DM

Development of Laponite® hydrogels for cisplatin delivery

MASTER DISSERTATION

Ana Sofia de Gouveia Duarte
MASTER IN APPLIED BIOCHEMISTRY

UNIVERSIDADE da MADEIRA
A Nossa Universidade
www.uma.pt

January | 2024

Development of Laponite® hydrogels for cisplatin delivery

MASTER DISSERTATION

Ana Sofia de Gouveia Duarte
MASTER IN APPLIED BIOCHEMISTRY

SUPERVISOR
Helena Maria Pires Gaspar Tomás

CO-SUPERVISOR
João Manuel Cunha Rodrigues

Development of Laponite® hydrogels for cisplatin delivery

Dissertation submitted to the University of Madeira in fulfilment of the requirements for the degree of Master in Applied Biochemistry

By Ana Sofia de Gouveia Duarte

Work developed under the supervision of

Prof. Dr. Helena Maria Pires Gaspar Tomás and

Co-supervised by Prof. Dr. João Manuel Cunha Rodrigues

Faculdade de Ciências Exatas e da Engenharia

Centro de Química da Madeira

Universidade da Madeira

Funchal – Portugal

2024

Declaration

"Plagiarism consists of the presentation, as your own and even if there has been translation, of ideas, opinions, phrases/texts, results, or conclusions of others. The practice of plagiarism is a serious violation of academic ethics and may lead to failure or withdrawal of the withdrawal of the degree, as well as civil, criminal, and disciplinary liability."

I hereby declare in my honor that this dissertation is of my own exclusive authorship, it is original, and that I have referenced and quoted all sources used in it.

Funchal, January 30, 2024

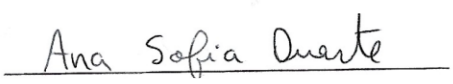

(Ana Sofia Duarte)

ACKNOWLEDGEMENTS

I would like to start by thanking Professors Helena Tomás and João Rodrigues for accepting to supervise me and for guiding me during my dissertation, for always being ready to help me with any difficulties I faced in my work, and for all the encouragement throughout the whole process.

Special thanks to Filipe Olim for helping me to accommodate in CQM as my co-supervisor in a previous internship, for giving me all the tools to perform my work in the materials' area of research, and for continuing to help me in any way he could. To Fátima Mendes and Helena Chá-Chá, thank you for becoming my great friends during this time in what I hope to be a long-lasting bond. To everyone at CQM who contributed to my work, I want to thank sincerely for all the help provided during my dissertation, with all the ideas and suggestions for the development of my work. To the people from room 0.99, thanks for all the laughs and company, all the peculiar lunch topics that were always so entertaining, and for all the advice you provided. An additional thank you to Mara Gonçalves, for all her assistance with the cells' related work, to Rita Castro, for all her help with SEM/EDS, and to Paula Andrade and the LQCMM team, for always helping me find what I needed to perform my work in the many different labs.

I want to thank my masters' colleagues, Verónica Pereira, Patrícia Silva, and Vera Oliveira for all the companionship during this masters, all the laughs and, honestly, us always sticking together through everything was a great help to get to the end of this journey so thank you very much. Finally, I want to thank my family for supporting me not only during the development of this dissertation but also throughout my entire academic journey so far. To my mother, for all her encouraging words in the toughest times, and for putting up with me whenever things were not going well, the biggest thank you. To the rest of my family, I thank you for all the support that you have given me. To my dad, for always encouraging me and cheering me up in dark times. Even though you are not here anymore, I hope that I am making you proud.

This work was supported by the *Fundação para a Ciência e a Tecnologia* (FCT) with Portuguese Government funds through the CQM Base Fund - UIDB/00674/2020 (DOI: 10.54499/UIDB/00674/2020) and CQM Programmatic Fund - UIDP/00674/2020 (DOI:10.54499/UIDP/00674/2020). Direção Regional da Juventude is acknowledged for their internship program Ingress@. The company BYK, Germany, is acknowledged for providing the Laponite XLG used in this thesis.

ABSTRACT

Cancer remains a major health concern worldwide and the development of effective therapies remains a challenge. Laponite® is a synthetic nanoclay that possesses properties such as easy functionalization, degradability, and biocompatibility. More importantly, Laponite® can form strongly thixotropic gels at higher concentrations which can be explored as an avenue to drug delivery. Amongst the drugs used for cancer therapy, cisplatin, a platinum-containing metallodrug, is especially used due to its mechanism of action, which involves interference with the cells' DNA. The main goal of this work was to formulate hydrogels composed by Laponite for the delivery of cisplatin. These gels are aimed for topical application or, eventually, for direct injection in the tumor site. As such, the preparation of Laponite hydrogels was first optimized (regarding type of liquid medium, temperature, Laponite concentration, solvent pH vs gelation time and gel consistency and transparency) and the gels were then studied to assess their ability to load (different cisplatin concentrations were assayed) and release cisplatin (at two different environmental pH values). Furthermore, the gels' cytotoxicity was evaluated *in vitro* in two cell lines, A2780 (human ovarian carcinoma) and its related cell line A2780cis (resistant to cisplatin). Cytotoxicity studies were carried out using two different approaches which mainly differed regarding the type of contact between the gels and the cells (direct and non-direct). Characterization of the gels by SEM/EDS showed that cisplatin enhances cohesion within the gels. Drug release was sustained but not sensitive to pH. Additionally, *in vitro* studies showed that non-loaded Laponite gels promoted cells' viability and gels containing cisplatin were cytotoxic in a concentration-dependent manner. Even though it was not possible to distinguish the two approaches used in this work regarding cytotoxicity, it was possible to conclude that Laponite hydrogels are promising platforms for cisplatin delivery.

Keywords: Laponite, Cisplatin, Hydrogel, Drug release, Cytotoxicity, Cancer

RESUMO

O cancro continua a ser um grande problema de saúde em todo o mundo e o desenvolvimento de terapias eficazes continua a ser um desafio. A Laponite® é uma nanoargila sintética que possui propriedades como fácil funcionalização, degradabilidade e biocompatibilidade. Mais importante ainda, Laponite pode formar géis fortemente tixotrópicos em concentrações mais elevadas, o que pode ser explorado como uma via para a entrega de fármacos. Entre os medicamentos utilizados para a terapia do cancro, a cisplatina, um metalofármaco contendo platina, é especialmente usada devido ao seu mecanismo de ação, que envolve interferência no DNA das células. O principal objetivo deste trabalho foi formular hidrogéis compostos por Laponite para a entrega de cisplatina. Estes géis destinam-se a aplicação tópica ou, eventualmente, a injeção direta no local do tumor. Como tal, a preparação de hidrogéis de Laponite foi primeiramente otimizada (em relação ao tipo de meio líquido, temperatura, concentração de Laponite, pH do solvente vs tempo de gelificação e consistência e transparência do gel) e os géis foram então estudados para avaliar sua capacidade de carregar (diferentes concentrações de cisplatina foram testadas) e libertar cisplatina (em dois valores de pH ambientais diferentes). Além disso, a citotoxicidade dos géis foi avaliada *in vitro* em duas linhas celulares, A2780 (carcinoma do ovário humano) e sua linha celular relacionada A2780cis (resistente à cisplatina). Os estudos de citotoxicidade foram realizados utilizando duas abordagens diferentes que diferiram principalmente quanto ao tipo de contacto entre os géis e as células (direta e não direta). A caracterização dos géis por SEM/EDS mostrou que a cisplatina aumenta a coesão dentro dos géis. A libertação do fármaco foi sustentada, mas não sensível ao pH. Além disso, estudos *in vitro* mostraram que géis de Laponite não carregados promoveram a viabilidade das células e géis contendo cisplatina foram citotóxicos de forma dependente da concentração. Embora não tenha sido possível distinguir as duas abordagens utilizadas neste trabalho em relação à citotoxicidade, foi possível concluir que os hidrogéis de laponite são plataformas promissoras para a entrega de cisplatina.

Palavras-Chave: Laponite, Cisplatina, Hidrogel, Libertação de fármaco, Citotoxicidade, Cancro

Contents

Figures Index

Tables Index

Abbreviations

3D Three-dimensional

BCA Bicinchoninic acid

CEC Cation Exchange Capacity

cisPt Cisplatin

DOX Doxorubicin

DMF Dimethylformamide

DNA Deoxyribonucleic acid

EDS Energy Dispersive X-ray Spectroscopy

EE Encapsulation Efficiency

FADH Flavin Adenine Dinucleotide

GNP Gold Nanoparticles

hMSC Human Mesenchymal Stem Cells

IC_{50} Half Maximal Inhibitory Concentration

LAP Laponite®

LDH Lactate Dehydrogenase

MRI Magnetic Resonance Imaging

MSC Mesenchymal Stem Cells

NADH Nicotinamide Adenine Dinucleotide

NADPH Nicotinamide Adenine Dinucleotide Phosphate

PBS Phosphate-Buffered Saline

PEG-PLGA Polyethylene glycol-poly lactic acid-co-glycolic acid

PPO-PEO Poly (propylene oxide)–poly (ethylene oxide)

PVA Polyvinyl alcohol

RPMI Roswell Park Memorial Institute

RT Radiation Therapy

SEM Scanning Electron Microscopy

1. Introduction

This thesis is focused on the development of hydrogels based on Laponite® for cisplatin delivery and cancer treatment. As one of the leading causes of death around the globe (1), cancer has been deeply studied in the past few decades. Many factors, both internal and external, have been linked to the appearance of the different cancer types but the unpredictability with which it manifests itself in the organism makes it one of the most demanding diseases to investigate potential therapies. There are currently several approaches for treatment for this disease such as chemotherapy, radiotherapy, immunotherapy, and surgery. Regarding chemotherapy, although there is a success rate associated with these treatments, there are also limitations such as harmful side effects, drug resistance or deficiency in tumor targeting (2). Hence, various drug delivery strategies have been developed and tested in recent years and, in particular, hydrogel-based systems should be highlighted.

1.1. Hydrogels and their biomedical applications

A hydrogel is a type of material that possesses a three-dimensional (3D) network structure, primarily composed of reticulated hydrophilic polymers (3). This network structure allows the hydrogel to retain a significant amount of water while maintaining its structural integrity. Hydrogels exhibit properties such as high water content, flexibility, and the ability to swell in response to changes in environmental conditions (4). These materials find widespread applications in various fields, including biomedical, pharmaceuticals, and environmental engineering, due to their unique ability to mimic biological tissues and provide a hydrated environment for cells or substances (5,6). These applications capitalize on the versatility of preparing hydrogels at various scales, including macro, micro, and nanogels (7).

In the biomedical field, especially, there are several areas where hydrogels' utility and benefits have been studied (Figure 1). One of the most important areas is that of wound dressing and healing. This is made possible by the hydrogel's creation of a moist environment that promotes tissue regeneration and accelerates the wound healing process (8). However, with the emergence of problems associated with the hydrogels' mechanical performance, the recurrent wound infections, and a low efficiency in the overall process (9), there was a necessity to develop hydrogels with more active roles in the healing procedure. Hence, there have been designed

systems in recent years involving hydrogels that are designed to release therapeutic agents to further enhance the wound's recovery (10).

Another area where there has been a lot of development for hydrogels is in tissue engineering. Organ donation and all the variables that the entire process entails and that could compromise it, such as compatibility, waiting time and survival benefit, is a very tricky procedure hence the need of the science community to find a suitable alternative. Therefore, hydrogels are a great strategy because they can serve as scaffolds for the cultivation and growth of cells while also providing a supportive structure that mimics the extracellular matrix, fostering cell attachment, proliferation, differentiation, and migration. Some of hydrogels' properties that may benefit regenerative medicine are their biocompatibility, thermal sensitivity, pH sensitivity, swelling properties, crosslinking degree, porosity, anti-microbial activity, and biodegradation (6).

For example, in the skeletal system, hydrogels can be used for bone tissue regeneration and cartilage tissue repair. As mentioned, the hydrogel's ability to deliver cells or growth factors to damaged cartilage areas make it a good candidate to support tissue repair (11,12). Hydrogels can also be used in ophthalmology, with soft contact lenses' manufacturing often using these materials. Their high water content and compatibility with the eye allow the necessary hydration for extended wear and can also provide comfort (13). In the area of diagnosis, hydrogels can be integrated into diagnostic devices for the identification of specific biomolecules. The hydrogels' capacity to immobilize and embed molecules in their 3D structure, their high permeability for small molecules and their viscoelastic properties enables the development and optimization of biosensors. Furthermore, they can also be used as responsive materials since changes in their properties, such as swelling or stiffness changes, can be indicative of the presence of specific analytes (14). Another area where hydrogels are applicable is in dentistry, where they can be used in oral delivery of substances such as drugs and antibacterial agents, as scaffold materials for dental implants and regeneration of dental tissues, and as a component in dental materials due to their biocompatibility (15). There is also a market for hydrogels in the cosmetic industry, such as reconstructive surgery. In their injectable capacity, hydrogels such as hyaluronic acid-based ones can be used as dermal fillers to enhance facial features or correct soft tissue defects, also providing a non-invasive option for augmenting or restoring volume (16).

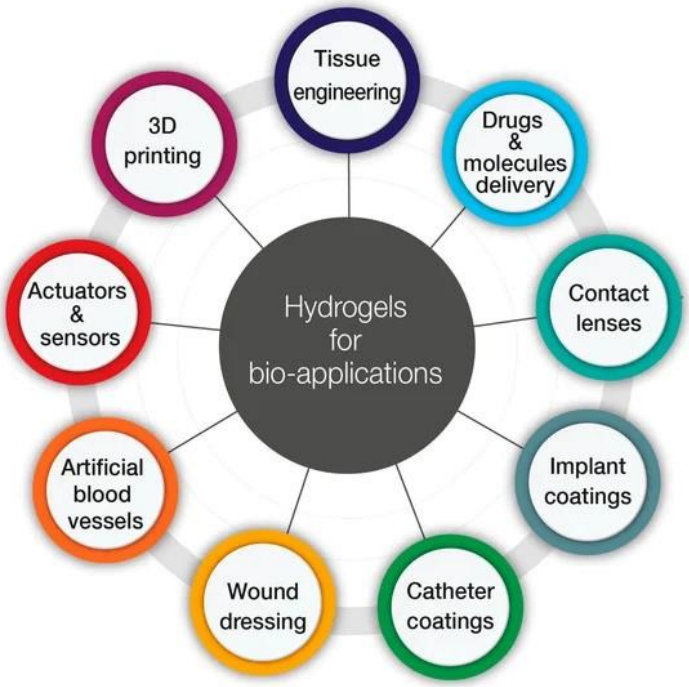

Figure 1 – Application of hydrogels in biomedicine (17)

Arguably one of the most important applications for hydrogels is drug delivery, particularly for cancer treatment (Figure 2). Due to some of their most attractive properties, such as their high biocompatibility, biodegradability, low levels of cytotoxicity, their capacity to encapsulate the drug and release in a sustained mode to the tumor (18) and due to their ability to absorb and retain water, hydrogels may serve as efficient drug delivery vehicles. They are particularly useful for the administration of medications over extended periods with minimization of side effects.

As briefly mentioned, chemotherapy presents several challenges in its clinical use which make it unable to completely eradicate all cancer cells while at the same time harming the organism (19). Hydrogels can be used to reduce these effects due to their potential sensitivity to temperature and pH changes, as evidenced by Lee et al. (20) with the development of a self-assembled hydrogel composed of transferrin protein and dithiothreitol (DTT) mixed in a salt solvent for the release of doxorubicin (DOX) into colon cancer cells. This system allowed for the encapsulation of the intended amount of drug and its release in both a temperature and pH-sensitive way and displayed cytotoxicity above 80% in the tested cells after 48 hours of incubation.

Similarly to chemotherapy, radiation therapy (RT) has been extensively used in cancer treatment because it leads to the tumors' reduction and potential eradication. Furthermore, the

ability to target this radiation to specific tissues enables both the killing of the cancer cells and the least possible damage to normal cells (21). However, this therapy is more effective in early-detected cancers vs in late stages due to the DNA's self-repair ability and cells' emerged resistance to the radiation. Hydrogel systems can prove beneficial due to their potential capability to inhibit these repairs and lessen the state of resistance, leading to more DNA damage (22,23). An injectable hydrogel based on Endostatin (ES) and hyaluronic acid-tyramine was developed by Wang et al. (24) with the goal of releasing ES in cancer cells due to its ability to reduce their microvascular density hypoxia which subsequently leads to an increase of the cells' sensitivity to radiation. They found that this hydrogel displayed sustained release, lower systemic toxicity and greater antitumoral action than ES alone. Furthermore, with the addition of RT, there was an increase in anti-angiogenic effects, the intended reduction in tumor hypoxia and overall improvement of RT in tested mice with Lewis lung cancer. Also to address RT's challenges, Zhang et al. (25) developed a versatile hybrid hydrogel by incorporating gold nanoparticle (GNP) aggregates and DOX into a polymeric hydrogel labeled with the radionuclide iodine-131. The investigated system demonstrated outstanding biocompatibility, stability in terms of photothermal and radiolabel properties, effective fluorescent imaging, and a sustained release of DOX. GNP aggregates functioned as both radio- and photosensitizers, enhancing DNA damage and contributing to photothermal therapy. This dual action impeded DNA self-repair and addressed tumor hypoxic conditions, resulting in an overall improvement in treatment effectiveness.

To fight the metastasis and recurrence phenomena associated with cancer, immunotherapy harnesses the organism's immune system to change the tumor microenvironment with the help of immune cells and signaling proteins such as chemokines and cytokines (26), creating anticancer effects and eradicating tumoral cells. However, the use of monoclonal antibodies as inhibitors limits their penetration in the cells owing to their big size and factors such as lackluster T cell infiltration rates and low immunogenicity provoke reduced sensitivity and responsiveness (27). Hydrogels can play a benefic role due to their ability to encapsulate these molecules and release them in a sustained way, increasing their effects. One example is the development by Jin et al. (28) of a hybrid peptide hydrogel combining melittin and RADA32, loaded with DOX, to achieve a potent chemoimmunotherapy against melanoma by actively regulating the tumor microenvironments (TMEs). The hydrogel displayed great biocompatibility, controlled drug release properties both in *in vitro* and *in vivo* studies and enhanced cytotoxicity against melanoma cells. The hydrogel activated natural killer cells, induced immunological responses, and depleted immunosuppressive elements, showcasing

robust anticancer efficacy against subcutaneous and metastatic tumors and potential for durable immunological memory against tumor rechallenge.

Hyperthermia is also a promising option for cancer treatment due to its fewer side effects, cost-effectiveness, and ability to be combined with other therapies, being usually applied as an adjuvant to chemotherapy or radiotherapy. It consists of the exposure of the organism to temperatures that exceed the physiological optimal level, around 39-45°C (29), which can destabilize cancer cells. This damage occurs due to a cascade of phenomena starting with protein denaturation, subsequent cell membrane and mitochondria disruption and deregulation of several biochemical pathways, particularly concerning DNA-related functions (30). Additionally, damage to the mitochondria compromises oxygen's uptake by the cells and induce hypoxia in the tumoral tissues, increasing their sensitivity to heat (31). Hyperthermia's effects on cancer cells enhance its potential synergistic effect with the previous discussed therapies via reduction of resistance to chemotherapy drugs, radiation, and acceleration of immune response. Hydrogels, particularly thermogels, have arisen as potential materials for a successful combination of therapies, including hyperthermia, due to their ability to not only load a variety of molecules and release them sustainably in the cancer cells but also respond to temperature variations. A thermogel that undergoes a sol-gel transition at a certain temperature (such as physiological temperature) can facilitate injectability in the organism which enhances its potential in several treatments (32). Yang et al. (33) developed a thermosensitive hydrogel based on PLGA-PEG-PLGA to deliver DOX and β-cyclodextrin-curcumin to osteosarcoma cells, in a dual delivery system. This system harnessed curcumin's ability to improve the cytotoxicity of several chemotherapy drugs by combining it with DOX in a hydrogel with a well-defined sol-gel transition temperature. This approach significantly improved cytotoxic efficiency and enhanced the pro-apoptotic effects of DOX when compared to single-drug treatments.

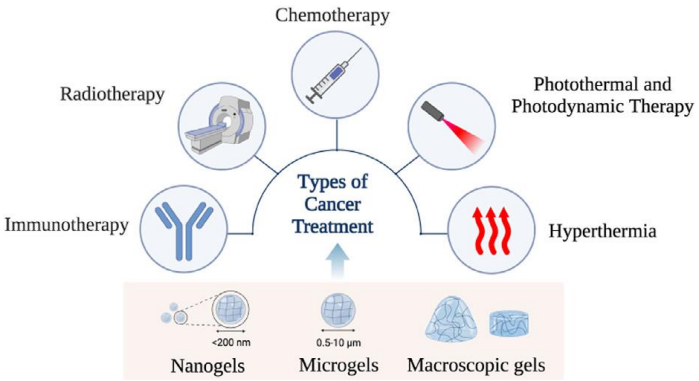

Figure 2 – Different types of hydrogels and potential applications in cancer treatment (adapted from (34))

As previously mentioned, hydrogels can also be classified by their size, with each having advantages, limitations and different potential applications, which are summed up in Table 1. These different sizes influence the methods of delivery and their efficiency. For example, a macrogel is more adequate for *in situ* delivery such as an injection or direct application in the wound or surgical cavity. On the other hand, microgels are more efficient via oral or pulmonary delivery rather intravascular applications due to their higher liability to phagocytosis by macrophages in the blood vessels (35). Finally, nanogels have the potential to overcome barriers imposed to larger hydrogels, such as the penetration of the blood-brain-barrier (BBB), which remains a challenge to this day.

Table 1 – Types of hydrogels classified by size

Type of hydrogel	Size	Advantages	Limitations	Example
Macrogel	>100 µM	High drug-carrying capacity, high stability, and high stimuli response (34)	Difficult to deliver (34)	Surface-filled hydrogel releases miRNA NPs with anticancer activity (36)
Microgel	0.5-10 µM	Delivery of hydrophobic drugs (34)	Prone to phagocytosis (34)	Pectin-based hydrogel for the release of 5-fluorouracil for colon cancer treatment (37)
Nanogel	<200 nm	Large surface area, high drug loading efficiency (34)	Rapid clearance (38)	Crosslinking of pullulan and poly(deca-4,6-diynedioic acid) (PDDA) to cross BBB (39)

1.2. Laponite

1.2.1. Structure, properties, and interactions with molecules

Clays are naturally occurring, fine-grained minerals or soil particles characterized by their small particle size and sheet-like structure. They are part of the larger family of phyllosilicates and are primarily composed of layered silicate minerals, such as kaolinite, montmorillonite, and illite (40). Clays have a high surface area and a significant capacity to

absorb water and other substances. Their properties can vary widely based on their mineral composition, and they often exhibit plasticity when mixed with water, allowing them to be molded and shaped (41). Clays are found in various geological formations and are commonly used in a range of applications, including ceramics, construction materials, cosmetics, and as a component in certain medical and industrial processes (42).

Due to their unique properties and versatile nature, clays have garnered increasing attention in biomedical applications. Specifically, certain types of clays, such as montmorillonite and halloysite nanotubes (43,44), exhibit characteristics that make them valuable in various medical contexts. These clays are explored for drug delivery systems, acting as carriers that can absorb/adsorb and release therapeutic agents in a controlled manner. Additionally, due to their natural antimicrobial properties, clays have been investigated for wound healing applications, with clay-based dressings providing a conducive environment for tissue regeneration. In tissue engineering, clays may contribute to scaffolds that support cell growth and differentiation (45). The biocompatibility and tunable properties of clays offer exciting prospects for advancing biomedical technologies and improving therapeutic outcomes, hence ongoing research continues to explore their full potential.

Laponite® is a nanoclay, classified as a synthetic smectite and whose structure and composition resemble that of hectorite, a natural clay mineral. Although Laponite® is a registered trademark, from now on it will be called Laponite for simplicity. These clays belong to the group of phyllosilicates, silicate structures defined as 2:1 crystals composed of layered units of two tetrahedral silica sheets that sandwich an octahedral metal cationic sheet (46). Figure 3 presents the idealized structure of the unit cell, where the magnesium ions are sandwiched between two layers of silicon atoms; these layers also contain oxygen atoms and hydroxyl groups (47). This unit cell would ideally have a neutral charge; however, as Figure 3 depicts, some of the divalent magnesium ions are sometimes replaced by monovalent lithium ions, leading to the following empirical formula:

$$Na^{+}_{0.7}\,[(Si_8\,Mg_{5.5}\,Li_{0.3})\,O_{20}(OH)_4]^{-0.7}$$

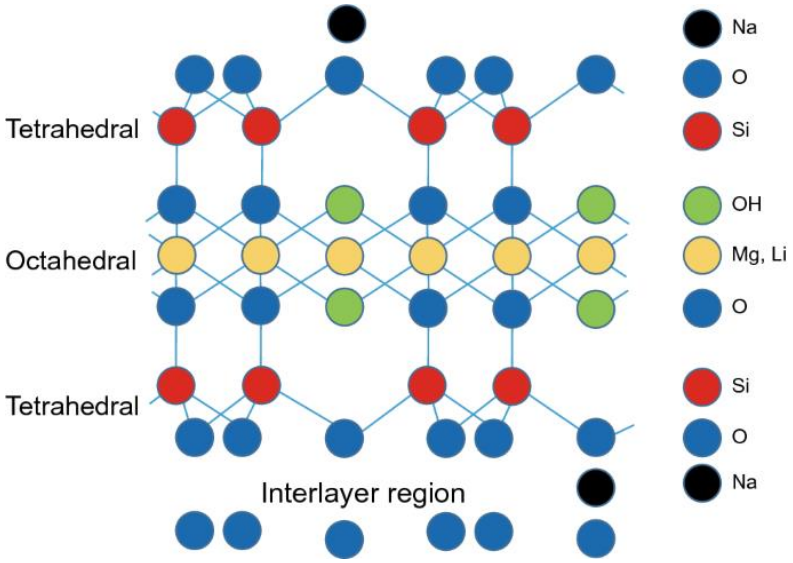

Figure 3 – Idealized crystal structure of Laponite (47)

The negative charge of 0.7 per unit cell is neutralized during the manufacturing process because of the sodium ions adsorbed on the crystal surfaces. When dispersed in water, Laponite's layer structure originates disk-shaped crystals. As displayed in Figure 4, the Laponite disks have about 25 nm of diameter and 0.92 nm of height (48) and it is estimated that a Laponite crystal has approximately 2000 unit cells.

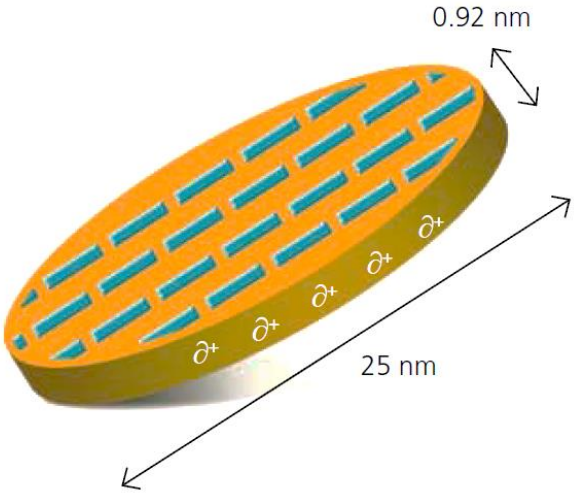

Figure 4 – Representation of a Laponite disk (48)

The structure of the groups present in the disks and the cation substitution previously stated (magnesium substituted by lithium ions) both cause their surfaces to be negatively charged, while having positively charged edges. The negative charge of the surfaces is balanced by the sodium ions present between the crystals and adjacent water molecules. These ions are responsible for the electrostatic interactions among the crystals in the interlayer regions, creating stacks of crystals that appear as a white dry powder. When the disks absorb water, Laponite can expand and delamination can occur. On the other hand, the disk edges possess hydroxyl groups and their charge depends on the surrounding pH, with previous studies indicating that the edges of the crystals possess a positive charge when the environmental pH is 11 (49). Studies on pH and conductivity have shown that Laponite acts as a base when dispersed in deionized water, with solutions having a pH of approximately 10, and that the positive charges of the crystal edges are approximately 10% of the negative charge on the disks' faces (48,49).

When Laponite is dissolved in water at a low concentration a colloidal dispersion is formed where all the crystals are surrounded by an electric double layer encompassing sodium cations. Because of the electrostatic forces between these sodium ions and the crystal surfaces, as well as osmotic pressure, which pulls them away from the surface, an equilibrium is created where the ions are in the vicinity of both sides of the Laponite crystal. These electric double layers create repulsive forces between the particles when they come into contact. When the experimental conditions are altered, such as the introduction of additional ions or polar molecules into the solution or the increase in concentration (50), there is interference with the electric double layers, where there is a decrease in the osmotic pressure and subsequent contraction of the layers. Consequently, this allows the weaker positive charges present in the crystal edges to bond with the negatively charged surfaces of neighboring crystals. These interactions can tip the balance in favor of attractive forces over repulsive forces, potentially resulting in the formation of gel-like structures (Figure 5) (48).

These gels have strong thixotropic properties, which signify that their viscosity decreases when shear stress is applied, and they can re-form once they are no longer under these conditions. The formation of gels occurs because of the negative surface interactions of the disks with the positive edges of other disks, which is commonly called a "House-of-Cards" structure, with the disks bonded together by weak ionic forces (51), as evidenced in Figure 5.

Figure 5 – House-of-Cards structure formed by electrostatic forces (47)

Laponite's composition and structure provide it with properties such as high aqueous stability (52)**,** cation exchange capacity (CEC) (53), and swellability, which is dependent on both the cations within the interlayer space and the solution's concentration of Laponite (54). Laponite exhibits versatile interactions with other molecules influenced by factors such as pH, molecular size, and electrostatic forces. Its potential for drug delivery systems lies in its capability to engage with drug molecules at different locations on its disks—interlayer spaces, between particles, and edges of the disks. Various mechanisms govern drug localization on Laponite nanoparticles, including Van der Waals bonds, cation exchange, water bridging potential, and hydrogen bonding. These mechanisms enable effective loading of drugs into interlayer sites and surface adsorption. The diverse ways drugs interact with Laponite nanoparticles underscore the complexity of their adhesion, determined by specific chemical features (55).

1.2.2. Applications

Due to several of its properties, Laponite has a broad range of applications. Its thixotropic properties allow it to be a rheology modifier in several contexts. For industrial functions, Laponite can be used in release suspensions, such as of mold, grinding pastes, oil drilling fluids, ceramic glazes, rubber latex and electrorheological fluids (48). Furthermore, this synthetic nanoclay has uses in personal care products, such as skincare emulsions, shampoos, and toothpastes; in household products, such as gelled bleach cleaners, air fresheners and sprayable cleaners; agricultural products, like seed germination gels and agrochemical flowables; in building products, such as wood treatment suspensions and adhesives. Moreover,

Laponite can be utilized for surface coatings, such as printing inks, pigment suspensions and decorative/architectural finishes. Another function Laponite possesses is that of a film forming agent, which can be taken advantage of for ink jet coatings, microparticle for retention and drainage systems and inert barrier films, for example (56).

Most relevant for this thesis is the potential Laponite has shown for biomedical applications (Figure 6). From bioimaging to regenerative medicine, several experiments have been carried out using Laponite due to many of its properties that are valuable for the intended goals.

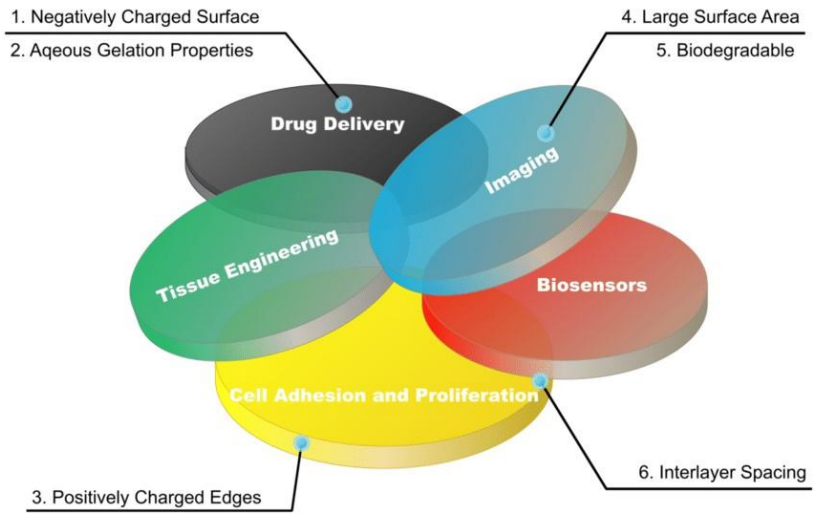

Figure 6 – Laponite's biomedical applications (56)

Tissue engineering and regenerative medicine

Tissue engineering is considered a subfield of regenerative medicine and its focus is the utilization of materials, cells, and biochemical and physicochemical factors to reconstitute biological tissues and to foster their regeneration in the long-run (57). One of Laponite's properties that is relevant to the tissue engineering field is its ability to interact with several molecules, which makes it an effective carrier of biochemical factors necessary in regenerative processes, while also being able to release them in a sustained manner. Laponite's ability to degrade is also relevant for its role in the fields of tissue engineering and regenerative medicine

since it leads to the release of orthosilicic acid ($Si(OH)_4$), an inorganic compound that has been shown to play a role in collagen type I synthesis in early osteoblastic cells (58). Type I collagen has been linked to the bone's formation, strength, and structure (59) with its genes' posttranslational modifications being crucial not only in bone turnover but also in the mechanical properties of the bone matrix (60). Therefore, type I collagen's synthesis by osteoblasts (in early stages) and deposition is important for the bone formation process. It has been investigated by Reffitt et al. that $Si(OH)_4$ stimulated type I collagen synthesis in human osteosarcoma cells, osteoblasts derived from the human bone marrow stromal cells and an osteoblast precursor line. Besides type I collagen synthesis, alkaline phosphatase (ALP) activity and osteocalcin synthesis also increased in the presence of $Si(OH)_4$, with the latter signifying osteoblastic differentiation (58). Moreover, Laponite's degradation process also causes the release of several ions, such as magnesium, lithium, and sodium. Magnesium plays numerous crucial roles in the organism due to its ability to both chelate with compounds like adenosine triphosphate (ATP), the cells' main energy provider, and compete with other ions, like calcium, for binding sites on proteins and membranes. It not only is a part of the synthesis of proteins and nucleic acids but also intervenes in metabolic processes and has more particular actions in a variety of organs and systems (61). Sodium also plays an important role in the human body, especially in the nervous system where it aids in generating electrical potential that allows the conduction of nerve impulses (62). Finally, lithium is said to interfere in neuronal behavior, being a mood stabilizer, while also having a reported role as an inhibitor in enzymatic reactions (63). In sum, Laponite's bioactivity as a material can be considered an advantage in regenerative medicine due to the beneficial biological roles its released products may have on the organism.

Laponite has also been studied regarding its potential in wound dressing. Gonzaga et al. formulated Chitosan/Laponite nanocomposite scaffolds via a freeze-drying process, while also testing different clay concentrations, for potential skin regeneration. It was concluded that chitosan alone provided some important properties to the material's application such as low levels of cytotoxicity, antimicrobial activity and swelling but these were enhanced in the presence of Laponite. Furthermore, this clay allowed for stronger mechanical properties, bio-adhesive strength *in vitro* and cell adhesion in the scaffold, as well as fitting porosity values for wound dressing. They also found that the higher Laponite's concentration was, the more efficient the bio-adhesion and its force were, with scanning electron microscopy (SEM) results demonstrating that fibroblast cells' attachment varied according to clay concentration present in the scaffold (64).

Bioimaging

One of the most important potential biomedical applications of Laponite is in bioimaging, in which non-invasive methods are applied to make possible the observation of biological processes, whether *in vitro* or *in vivo*. Laponite's ability to interact with many biochemical factors is beneficial to this application, since it means that several dyes, such as fluorophores, can be linked to it. Furthermore, Laponite also facilitates the solubilization of hydrophobic compounds by serving as a carrier of these dye molecules (46). Felbeck et al. formulated Laponite nanoparticles functionalized with 3-aminopropyldimethylethoxysilane (APES) and subsequently tested several dyes with these particles. The results showed that the dyes' bond with the Laponite's disks' edges influenced their charges and accumulation (65). It is also possible to utilize Laponite in magnetic resonance imaging (MRI) applications, where magnetic materials such as iron oxide nanoparticles can be blended with Laponite in nanocomposites, as investigated by Tzitzios et al. (66). In this work, laponite-gamma-iron oxide (LAP/ɣ-Fe_2O_3) composite nanomaterials were synthesized and several of their properties were subsequently studied, including magnetism. The nanoparticles exhibited much higher T2-weighted MRI divergence in comparison with Fe_2O_3 not intercalated with Laponite. However, *in vivo* results were not as satisfactory. Ling et al. introduced a different synthesis method based on co-precipitation and prepared LAP-Fe_3O_4 nanoparticles with properties such as colloidal stability, water dispersibility and cytocompatibility (67). Both in *in vitro* tumor cell imaging MRI and *in vivo* tumor grafted nude mice MRI there was a clear alteration of signal intensity in the presence of the LAP-Fe_3O_4 nanoparticles, due to their efficient cellular uptake. The fact that Laponite possesses unique properties makes it so that it can be loaded with anti-cancer drugs or modified for active targeting and makes this system effective for theranostic applications. This was demonstrated later when the LAP-Fe_3O_4 nanoparticles were modified with folic acid and were able to target cancer cells with overexpressed folate receptors (68).

For theranostics the main draw is the synergistic effect of combining both imaging and therapy in the same process, which not only is a time-saver but also strengthens both applications. More recently, Liu et al. synthesized nanoplatforms where Laponite was coated with polydopamine (PDA), loaded with a photothermal dye, indocyanine green (ICG), and an anti-cancer drug, DOX as well as modified with polyethylene glycol-arginine-glycine-aspartic acid (PEG-RGD) for photoacoustic imaging-guided chemotherapy on cancer cells with an overexpression of αvβ3 integrin (69). This integrin plays a critical role in tumor growth and controls cancerous cells' survival. The nanoplatforms displayed good imaging properties, both

photothermal and photoacoustic, were successful in releasing DOX in a pH-sensitive way and had good cellular uptake in the 4T1 cells (derived from mouse's mammary gland tissue) with αvβ3 overexpression, serving also as a great contrast agent for *in vivo* imaging of these cancer cells. Overall, these nanoplatforms were presented as an effective method for theranostics.

Drug delivery

There is no doubt that drug delivery has been one of the most important challenges in the biomedical field. Whenever drugs started being conceived for the treatment of several diseases, the way the substance was delivered to the damaged organ and its cells became also the subject of much investigation. There are many factors that contribute to a drug's therapeutic efficacy in the organism, such as the dosage administered and the frequency of administration but these often result in toxicity and side effects (55). Hence, drug carriers must be able to successfully encapsulate the drug and deliver enough of it to the specific site but also maintain its frequent release for maximum therapeutic efficiency.

Laponite as a nanomaterial, alone or in combination with other materials, is an interesting prospect for drug delivery (Figure 7) due to its ability to encapsulate or "trap" cationic compounds in the large surfaces of its interlayer spaces as well as the high negative charge from these surfaces. As mentioned before, these properties allow the adsorption of molecules with positive charges on Laponite's surfaces and an eventual controlled release through an ion-exchange mechanism dependent on ambient pH, size, and electrostatic properties of the interacting molecule (70,71).

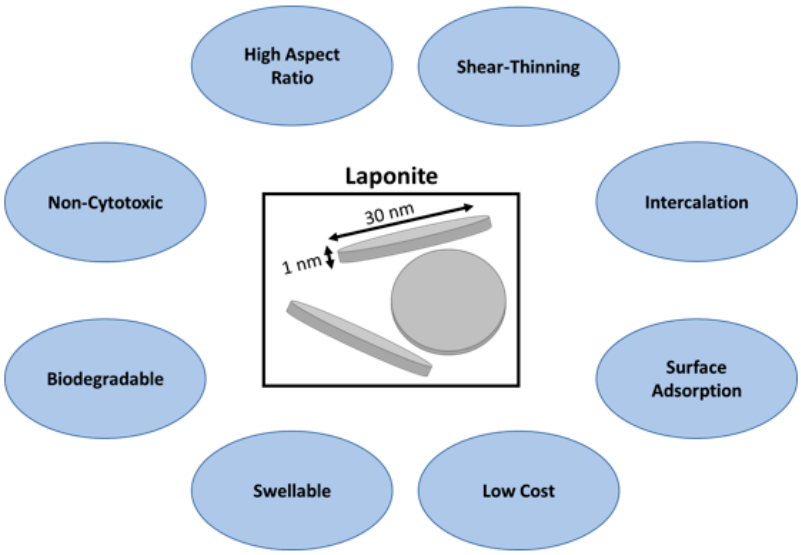

Figure 7 – Laponite's properties that make them suitable for drug delivery (adapted from (72))

Several factors affect both the drug encapsulation efficiency (EE) and the drug release from Laponite. For the encapsulation of the drug molecule by Laponite, the mechanism is mainly intercalation due to the spaces created by the electrostatic forces amongst the negatively charged interlayers (73). The drug molecules are encapsulated by one of two mechanisms, an ion-dipole interaction with hydrophilic molecules or an ion-exchange with ionic compounds (74). Some of the factors influencing the EE are both the drug and Laponite's net charges which are always dependent on pH. Furthermore, the drug's net charge influences the force of the electrostatic interactions amongst both compounds and the stronger these are the more efficient the encapsulation of the drug is. Moreover, the ionic strength can also influence the drug's net charge by pK_a modulation. Both the drug and Laponite's concentrations are also crucial factors in EE. Regarding Laponite, there are two contradicting theories on concentration versus EE. There are reported results of EE increasing with the increase of Laponite's concentration, with an example being Laponite/chitosan beads loaded with ofloxacin where the EE increased from 50% to 91% when Laponite's concentration varied between 10 to 40 $mgmL^{-1}$ (75). Results such as these could support the idea that higher concentrations of Laponite would lead to a more efficient dispersion of the drug in its interspaces. However, the second theory states the opposite of the first and is supported by results showing that, with the increase of Laponite's concentration, EE decreases. For example, Wang et al. found that the increase of Laponite from 3 $mgmL^{-1}$ to 10 $mgmL^{-1}$ in amoxicillin-loaded Laponite/chitosan nanofibers caused a decrease of the EE from 10% to 3% (76). It's been posited that increasing the concentration of Laponite could lead to the aggregation of its disks and therefore interfere with the drug's entrapment and consequently its loading. For the drug's concentration, it has been reported, for example, that tetracycline's concentration increase in a Laponite dispersion will lower the EE (74). The success of the drug's loading can be characterized by several techniques such as SEM, zeta potential, Fourier-transform infrared spectroscopy (FTIR), and X-ray diffraction (XRD).

Regarding the drug release, there are also a set of factors that influence the process. There are two main mechanisms by which the release can happen which are drug diffusion and the carrier's degradation. The former is more common, as the drug is more rapidly diffused than the carrier is degraded. What happens is the intercalated drug is released from the carrier and while the drug is diffused out, water is diffused into the carrier and any interfering factors will have an impact on the release (55). Firstly, the physicochemical properties of the drugs play a crucial role in whether the molecules will be released at a faster rate or suffer a bigger retention. For example, hydrophilic and protonated compounds are evidently more retained due to their interactions with Laponite's negative surfaces and therefore will display a more sustained

release profile (77,78). Furthermore, the microenvironment's pH also has an important role in drug release since physiological variations of pH levels always happen, especially in conditions such as cancer or inflammation, with a lower pH being observed in these scenarios. This variation in pH has long been studied for its potential in targeted drug delivery (79) and it is particularly relevant for Laponite with its negative surface charges and pH-responsive edges with its amphoteric groups (80). The reversible protonation and deprotonation of Laponite in response to environmental pH and its influence on the electrostatic interactions between drugs and Laponite make it suitable for controlled drug release as a pH-responsive material (46,81). For example, the release of cationic drugs like DOX is due to an ion-exchange mechanism and it has been shown that it occurs at a faster rate in an acidic pH, with Xiao et al. demonstrating that at a pH of 5.4 there was a faster release for their compounds than at pH 7.4, where there was only 10% of DOX released (82).

Other factors that play a role in drug release include Laponite's CEC, swelling behavior, its own concentration and drug solubility. Drug's solubility in water is a big factor in its release rate and subsequent bioavailability in the organism. Regarding the CEC, a drug's deintercalation from the Laponite layer is significantly influenced by the quantity of drug released (83). The substitution of the protonated drug with cations in the solution is a process whose pace is governed by the physicochemical characteristics of both the drug and the clay (81). A greater clay CEC signifies a more robust interaction between the drug and the clay, potentially resulting in a slower release of the drug (55). On its swelling behavior, studies indicate that the inclusion of Laponite has the capacity to influence the swelling behavior of hydrogels that incorporate it (84) and it is known that the process of rehydration plays a crucial role in facilitating the release of encapsulated drugs from Laponite (85). The concentration of Laponite is also important and studies have shown that increased clay concentration may slow the drug's release due to possibly a more gradual degradation or a reduced diffusion (75,86).

As a drug carrier, Laponite has other appealing factors such as its degradation ability, particularly in acidic environments. Some studies have shown that in the presence of solutions with pH ≤ 7, there is a higher concentration of silica, magnesium, and sodium ions dissolved in the medium than in alkaline solutions. This implies that under acidic conditions, Laponite is more degradable, and the ions in its composition are released into the solution, which is dissolved in (87). Furthermore, some of the contributing factors to the chemical degradation of Laponite were studied and it was found that time, salt concentration and Laponite concentration had a significant influence in Laponite's degradability, in which older suspensions with low salt and

low Laponite concentrations displayed bigger degradation (52,88). Moreover, the cytotoxic behavior of Laponite is crucial for its potential biomedical applications. This property has been studied using a lactate dehydrogenase (LDH) assay in human mesenchymal stem cells (hMSCs), and it has been reported that the addition of Laponite XLG at concentrations lower than the Half Maximal Inhibitory Concentration (IC_{50}) values did not cause a change in the LDH level in the media, showing that at concentrations lower than 1 $mgmL^{-1}$, no significant cytotoxicity was observed in hMSCs (89). Finally, one of the most important properties Laponite possesses is its biocompatibility, with several studies showing that it doesn't generally induce cytotoxicity in the organism, can increase cell growth (90) and can enhance the attachment and proliferation of cells such as mesenchymal stem cells (MSCs) (91).

Similarly to its role in nanoparticles, Laponite has been integrated with various polymers to create hydrogels for drug delivery, showcasing diverse applications, including anti-cancer, anti-inflammatory, and anti-bacterial activities (Table 2).

Table 2- Summary of some of Laponite's past works in different applications

Application	Polymer	Synthesis Method	Drug delivered	References
Anti-cancer	PPO-PEO	Solution mixing	β-Lapachone	(92)
	Chitosan-PVA		Curcumin	(93)
	Alginate		Doxorubicin	(94,95)
	None	Inverse miniemulsion technique	Cisplatin, cyclophosphamide, 4-fluorouracil	(96)
Anti-inflammatory	Alginate	Solution mixing	Theophylline	(53)
Anti-bacterial	Chitosan	Co-precipitation	Ofloxacin	(97)
	Dextran	Free radical polymerization	Ciprofloxacin	(98)

For the delivery of small molecules like anti-cancer drugs, some Laponite-polymer composite hydrogels have been developed, like Laponite-alginate for delivery of DOX (95) that displayed high encapsulation efficiency, sustained drug release behavior, successful cell internalization and high cytotoxicity in CAL-72 cells in comparison with the free drug. Becher et

al. (96) designed a nanohydrogel platform based on Laponite nanodiscs, polyacrylate, and sodium phosphate salts with tailored stiffness for drug delivery. Three drugs tested, which were 4-fluorouracil, cyclophosphamide, and cisplatin, and *in vitro* studies showed the nanohydrogels displayed a lower IC_{50} in MCF-7 cells in comparison with the free drugs. Furthermore, *in vivo* studies demonstrated the nanohydrogels' biocompatibility and non-accumulation in central organs.

One of the anti-neoplasic drugs utilized in the aforementioned work is cisplatin, a well-known metallodrug used for cancer treatment which will be further explored within the scope of this work.

1.3. Platinum-based metallodrugs for cancer treatment

Metallodrugs, also known as metallopharmaceuticals, are compounds featuring a metal atom as their active agent and are activated by ligand substitution or metal- or ligand-based redox reactions. Their significance in clinical applications stems from their mechanisms of action, which are primarily active targeting processes, through favorable interactions with various biological molecules within the human body (99). Metallodrugs find application in treating a multitude of diseases, particularly cancer. Notably, platinum-based metallodrugs exhibit substantial anti-cancer potential. The electrophilic nature of platinum allows its reaction with nucleophilic residues in DNA molecules, functioning akin to an alkylating agent.

Since the 1970s, three major drugs within the platinum-based antineoplastic medication family have been available in the market: cisplatin, carboplatin, and oxaliplatin. These drugs have demonstrated their capacity to disrupt DNA functions in cancer cells by forming monoadducts and DNA crosslinks (100). Both carboplatin and oxaliplatin are derivatives of cisplatin, distinguished mainly by their structures and toxicity levels. Carboplatin incorporates a bidentate dicarboxylate-substituted ligand and is associated with significant myelosuppressive effects in the organism, acting as its dose-limiting factor (101). Oxaliplatin, classified as an organoplatinum compound, features a platinum atom complexed with *trans*-1,2-diaminocyclohexane and a bidentate oxalate group and it causes side effects such as neurotoxicity and ototoxicity (102).

The primary platinum-based compound employed in cancer treatment is *cis*-diaminedichloroplatinum (II) [Pt $(NH_3)_2Cl_2$], medically referred to as cisplatin. Cisplatin features a square planar molecular geometry, with two chloride ligands and two ammonia groups

complexed to the platinum atom in a *cis*- configuration (Figure 8). Upon entering the organism, this molecule undergoes aquation, during which its chloride ions are displaced and replaced by two water molecules (Figure 9). The resulting aquocomplex, cis-[Pt $(NH_3)_2(H_2O)_2]^{2+}$, is considered crucial in the DNA platination process, which is the basis for its mechanism of action (103).

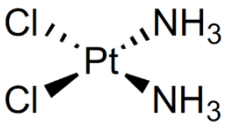

Figure 8 – Chemical structure of cisplatin (100)

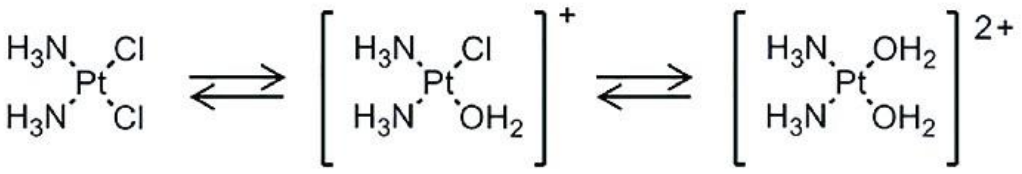

Figure 9 – Cisplatin's aquation process (adapted from (104))

Cisplatin's mechanism of action, akin to other platinum-based drugs, involves inducing cytotoxicity by impairing the DNA within the cells. The interference with DNA functions, including replication and transcription, impacts processes such as cell mitosis. Cisplatin damages DNA by crosslinking it, triggering DNA damage repair mechanisms that, if unsuccessful, result in apoptosis (105).

However, the utilization of cisplatin in cancer treatment is constrained by various limitations. Besides the occurrence of toxic side effects such as neurotoxicity, nephrotoxicity, and the potential for nausea and vomiting, there is also the emergence of resistance mechanisms in tumor cells. This resistance phenomenon has been attributed to several self-defense mechanisms developed by the cells, including blocked endocytosis or mislocalization of membrane transporters, which hinder cisplatin's influx and accumulation while promoting increased efflux (106). Consequently, numerous preclinical models are dedicated to understanding and addressing these resistance mechanisms, seeking ways to overcome these challenges (100).

2. Thesis Objectives

As a powerful anti-neoplasic drug, cisplatin has been used for cancer treatment since its inception but its limitations make it imperative that new delivery methods are developed. In this work, Laponite's advantageous properties as a drug carrier and, most importantly, its thixotropic nature, were harnessed to develop gels as new delivery method for cisplatin in cancer cells. These gels are aimed for topical application or, eventually, for direct injection in the tumor site. In this scope, research was mainly focused on the gels' optimized formulation, physicochemical characterization, efficacy in releasing the drug in different environmental conditions (namely pH) and cytotoxic effects on tumor cells.

More specifically, the main goals proposed for this dissertation were:

a) The establishment of an optimized formulation of Laponite gels and Laponite-Cisplatin gels in terms of gel-forming conditions, namely gelation time and gel consistency; the effect of variables such as temperature, pH, and concentration of both Laponite and Cisplatin on gels' properties were studied.
b) The characterization of the gels, namely their water content, their morphology and their composition, the latter two analyzed by Scanning Electron Microscopy and Energy-dispersive X-ray spectroscopy (SEM/EDS).
c) The evaluation of cisplatin's release profile at two different environmental pH values (the physiologic pH value of 7.4 and the pH value of 6.5 that, being more acidic, can possibly be reached in the tumor microenvironment); here, the drug release was followed by cisplatin's quantification through a chemical derivatization method and the possible sustained release behavior of the drug was investigated.
d) The evaluation of the Laponite and Laponite-cisplatin gels' cytotoxicity in vitro; these studies were performed using two different cell lines, the A2780 (human ovarian carcinoma) and the A2780cis (resistant to cisplatin) cell lines; moreover, two different approaches regarding the type of contact between the gels and the cells were tested (direct and non-direct contact with the gel); in all studies, cell viability was indirectly assessed through a metabolic activity assay (the resazurin reduction assay). In this context, in order to validate the application of the resazurin reduction method to assess cytotoxicity, the total protein quantification in culture (by the bicinchoninic acid protein assay) was also performed in selected experiments.

3. Materials and Methods

3.1. Materials

Laponite XLG was kindly donated by BYK, Germany. According to the supplier, it is a gel forming grade Laponite with high purity, and certified low heavy metal and low microbiological content (see the data sheet in Annex 1). Cisplatin (cisPt, IUPAC name: cis-dichlorodiamineplatinum (II)) was purchased from Acros Organics (99.99%). For the phosphate buffered saline (PBS) solution without calcium and magnesium ions, dibasic sodium phosphate was purchased from Panreac, monobasic potassium phosphate from Panreac, sodium chloride from Fisher and potassium chloride from Panreac. The pH was adjusted to 7.4 with sodium hydroxide (NaOH) 0.01 M.

For cisplatin quantification, o-phenylenediamine was purchased from Aldrich (99.5%) and for the potassium dihydrogen phosphate (KH_2PO_4) buffer, the potassium dihydrogen phosphate was purchased from Merck and sodium hydroxide from Fisher. Dimethylformamide (DMF) was purchased from Fisher.

3.2. Formulation of the gels

For the optimization of the Laponite gels forming method, several variables were studied including different ions present in the solvent (water), solvent pH, temperature of incubation, Laponite concentration and mixing process. Furthermore, cisplatin concentration was also assessed as a variable when cisplatin was added to prepare the Laponite-cisplatin gels.

To form pristine Laponite gels, a Laponite solution at the desired concentration (20 to 40 $mgmL^{-1}$) was prepared in distilled water (depending on the cases , without or with pH adjustment to 7.0 using NaOH 0.01 M) and mixed vigorously by vortexing for 10s. The solutions were incubated at 37 °C until complete gelation was achieved (a Wisd incubator was used).

To form Laponite-cisplatin gels, a cisplatin solution was prepared at the desired concentration in distilled water adjusted to a pH of 7.0. Subsequently, Laponite was poured into the solution to obtain a final Laponite concentration of 30 $mgmL^{-1}$, and the solution was mixed vigorously by vortexing for 10s. The solution was incubated at 37 °C until complete gelation was achieved.

3.3. Characterization of the gels

3.3.1. Water content

Laponite and Laponite-cisplatin gels (2 Laponite gels at 30 $mgmL^{-1}$ with 0 and 3 $mgmL^{-1}$ of cisplatin, respectively) were prepared by the previously described methods and weighed ($m_{hidrated\ gel}$) (Ohaus). Subsequently, the samples were lyophilized (Labconco) and weighed again ($m_{lyophilized\ gel}$) to evaluate the water content of the gels using the following formula:

$$\%\ water\ content = \frac{(m\ hidrated\ gel - m\ lyophilized\ gel)}{m\ hidrated\ gel} x100$$

3.3.2. Morphology and composition of the gels by SEM/EDS

Several Laponite gels were prepared by the previously described methods, namely: a pristine Laponite gel (30 $mgmL^{-1}$) and two Laponite-Cisplatin gels (containing 30 $mgmL^{-1}$ in Laponite and 1 $mgmL^{-1}$ or 3 $mgmL^{-1}$ of Cisplatin). Subsequently, the gels were lyophilized and later analyzed by SEM/EDS (Bench SEM Phenom ProX) at 10-15 kV with different magnifications (210x, 250x, 500x, 1000x, 2000x and 4000x).

3.4. *In vitro* drug release studies

To evaluate the effect of the environmental pH in the cisplatin's release from the gels, two different pH values were used in the drug release assays, namely the pH of 7.4 to mimic the physiological pH of the human body and a pH of 6.5 to simulate the pH of the tumor microenvironment (107).

To perform the cisplatin release assay, Laponite-cisplatin gels were prepared as previously described. The Laponite concentration utilized for all solutions was 30 $mgmL^{-1}$ while several cisplatin concentrations were used (0.08, 0.8, 8, 83, 833, 1700, 3300, 6700 and 10000 µM). Four gel replicates were prepared for each cisplatin concentration. Briefly, 0.1 mL Laponite-Cisplatin gels were prepared in small flasks and once they were gelled, 2 mL of PBS (pH=7.4 or 6.5) were deposited on the top. Afterwards, the flasks were incubated at 37 °C, under stirring

(Heidolph Unimax 1010), and, at determined times, 0.1 mL of PBS were removed from the flask, stored, and 0.1 mL of fresh PBS were added to the flask again. For the controls, 0.1 mL of each cisplatin solution were also deposited at the bottom of the flasks and 2 mL of PBS were deposited on the top. The controls were then subjected to the same conditions as the samples. The time points used for cisplatin analysis in solution were 30 min, 1h, 2h, 3h, 4h, 5h, 6h, 7h, 8h, 24h, 25h, and 26h in the first assay performed. For practical reasons, the following assays were performed with the following times: 30 min, 1h, 2h, 4h, 6h, 8h, 24h, and 26h.

To quantify the cisplatin present in the PBS removed from each flask at the aforementioned time points, a derivatization method was used which was adapted from literature (108). For the experiment, a standard calibration curve was prepared by diluting a 1 $mgmL^{-1}$ cisplatin stock solution to obtain six concentrations. These concentrations were 1, 5, 10, 20, 50, and 100 μgmL^{-1}, respectively. All dilutions were performed in PBS, and a blank was prepared as a control. For the standard curve, four replicates were prepared for each concentration, and for the samples obtained from the release assay, four replicates were prepared too. In each *Eppendorf* tube, 0.1 mL of the cisplatin solution, 0.1 mL of a previously prepared o-phenylenediamine solution (1.4 $mgmL^{-1}$, using DMF as solvent), and 0.2 mL of a previously prepared KH_2PO_4 buffer (0.1 M, pH=6.8) were added. Afterwards, all Eppendorf tubes were incubated at 90°C in a bath (Grant) for 30 min for the reaction between cisplatin and o-phenylenediamine to occur. Finished this period and after the subsequent cooling of the *Eppendorf* tubes, the volume of each *Eppendorf* tube (1.5 mL) was completed with DMF, and the absorbance was read at 703 nm in the UV-Vis spectrophotometer (Thermo Scientific, Genesys™ 180).

3.5. Cell culture

Two cell lines were used in these experiments: A2780 (ECACC 93112519), a human ovarian cancer cell line, and A2780cis (ECACC 93112517). A2780 is the parent cell line of A2780cis, a cisplatin-resistant cell line. Both cell lines were kept in culture in Roswell Park Memorial Institute (RPMI) medium (Gibco, Thermo Fisher) supplemented with 10% fetal bovine serum (FBS), 1x AA (antibiotic-antimycotic), and 1% L-glutamine (200 mM). A2780cis cells were treated with 1% cisplatin (100 µM in 0.9% NaCl) added to the culture medium every time there was a medium change which was performed 2-3 times a week (cisplatin was not added for trypsinization). All additives were purchased from Gibco (Thermo Fisher Scientific).

3.6. Cytotoxicity assays

3.6.1. Cells in direct contact with the hydrogels

Laponite and Laponite-cisplatin gels were prepared according to the previously described method and added to the bottom of the wells of 96-well plates, with 0.05 mL of gel added to each well. After the gels were prepared, cells (A2780 or A2780cis cells) were seeded on the top of the gels at a cell density of $1.5x10^4$ cells/cm^2 (Figure 10-A) and incubated for 24h and 48h, at 37 °C, and a 5% CO_2 humidified atmosphere (NUAIRE, 5800 incubator). For the experiments with pristine Laponite gels, three concentrations of Laponite were tested (25, 28, and 30 $mgmL^{-1}$). For the experiments with Laponite gels containing cisplatin, several cisplatin concentrations were used in the gels: 0.08, 0.83, 8.3, 83, 833, 1700, 3300, 6700, and 10000 µM. Depending on the experiments, negative control experiments involved cells only cultured with medium (RPMI, CONTROL 1) and cells cultured on the pristine Laponite gel (30 $mgmL^{-1}$, CONTROL 2). The positive control was 1% (v/v) Triton-X (Fisher) solution in RPMI. Additionally, cisplatin controls of all concentrations present in the Laponite-cisplatin gels were used.

After 24h or 48h in culture, the cells were exposed to a 10% resazurin solution and incubated for another 3h for metabolic activity assessment. Next, 0.1 mL of each well was transferred to a microplate, and resorufin fluorescence was measured (λex =530nm, λem= 590nm) using a microplate reader (Victor3 1420, Perkin Elmer).

A)

B)

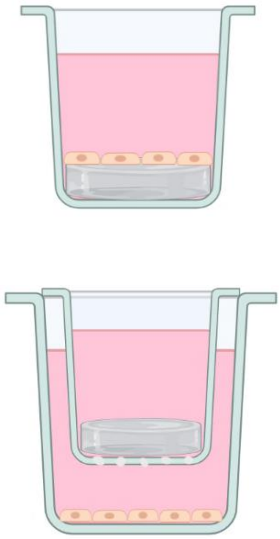

Figure 10 – Scheme representing the well of the 96-well plate (A) and the 24-well plate with the insert (B)

3.6.2. Cells in non-direct contact with the hydrogels

These assays evaluated the cytotoxic effect of cisplatin released from gels on 24-Well Millicell® Hanging Cell Culture Inserts, which were placed in the wells of a 24-Well Plate as presented in Figure 10-B.

Laponite and Laponite-cisplatin gels were prepared according to the previously described method, with 0.1 mL of the gel added to each insert. After the gels were prepared, the cells (A2780 or A2780cis) were seeded at a cell density of $1.5x10^4$ cells/cm^2 (Figure 10-B) at the bottom of the wells and incubated for 24h and 48h at 37 °C, and a humidified 5% CO_2 atmosphere. The concentration of Laponite in the gels was fixed at 30 $mgmL^{-1}$, and the cisplatin concentrations in the Laponite gels were 0.83, 8.3, 833, 1700, 3300, and 10000 µM. The negative controls used were cells only cultured with medium (RPMI, CONTROL 1) and cells cultured with medium but exposed to the Laponite gel without cisplatin (30 $mgmL^{-1}$, CONTROL 2). The positive control was 1% (v/v) Triton-X (Fisher) solution in RPMI. Additionally, cisplatin controls were used of all concentrations present in the Laponite-cisplatin gels.

After this period (24h or 48h), the cells were exposed to a 10% resazurin solution and incubated for another 3h for metabolic activity assessment. Next, 0.1 mL of each well was transferred to a microplate, and resorufin fluorescence was measured (λex = 530 nm, λem = 590 nm) using a microplate reader (Victor3 1420, Perkin Elmer).

After the resazurin reduction assays performed on non-adherent cells (section 3.6.2), the total protein content (BCA assay) was determined on both cell lines (it was assumed that the protein content was proportional to cell number). The bicinchoninic acid (BCA) assay, also known as the Smith assay, is a biochemical assay performed for colorimetric detection and quantitation of total protein in a sample. The method is based on the formation of a Cu^{2+} protein complex, with a bicinchoninic acid reagent, in an alkaline medium followed by the reduction of Cu^{2+} to Cu^{+} (biuret reaction) (109). What occurs is the chelation of two BCA molecules to a cuprous cation (Cu^{+}), resulting in a color change from green to a purple reaction product that displays a strong absorbance at 562 nm. The quantity of protein present in the sample will be proportional to the amount of Cu^{2+} that's reduced to Cu^{+} in an almost linear way within a certain range (20–2000 $µgmL^{-1}$). The BCA/Cu^{+} complex is affected by several factors, such as the number of peptide bonds and the presence of amino acids cystine, cysteine, tyrosine, and tryptophan side chains (110).

The assay was conducted using the Sigma-Aldrich “Bicinchoninic Acid Protein Assay Kit” following the standard protocol described on Annex 2, provided by Sigma-Aldrich.

4. Results and Discussion

4.1. Optimization of the Laponite gels forming method

In line with the primary goal of this thesis, focused on developing hydrogels based on Laponite for the localized delivery of the anticancer drug cisplatin, the initial phase of the work involved the investigation of clay's gelation conditions. Importantly, considering that the hydrogels are aimed at being applied in the biomedical field, Laponite XLG was selected for the present studies due to its high purity and certification confirming low levels of heavy metals and the absence of microbial contamination.

In fact, as described in the literature (50,51), the gelation process of Laponite can be very complex. This is because the Laponite disks possess charges that are not homogeneously distributed, that is, they are different in the faces and the edges, thus leading to a range of repulsive (face-to-face, edge–edge) and attractive (face to edge) electrostatic interactions which are very sensitive to changes in clay concentration, ionic force, type of ions present in the environment, pH, and also the presence of other molecules (46). All of this justifies the need to study the gelation process of Laponite under actual laboratory working conditions. As such, the gelation process was here investigated in terms of capacity/time needed for the material to achieve a self-standing behavior (hold its shape and stand independently without the need for a container or additional support structure) and also regarding optical transparency. The impact of the presence of cisplatin on the gelation behavior was also evaluated.

4.1.1. Formation of Laponite gels

To evaluate the gel-forming process of Laponite, a first set of experiments was made where several clay concentrations were tested and 3 different liquid media were used: distilled water, sodium chloride (0.15M NaCl) and PBS (pH=7.4). The experiments were also performed at two different temperatures: 21 °C (room temperature) and 37 °C (Table 3). The initial

dissolution of Laponite within the liquid media was always achieved by vigorous mixing using a vortex for 10s.

Table 3- Results obtained regarding gel formation/time needed to achieve gelation by varying several parameters: Laponite concentration, temperature, and liquid media (gelation was carried out at 21 and 37 °C after vigorous stirring for 10s).

[LAPONITE] ($mgmL^{-1}$)	H_2O**		0.15 M NaCl**		PBS (pH= 7.4)	
	Room temperature (21 °C)	37 °C	21 °C	37 °C	21 °C	37 °C
20	No	Yes–more than 24h	No	No	No	No
25	Yes - overnight *	Yes - 5h	No	No	No	No
28	Yes - overnight *	Yes - 5h	No	No	No	No
30	Yes - 5h	Yes - 4 to 5h	No	No	No	No

* Highly viscous solution; **pH was not adjusted

Overall, it was possible to observe that the solutions exposed to 37 °C were faster in gel formation than the ones at 21°C, with the same being observed in the solutions with higher concentrations of Laponite versus the lower-concentrated ones. Furthermore, it was also possible to conclude that only the Laponite solutions in distilled water suffered gelation as opposed to the ones prepared with 0.15 M NaCl and PBS.

Regarding the effect of Laponite concentration on gelation, at higher concentrations, there are more particles in close proximity, and this increased density can facilitate interparticle interactions (50). This may lead to a faster gelation process but will not necessarily imply a higher level of organization within the gel (aggregates of Laponite disks may form inside the gel with an impact in gel structure). A higher temperature may, by itself, accelerate the proximity among particles due to the associated increase in kinetic energy in the overall system, thus also contributing for a faster gelation. Concerning the presence of other ions in solution (such those present in the 0.15 M NaCl solution or in PBS), this may lead to an increase in the ionic force in the medium that will impair the establishment of the electrostatic forces among the Laponite disks.

Following these results, a second set of experiments was carried out where Laponite solutions were always prepared in distilled water and incubated at 37 °C. In this case, the variable tested was the pH of the water used in the Laponite solutions. Here, the Laponite concentration was fixed at 30 $mgmL^{-1}$ (3% wt) and the mixing process was maintained (Table 4).

Table 4- Results obtained regarding gel formation/time needed to achieve gelation by varying the pH value of the distilled water (Laponite concentration was fixed at 30 $mgmL^{-1}$; gelation was carried out at 37 ^{o}C after vigorous stirring for 10s).

WATER PH	TIME	OPTICAL TRANSPARENCY
3.0	Overnight *	YES
5.0	Overnight *	YES
7.0	1 h	YES
9.0	Overnight	YES
11.0	Overnight *	YES

* In the first 5 hours it was possible to observe the formation of 2 phases: gel and sol

With the variation of the pH values, it is possible to conclude that Laponite solutions prepared in distilled water with a pH of 7.0 suffered faster gelation than at any of the other pH values tested. Thus, there is an optimal pH range that leads to a faster gelation. In agreement, when comparing with the results obtained in the first set of experiments where simple distilled water was used (which may have a slight acidic pH due to atmospheric exposure), gelation took considerably less time (1h with distilled water adjusted to a pH of 7.0 *vs* 4/5h with simple distilled water). This result shows that gelation time is very sensitive to pH. Not only can the edges of Laponite disks be deprotonated at very high pH values, but also the charge on the faces of Laponite disks can become less negative at very low pH values, in both cases impairing gelation (52). Also, changes in the ionization state of water molecules may strongly alter the electrostatic forces at play in solution.

After assessing that distilled water with a pH value of 7.0 was the best option for faster gelation, different concentrations of Laponite were tested (from 28 to 40 $mgmL^{-1}$), being the results summarized in Table 5.

Table 5- Results obtained regarding gel formation/time needed to achieve gelation by varying Laponite concentration (distilled water with a pH adjusted to 7.0 was used; gelation was carried out at 37 °C after vigorous stirring for 10s)

[LAPONITE] ($mgmL^{-1}$)	TIME	OPTICAL TRANSPARENCY
28	1h15	YES
30	1h10	YES
32	25 min	YES
35	25 min	YES
40	10 min	YES

With the variation of the concentration, it is possible to observe that the solutions with higher concentrations suffered a faster gelation (Table 5). This also aligns with the prior results based on solutions prepared using simple distilled water (without pH adjustment to 7.0). In this third set of experiments, the Laponite concentration was further increased, clearly showing the favorable effect on gelation time due to a closer proximity among particles.

The effect of the mixing process on gelation time was also investigated. It was found that the vigorous agitation applied (10 seconds using a vortex) was also an important experimental parameter. A gentler stirring using a magnetic stirrer increased the gelation time by 1.5 times for gels prepared at a concentration of 30 $mgmL^{-1}$ of Laponite at 37 °C. A strong mixing is for sure important for Laponite dispersion in water, thus turning the gelation process more effective.

Interestingly, all hydrogels obtained showed transparency. In the context of hydrogels, transparency is often associated with a homogeneous structure, in the present case indicating that the Laponite network is well-dispersed and there are minimal impurities or phase separations. Transparency is also a property usually important if hydrogels are aimed at biomedical applications (111). Transparent hydrogels are often preferred because they allow for easy visual observation of cells, tissues, or any incorporated therapeutic agents.

With all these experiments conducted, an “optimized” method for the preparation of Laponite hydrogels could be established. From this point further, Laponite gels were all made at 37 °C, in distilled water previously adjusted to a pH of 7.0, and vigorously mixing Laponite with water using a vortex for 10s. Although the gelation process was faster for the higher Laponite concentration tested (10 min at 40 $mgmL^{-1}$), a concentration of 30 $mgmL^{-1}$ was anyway

established for future studies. This decision was based on: (a) the fact that a very high Laponite concentration could strongly affect the internal structure of the gels giving rise to a less ordered material (due to a faster gelation); (b) a slower gelation would be more advantageous in terms of handling the gels for use in future studies with cell cultures (1h at 30 $mgmL^{-1}$).

Furthermore, since these Laponite hydrogels are aimed at being used as drug delivery systems, the influence of the addition of PBS (pH=7.4) on gel integrity and optical properties was also evaluated at this point of the thesis (Figure 11). Two experiments were then conducted, one where PBS was added right after the Laponite solution was mixed with distilled water (control) and the other where PBS was added after the gelation of the solution. In the control, gelation did not occur although two liquid phases were apparently formed in the flask – a white one in the bottom and another one in the top that was transparent (the white color observed in the bottom solution could be due to some particle aggregation due to the presence of ions coming from PBS; these heavier particles would tend to deposition). On the other hand, when PBS was added after gelation, two transparent separate phases were created – the Laponite gel in the bottom with the PBS solution in the top. One could then conclude that the formulated gels could be used in the following drug delivery studies without special difficulties being expected.

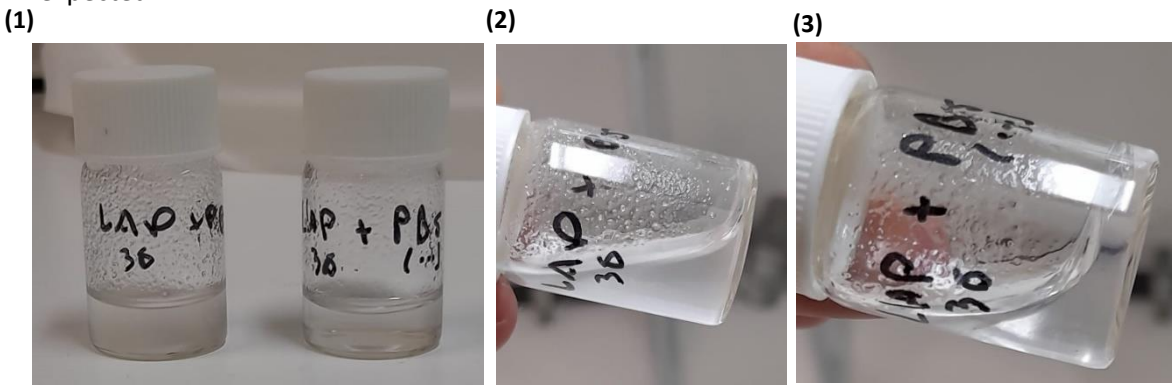

Figure 11 – Laponite gels in contact with PBS (pH=7.4). (1) Left: PBS added right after mixing ; Right: PBS added after gelation was complete; (2) PBS added right after mixing; (3) PBS added after gelation was complete.

4.1.2. Formation of Laponite-Cisplatin gels

To employ laponite hydrogels as cisplatin delivery systems, it is essential to examine how the incorporation of this drug influences the gelation process. As such, Laponite-Cisplatin hydrogels were formulated with varying concentrations of cisplatin (ranging from 0.5 to 3.0 $mgmL^{-1}$) by preparing a cisplatin solution at the desired concentration in distilled water adjusted to a pH of 7.0. Afterwards, Laponite was poured in the solution, to obtain a final concentration

of 30 $mgmL^{-1}$, and the solution was vigorously mixed with the vortex for 10s. Finally, the solution was incubated at 37 °C until gelation was completely achieved. The evaluation encompassed both gelation time and the transparency of the resulting gels (Table 6). It was possible to observe that gelation time was slightly shorter with the increase in cisplatin concentration. Furthermore, the two highest concentrations of cisplatin led to the gels' light yellow color and slight turbidity as opposed to the optical transparency displayed by the other concentrations (Figure 12). These observations suggest that cisplatin may contribute to strengthening cohesion forces within the gel.

Table 6- Results obtained regarding gel formation/time needed to achieve gelation by varying cisplatin concentration in the distilled water with a pH adjusted to 7.0 (Laponite concentration was fixed at 30 $mgmL^{-1}$; gelation was carried out at 37 °C after vigorous stirring for 10s).

Cisplatin concentration ($mgmL^{-1}$)	Time	OPTICAL TRANSPARENCY
0	1h30	YES
0.5	1h15	YES
1.0	1h15	YES
2.0	1h	Some turbidity – light yellow
3.0	1h	Some turbidity – light yellow

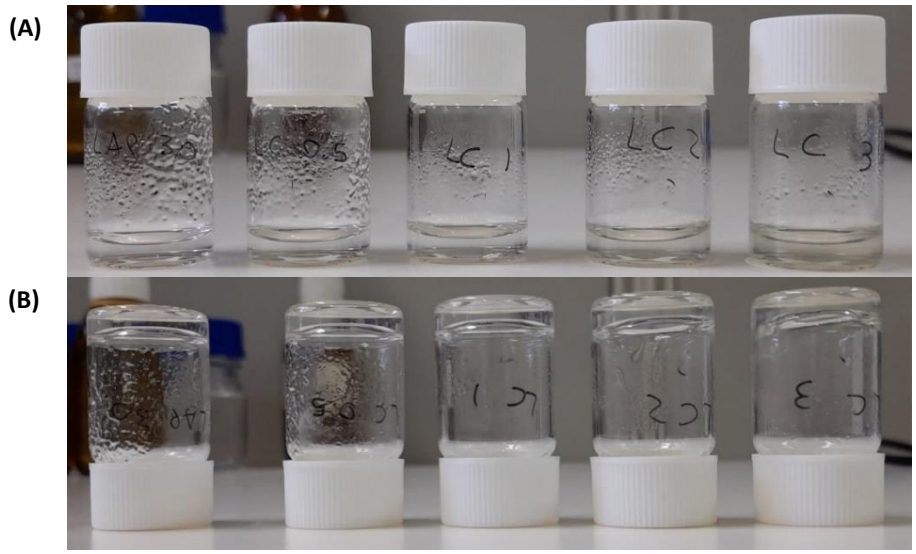

Figure 12 – (A) Gels obtained with the different concentrations of cisplatin displayed in Table 6 and respective characteristics (left to right in concentrations of cisplatin: 0, 0.5, 1, 2 and 3 $mgmL^{-1}$); (B) Display of gels' self-standing behavior, in the same order as previous picture.

4.2. Characterization of the gels

4.2.1. Water content

The water content of a hydrogel is a very important parameter that influences several key properties of hydrogels. For example, since hydrogels with high water content can mimic the natural environment of living tissues, they usually show higher biocompatibility. Hydrogels with appropriate water content can support cellular activities, including adhesion, proliferation, and migration (112). The water content also plays a significant role in determining the mechanical properties of hydrogels. The high-water content contributes to the soft and pliable nature of hydrogels, making them suitable for applications where flexibility and compliance with surrounding tissues are essential. Moreover, if hydrogels are aimed at being used as drug delivery platforms, as is the present case, water within hydrogels provides a medium for drug dissolution and release. The water content thus may affect the rate and mechanism of drug release, making it a critical factor in the process.

The water content was determined for both Laponite and Laponite-cisplatin gels and the average of 3 replicates is presented in Table 7. The results obtained allow to infer that the presence of cisplatin in the gels affected their hydration characteristics, probably by the establishment of bonds between the drug and the Laponite disks. Anyway, the water content still remained very high. It is possible to observe in Figure 13 the gels post-lyophilization and their major differences namely in color (cisplatin's presence causes the gel's yellow color) but it was also noted a difference in consistency of the materials.

Table 7– Water content of Laponite and Laponite-Cisplatin gels. Laponite concentration was 30 $mgmL^{-1}$ and cisplatin concentration, when present, was 3 $mgmL^{-1}$. Results are the average of 3 replicates.

	Laponite	Laponite-cisplatin
Water content (%)	96±2	85±4

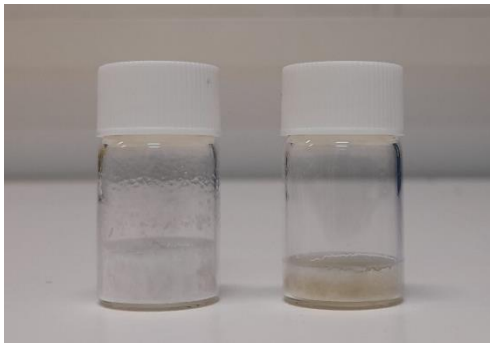

Figure 13 – Gels post-lyophilization (left: Laponite gel; right: the Laponite-cisplatin gel at 3 $mgmL^{-1}$)

4.2.2. Morphology and composition of the gels by SEM/EDS

The gels formulated were also characterized by scanning electron microscopy (SEM) and Energy-dispersive X-ray spectroscopy (EDS) by using dehydrated samples obtained by hydrogel lyophilization. Three different samples were analyzed: a) LAP30 (Laponite gel with a concentration of 30 $mgmL^{-1}$); b) LAP30/cisPt-1 (Laponite gel with a Laponite concentration of 30 $mgmL^{-1}$ and a cisplatin concentration of 1 $mgmL^{-1}$); c) LAP30/cisPt-3 (Laponite gel with a Laponite concentration of 30 $mgmL^{-1}$ and a cisplatin concentration of 3 $mgmL^{-1}$). The results are shown in Figure 14 (A-C), as well as in Table 8.

(A)

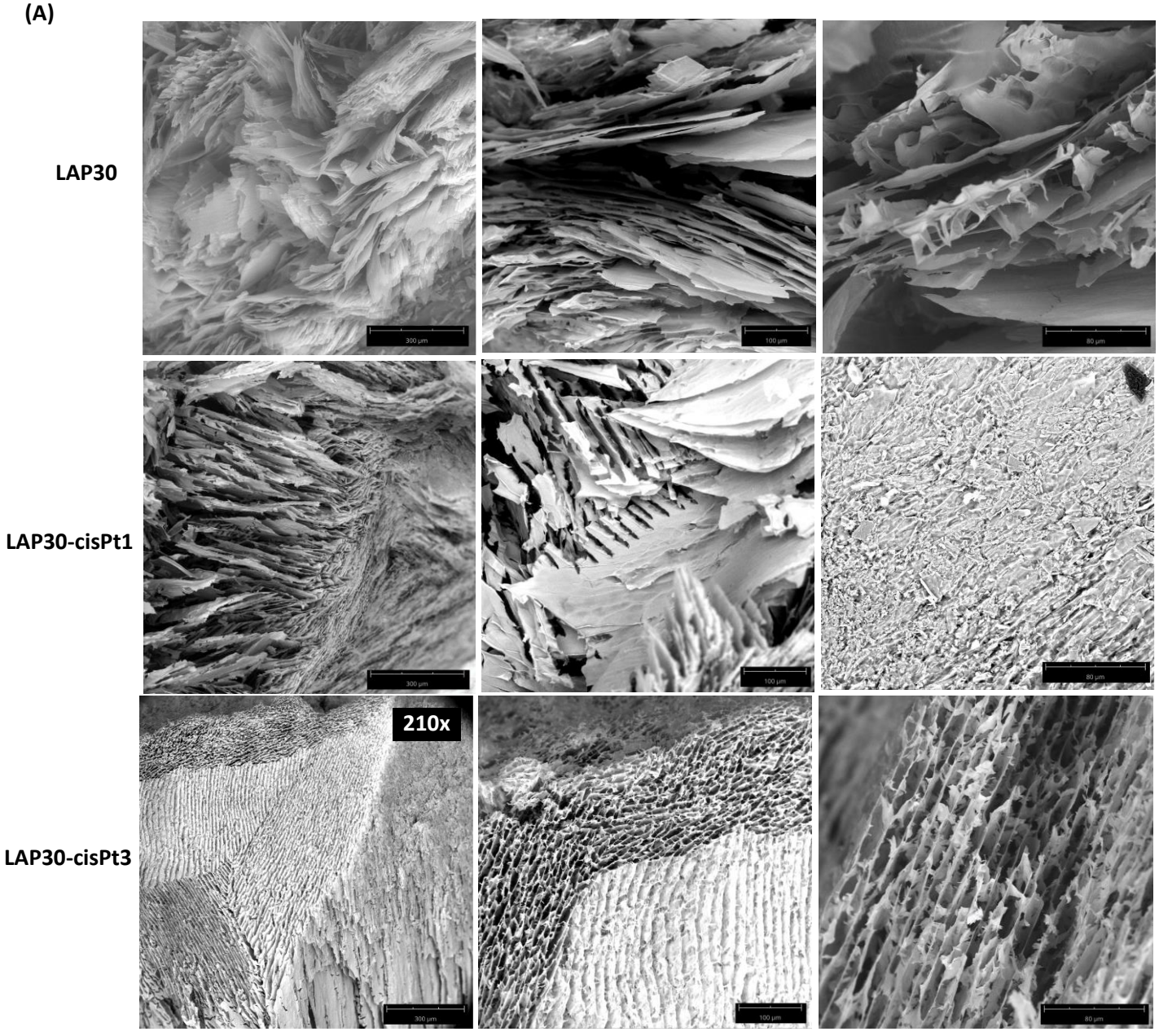

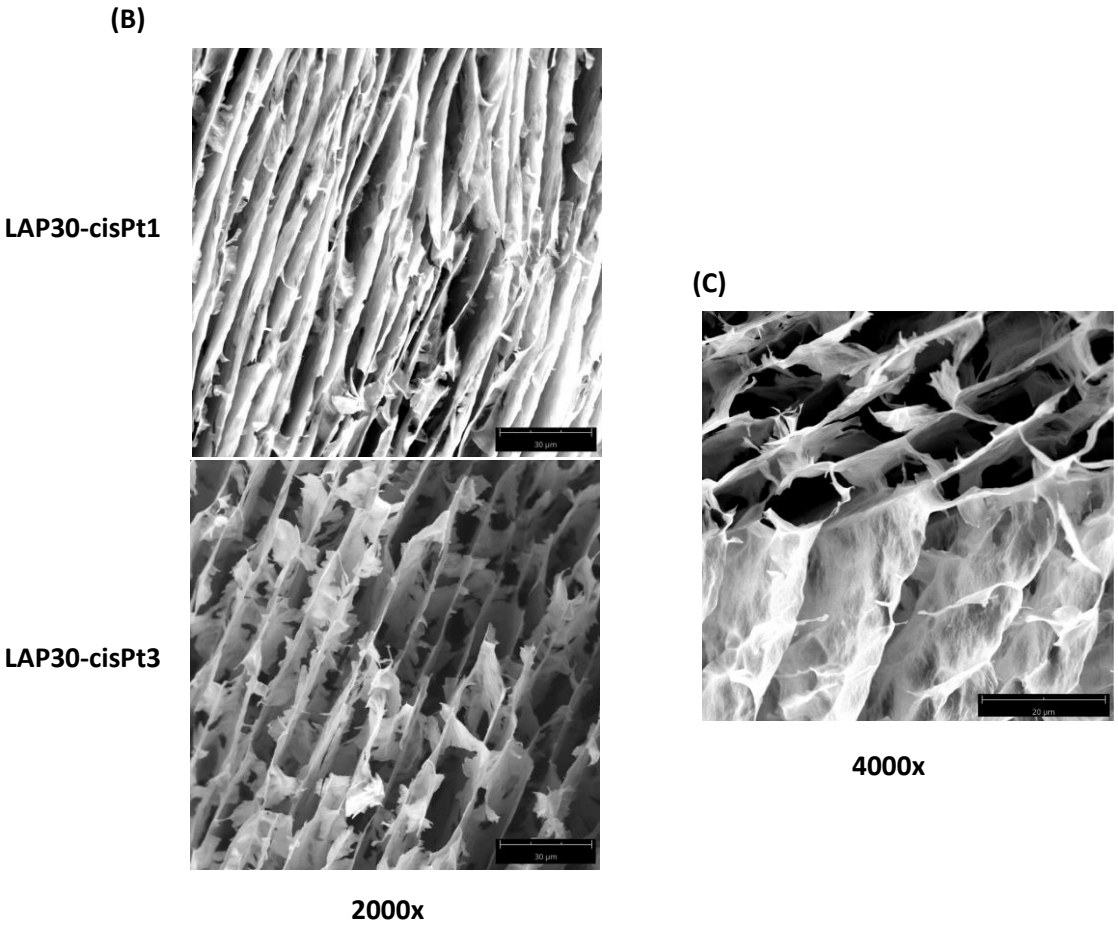

Figure 14 - SEM micrographs of Laponite gels and Laponite-Cisplatin gels. **(A)** SEM micrographs of LAP30, LAP30-cisPt1 and LAP30- cisPt3 samples at 250x, 500x and 1000x (except for LAP30-cisPt3, that was 210x instead of 250x). **(B)** SEM micrographs of LAP30-cisPt1 and LAP30-cisPt3 at 2000x. **(C)** SEM micrograph of LAP30-cisPt3 at 4000x.

Table 8- EDS analyses of Laponite gels (LAP30) and Laponite-Cisplatin gels (LAP30-cisPt1 and LAP30-cisPt3).

Element symbol	Atomic concentration (%)		
	LAP30	LAP30/CisPt-1	LAP30/CisPt-3
O	65.8	65.0	62.9
Si	19.2	16.1	14.5
Mg	13.0	11.6	10.3
Na	1.9	1.7	1.1
Pt	-	1.5	6.4
N	-	3.5	3.9
Cl	-	0.4	0.6

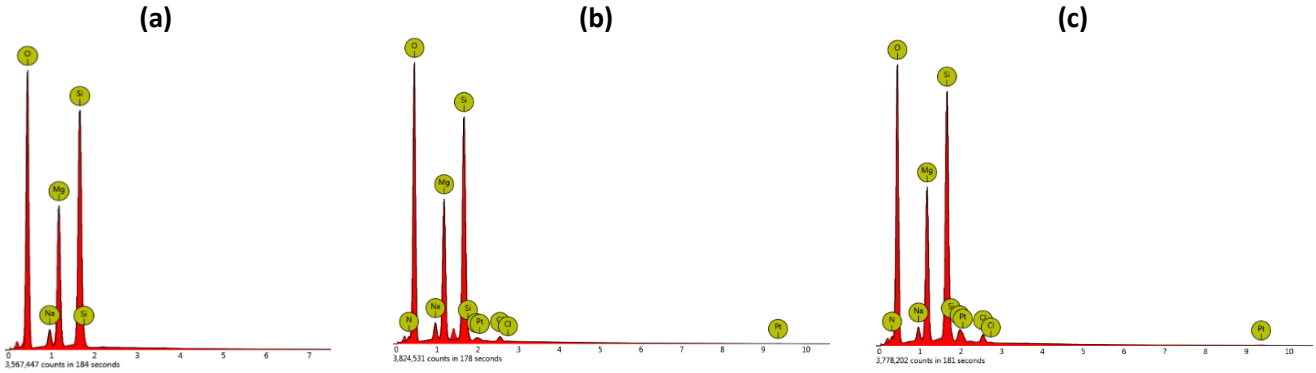

Figure 15- Graphs representing the EDS analysis of Laponite gels (LAP30-a) and Laponite-Cisplatin gels (LAP30-cisPt1-b and LAP30-cisPt3-c).

The SEM images of the lyophilized Laponite gels (Figure 14) reveal the presence of stacks of sheets in all hydrogels which show a high aspect ratio, that is, their length is significantly larger than their thickness. These sheets should be composed of Laponite disks with some degree of overlapping. At lower magnifications, the presence of areas in the material where these sheets appear with different orientations is noticeable. These areas essentially constitute grains within the material that resulted from the growth of independent "crystallization nuclei".

The effect of lyophilization (water removal) is particularly evident in the LAP30 samples. The correspondent micrographs clearly show collapsed structures that were not able to resist the forces involved in the dehydration process. Therefore, one is led to believe that the forces established within the material were relatively weak. This was not a surprise as, indeed, there are many works in the literature that describe the inclusion of polymers in Laponite gels in order to increase their mechanical resistance. For example, in the biomedical field, collagen-Laponite nanoclay hydrogels were prepared for tumor spheroid growth by Alamán-Díez et al (113). The presence of collagen in the hydrogels conceived by these researchers resulted in a more resistant material which was also possible to be observed in their SEM analysis.

Very interesting is the fact that the gels, after lyophilization, do not appear so collapsed in the presence of cisplatin, especially at higher concentrations of this drug (sample LAP30-cisPt-3). SEM images still exhibit stacks of Laponite sheets but, upon closer inspection, it is possible to perceive a more organized structure inside the material. It can be inferred that the presence of cisplatin at a higher concentration in the sample may lead to a higher level of cohesion between the Laponite sheets, that is, interactions among particles are stronger. Although the conducted

studies do not precisely reveal the type of interactions established between cisplatin and Laponite in the gel, it is possible that the drug adsorbs to the surface of Laponite disks or reacts with existing chemical groups on the surface, modulating the electrostatic interactions established within the material.

EDS is a technique that analyzes the characteristic X-rays emitted by a sample when it is bombarded with high-energy electrons. Each element has a unique X-ray signature, and by measuring the energy and intensity of the X-rays emitted, one can identify the elements present in the sample (114). In terms of EDS analysis (Table 8, Figure 15), it is possible to observe the presence of silicon, magnesium and sodium in all hydrogels and in proportions identical to those present in the empirical formula of Laponite. These are all elements characteristic of Laponite. The element lithium was not detected but the sensitivity of EDS for detecting lithium depends on several factors, including the concentration of lithium in the samples which is very low. Moreover, lithium has a relatively low atomic number, and its X-ray signals might overlap with those of lighter elements, making detection more challenging.

Regarding the EDS analysis of the hydrogels containing cisplatin (Table 8, Figure 15b and 15c), the elements platinum, nitrogen and chloride were also detected. This was expected since they are present in cisplatin's molecular structure. Moreover, the atomic concentration of platinum detected in the samples increased with cisplatin's concentration in the gels (1 to 3 $mgmL^{-1}$) in approximate proportion.

4.3. *In vitro* drug release studies

To evaluate the release of cisplatin by the gels over time, assays were conducted where the gels, with different cisplatin concentrations, were incubated with PBS at 37 °C with stirring. The cisplatin that was released was quantified through a chemical derivatization process and the cumulative release of the drug was calculated (the standard curves performed for both assays can be found in Annex 3). In these studies, it was decided to use a broader range of cisplatin concentrations in the gels (0.08, 0.8, 8, 83, 833, 1700, 3300, 6700, and 10000 µM) but the cisplatin quantification method proved not to be sensitive enough to be used with low concentrations. Therefore, results are only presented for cisplatin concentrations in the gels equal to or greater than 1700 µM.

Figure 16 shows the results obtained in the assays conducted in PBS at pH=7.4. In the upper graph, the experimental points correspondent to cisplatin release (cumulative release) are presented, whereas the graph below shows the logarithmic functions adjusted to those points. Based on these results, it is possible to conclude that all gels tested, independently of the cisplatin concentration, tend to release the drug in a sustained mode with the passage of time at physiological pH. The release is faster during the first 2h, and then it slows down. At the end of the assays, a plateau seems to be reached (above 24-26h). These observations are consistent with the idea that cisplatin is retained inside the gels in two different forms: a "less-bound" form that tends to be released more rapidly (likely cisplatin encapsulated in the gel pores), and a "more-bound" form (likely cisplatin that is adsorbed or chemically bound to the laponite disks and thus establishes stronger interactions with the gel). It should be noticed that, after 24-26h, only 70 to 85% of the drug initially incorporated in the gels was released. Of course, the drug release profile may also be impacted by diffusion phenomena as drug molecules that are immobilized in deeper regions of the gel need more time to reach their surface. However, since the drug release profiles do not seem to vary significantly with the concentration of cisplatin initially present in the gel, one may conclude that the diffusion of drug molecules within the gel should be relatively facilitated.

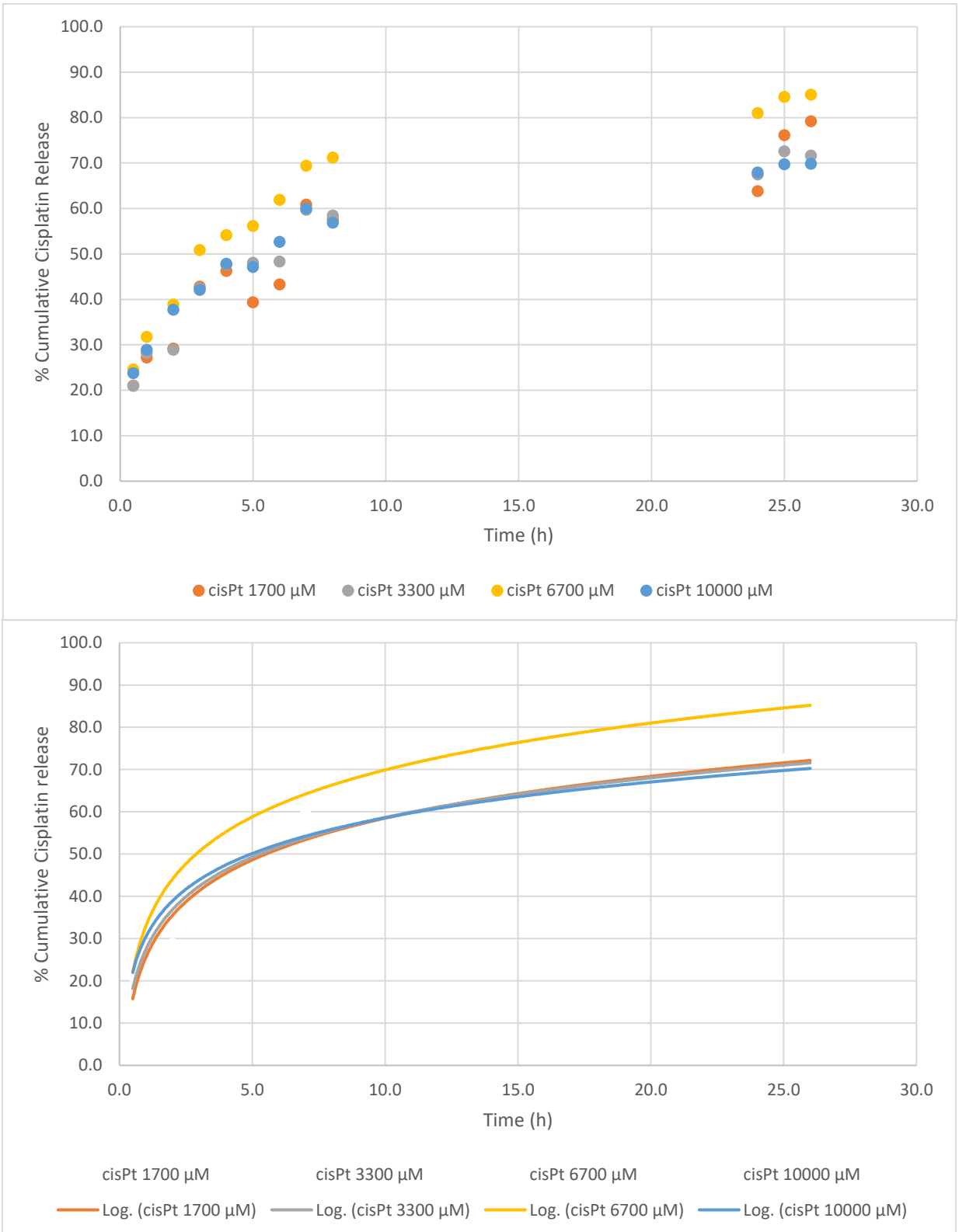

Figure 16 - *In vitro* release behavior of cisplatin in PBS (pH=7.4) for gels with the following cisplatin concentrations: 1700, 3300, 6700 and 10000 µM (results are presented as a percentage of the total cisplatin initially incorporated in the gels and are the average of 4 replicates). Graph on top: shows the experimental points (average); Graph below: a logarithmic function was adjusted to the experimental points.

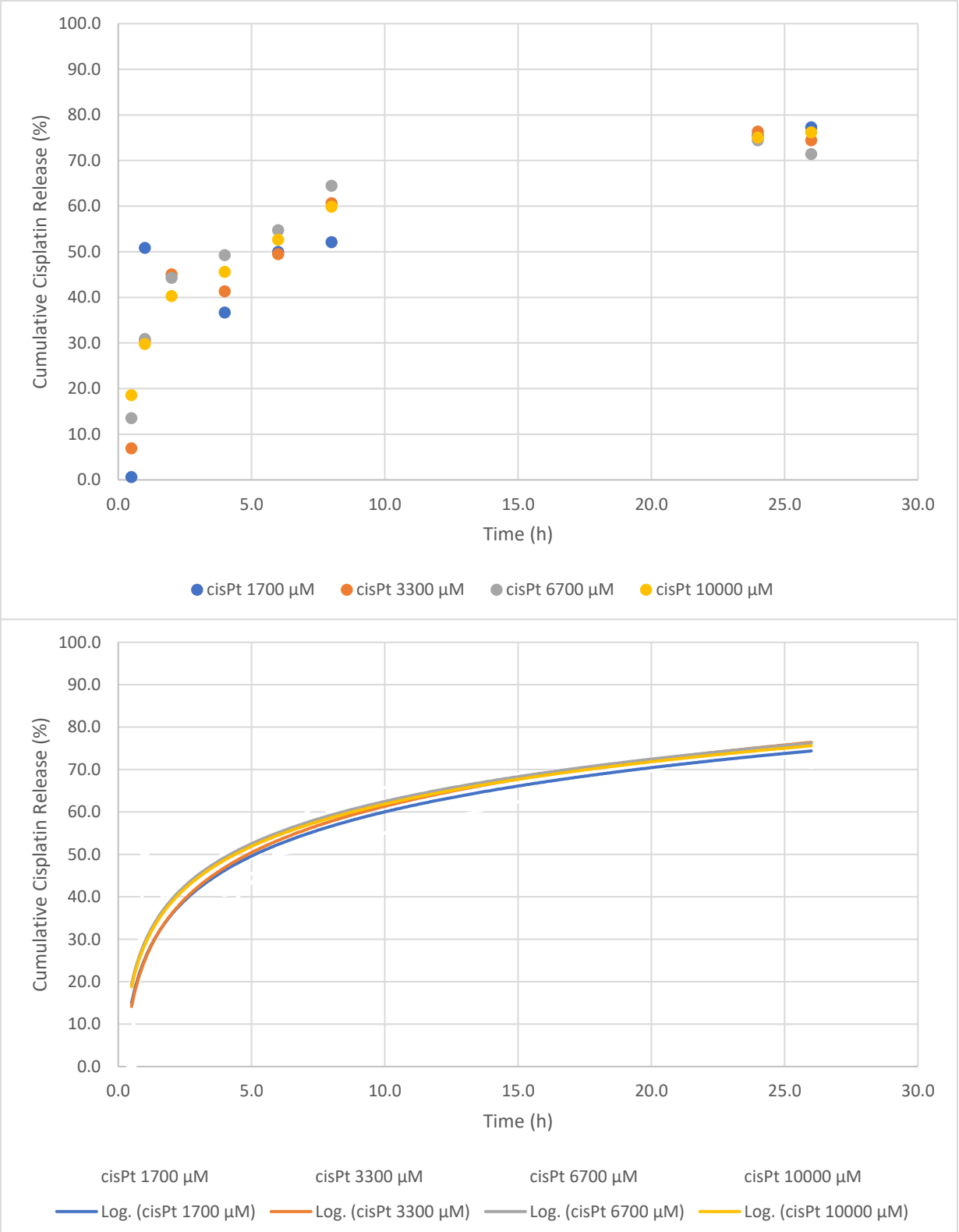

Figure 17 - *In vitro* release behavior of cisplatin in PBS (pH=6.5) for gels with the following cisplatin concentrations: 1700, 3300, 6700 and 10000 µM (results are presented as a percentage of the total cisplatin initially incorporated in the gels and are the average of 4 replicates). Graph on top: shows the experimental points (average); Graph below: a logarithmic function was adjusted to the experimental points.

The results obtained in the assay conducted with PBS at pH=6.5 are shown in Figure 17. Amongst the concentrations tested, there is not a notable difference in terms of the release pattern. Indeed, the drug release profiles are very similar to those obtained at a pH of 7.4, showing a sustained release behavior but absence of response to the change in the pH. This result can be explained by the fact that cisplatin, although being a polar molecule, is not charged at pHs near neutrality. As charges in Laponite disks strongly depend on pH and the capacity of Laponite to release drugs in response to the pH is mainly due to its capacity to hold exchangeable cations (CEC), since cisplatin is not charged, its release will not be importantly affected by proton concentration in solution (55). However, it must be said that many other anticancer drugs incorporated in drug delivery systems based on Laponite, such as DOX, show drug release profiles sensitive to different environmental pH values (115). Several studies showed that when this drug is released in PBS with pH=5.0, the release rate is notably more accelerated, and the amount of drug released in the medium is higher (116). Also, when using other delivery platforms, there is record of cisplatin release profiles at pH=7.4 and pH=5.0 that show no noteworthy difference between them in terms of amount of drug released or release rate (117).

4.4. Cytotoxicity assays

As mentioned earlier, the main objective of this work was the development of Laponite-based hydrogels for the localized delivery of cisplatin. Therefore, various exploratory assays were conducted using cultured cells to assess the cytotoxicity of the Laponite-Cisplatin hydrogels. These studies used A2780 and A2780cis cells and cytotoxicity was determined using the resazurin reduction assay.

The A2780 cell line utilized derives from human ovarian carcinoma in an untreated patient (118) and it is parent-line to the A2780cis cell line, with this one being obtained by chronic exposure of the parent cisplatin-sensitive A2780 cell line to increasing concentrations of cisplatin (119). Cisplatin and other platinum-compounds have been used to treat ovarian cancer since their inception in 1978 and one of the main limitations to overcome has been the resistance mechanisms the cells create to these compounds, which is an important focus of the research regarding their pharmacology (120).

Resazurin (also known as Alamar Blue) is a phenoxazine dye with a blue, non-fluorescent appearance in its oxidized form (resazurin). Resazurin can be reduced to a pink, highly fluorescent compound called resorufin as a result of active cells' metabolic activity (121), induced by reductive species such as NADH, NADPH and FADH (122). This conversion from

resazurin to resorufin at pH=7.4-7.5 is linked with a shift in the absorbance spectrum (λ_{max}=600 nm for resazurin and λ_{max}=570 nm for resorufin). Moreover, when resorufin is excited at wavelengths matching its peak absorbance (λ_{max}=590 nm), it exhibits fluorescence that can be detected. In contrast, resazurin has weak fluorescence properties in the visible spectrum (121). The dependence of this assay on cellular metabolism makes it useful for measuring cell proliferation, cytotoxicity, and general health of a cell culture (123). Resazurin reduction assays have been used for over 50 years to study cells' metabolic activity in several systems, be it biological or environmental, and they present several advantages in comparison with other assays. Factors such as low cost, low cytotoxicity, high sensitivity, speed, and ability to be combined with other assays for confirmation of the results make this method ideal for a simple and efficient evaluation of cell viability (124–126). However, there are also disadvantages to this assay, such as the possible interference of chemical interactions between the compounds being tested and the resazurin (124).

The biological assays were conducted using two different approaches: a) direct contact with the gel (with the cells seeded on top of the gels); and b) non-direct contact with the gel (with the help of inserts, where the gel is in the insert and the cells are seeded in the bottom of the well). Cytotoxicity was evaluated in both these cases by assessing the metabolic activity of cells and, in non-direct contact experiments, it was also studied through total protein quantification in culture using the bicinchoninic acid protein assay. The use of these two approaches allowed to study the effect of cisplatin release on cell viability, but also on cell adhesion/proliferation on pristine Laponite gels and cisplatin-loaded gels.

4.4.1. Cells cultured on the surface of pristine Laponite hydrogels

In a first set of experiments, the objective was to study the possibility of culturing cells in the surface of pristine Laponite gels. Here, cell viability was evaluated using Laponite gels at different concentrations (25, 28 and 30 $mgmL^{-1}$) and using both A2780 and A2780cis cell lines. The results are shown in Figures 18 and 19. All graphs represent the average of 3 assays. In each figure, the graphs in the top show cell viability as a percentage of the control (cells adherent to the cell culture dish) and the graphs below show cell viability as fluorescence intensity.

Importantly, cells were able to adhere and grow in direct contact with the surface of Laponite gels. For both cell lines studied, it is possible to observe that, in general terms, there is an increase in cell viability between, not only both times studied (24h and 48h), but also the different Laponite concentrations tested. For the A2780 cell line, it can be inferred that the

Laponite gels promoted the cells' metabolic activity, notably with the increase in Laponite concentration and with the passage of time. For the A2780cis cell line, there is also an increase of cell viability with time, but it is not possible to observe the same trend in relation to the Laponite concentrations (in this case, cell growth was higher between 24 and 48h in culture in the gels having a lower Laponite concentration). Indeed, it is described in the literature (61–63) that Laponite can degrade and release ions that may contribute to a lower rate of cellular proliferation. At this point, it should be noticed that reproducibility was an important issue when working with these hydrogels and cells cultured on their surfaces due to higher difficulties in the manipulation of these systems in the laboratory.

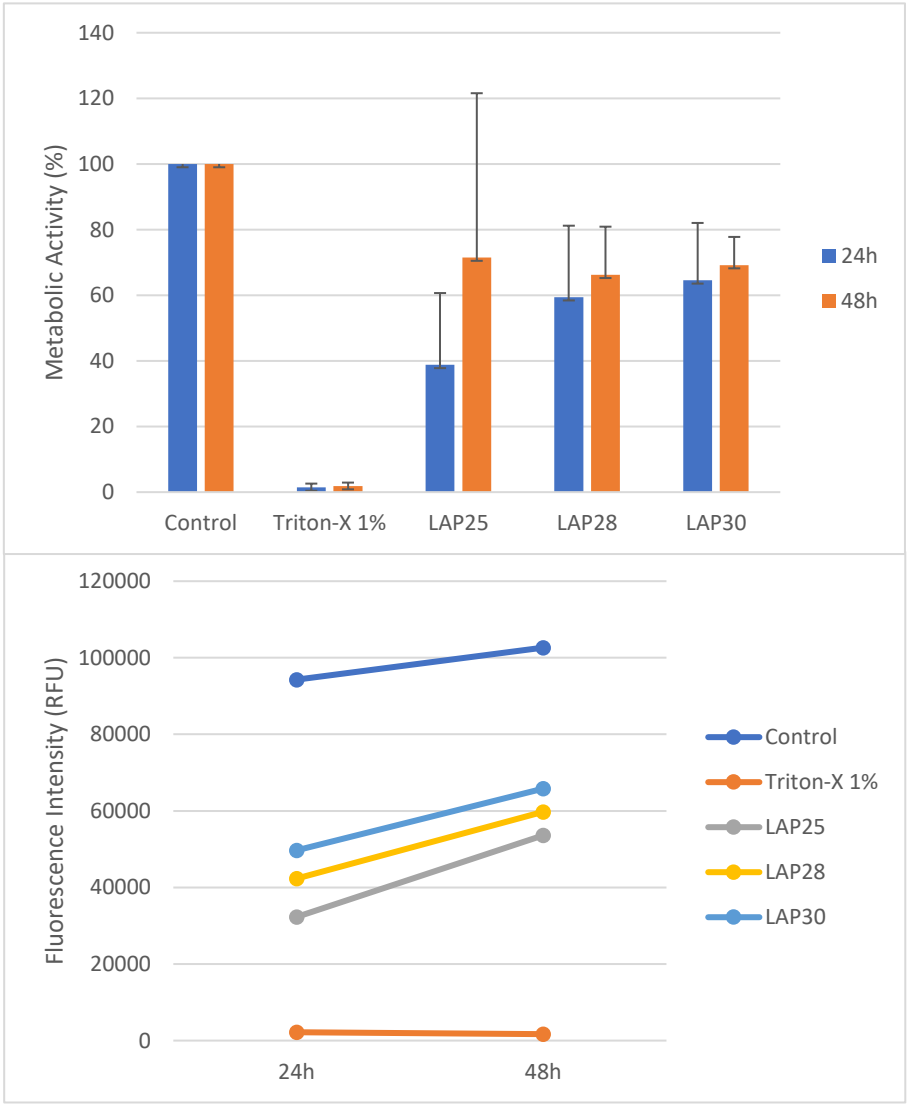

Figure 18 - Cell viability of A2780 cells cultured on the surface of pristine Laponite gels of different concentrations (LAP25=25 $mgmL^{-1}$; LAP28=28 $mgmL^{-1}$ and LAP30=30 $mgmL^{-1}$) for 24h and 48h (results are an average of the 3 assays performed). Top graph: cell viability as a percentage of the control (cells adherent to the cell culture dish). Bottom graph: cell viability as fluorescence intensity.

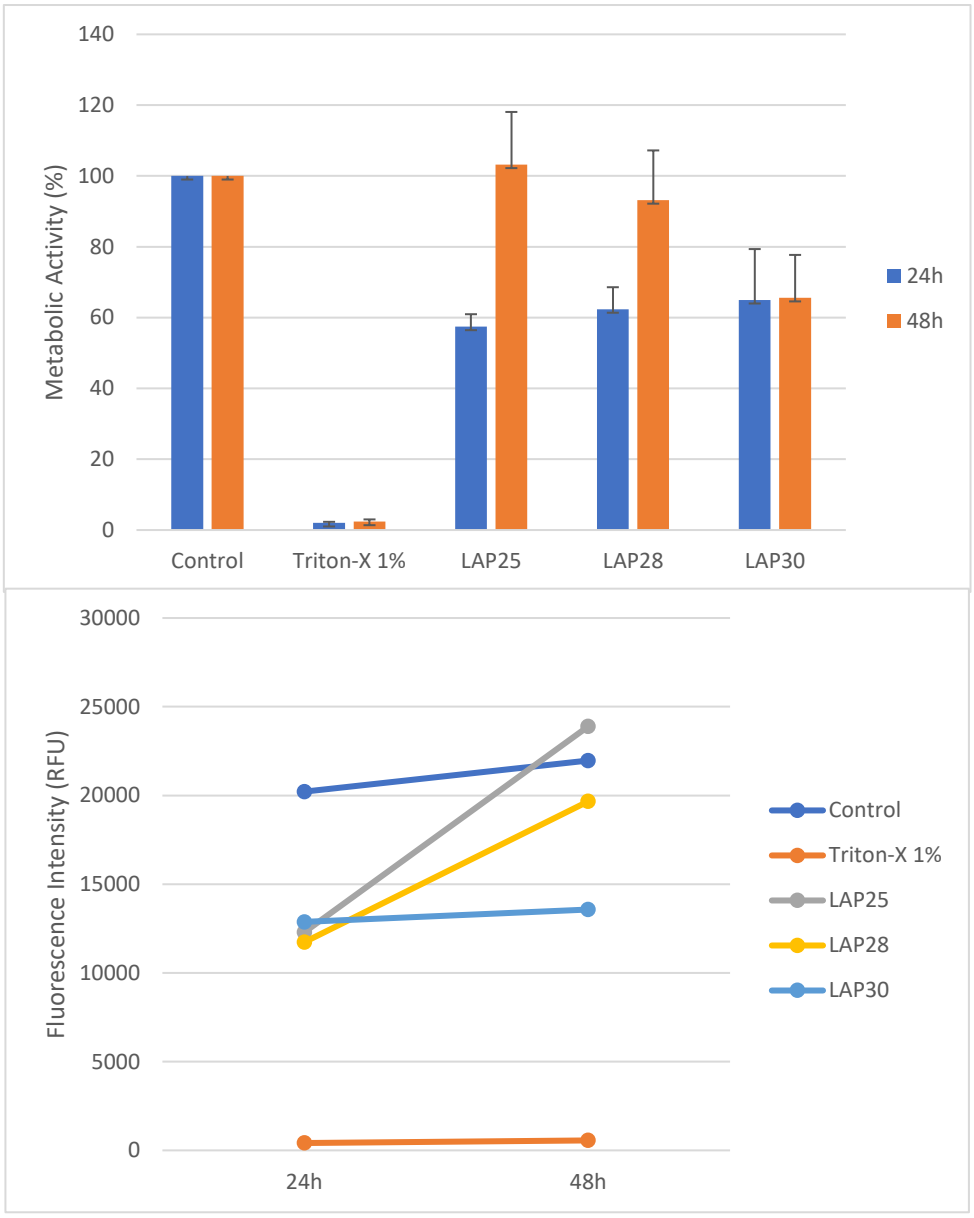

Figure 19 - Cell viability of A2780cis cells cultured on the surface of pristine Laponite gels of different concentrations (LAP25=25 $mgmL^{-1}$; LAP28=28 $mgmL^{-1}$; and LAP30=30 $mgmL^{-1}$) for 24h and 48h (results are an average of the 3 assays performed). Top graph: cell viability as a percentage of the control (cells adherent to the cell culture dish). Bottom graph: cell viability as fluorescence intensity.

4.4.2. Cells cultured on the surface of Laponite-Cisplatin hydrogels

The cytotoxicity of Laponite-cisplatin gels, with different cisplatin concentrations, was evaluated for both cell lines when cultured in direct contact with the gel surface after 24 and 48h. The results of representative experiments are summarized in Figures 20, 21, and 22.

Figure 20 shows the results obtained with the A2780 cell line when using gels containing cisplatin at high concentrations (in the range 833-10000 µM). Graph A shows cell viability as a percentage of the control (CONTROL 1: cells adherent to the cell culture dish and cultured only in the presence of cell culture medium) and graph B shows cell viability as fluorescence intensity. Graph C is the same as graph A but cell viability is presented as a percentage of the "real" control (CONTROL 2: cells adherent to the surface of the pristine Laponite hydrogel but not exposed to the drug) for the experiments where gels were present. Overall, one can observe that cells grew from 24 to 48h in both CONTROL 1 and CONTROL 2 experiments, while in the presence of cisplatin their metabolic activity always decreased in that period of time. As expected, cytotoxicity was dependent on cisplatin concentration, increasing for higher drug concentrations. When comparing the experiments where cisplatin was released by the Laponite gels to those where cells were directly exposed to free cisplatin solutions, one can conclude that the cytotoxic effects were higher in the last case. This is consonant with a controlled release of cisplatin from the gels.

Since cytotoxicity was very high in the previous experiments, one has decided to do similar experiments with lower cisplatin concentrations (in the range 0.083-83 µM, according to the literature (127)), although evaluating cytotoxicity only for 24h. The objective was to be able to determine the IC_{50} for cisplatin when loaded on Laponite hydrogels to have a quantitative idea of the efficacy of the systems. These results are shown in Figure 21. Graph A shows cell viability as a percentage of CONTROL 1 and graph B shows cell viability as a percentage of CONTROL 2 for the experiments where gels were present. After determination of the IC_{50} values using CONTROL 1 as 100% of cell viability, it was possible to see that the IC_{50} for cisplatin in A2780 cells was 1.6 µM when cells were cultured directly on gel surface, whereas it was higher (5.1 µM) when free cisplatin was used. However, since cell adhesion on the gels surface seems to be lower when compared to that on the substrate of the cell culture dish, CONTROL 2 corresponding to 100% cell viability is a better (more real) option to calculate the IC_{50}. In this case, the IC_{50} value for cisplatin is 21.4 µM. One can thus conclude that the use of gels to deliver cisplatin seems not to

emphasize cisplatin toxicity. Likely, A2780 cells are not so much affected at the same cisplatin concentrations because of the beneficial effect of Laponite in cell proliferation.

Figure 22 shows the correspondent results for A2780cis cells. Again, graph A shows cell viability as a percentage of CONTROL 1 and graph B shows cell viability as a percentage of CONTROL 2 for the experiments where gels were present. The IC_{50} values were >83 μM for free cisplatin (CONTROL 1 was used as 100% cell viability) as well as for cisplatin released from the gels (CONTROL 2 was used as 100% cell viability). These results led to two important conclusions. First, it was confirmed that A2780cis cells were resistant to cisplatin (one can see that the IC_{50} values are much higher than when using A2780 cells which is associated with cell resistance to the drug). Second, it was not possible to distinguish cytotoxicity between the two conditions.

It is important to note that the IC_{50} values found in the literature for cisplatin are indeed different from those determined in the present work, likely due to a myriad of factors such as the type of assays being performed, the methodology and time of exposure, all of which influence calculation of IC_{50}. Anyway, IC_{50} values of 1.1 μM and >50 μM were found using A2780 and A2780cis cells by Gouveia et al. (127), respectively, but the values determined are for 72h of exposure, which is not comparable to the present work.

In summary, Laponite hydrogels demonstrated effectiveness as a delivery system for both A2780 and A2780cis cells in cancer treatment. They exhibited cytocompatibility, the capacity to release cisplatin, and the drug exerted a cytotoxic effect on the cells.

A

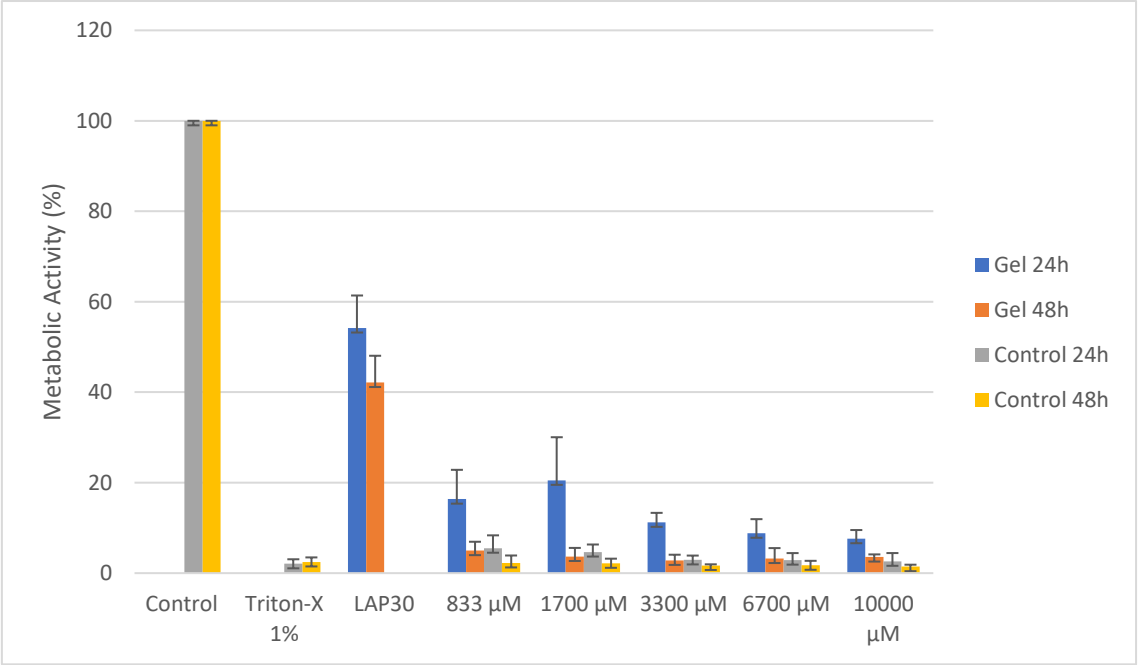
120
100
80
60
40
20
0
Metabolic Activity (%)
Control
Triton-X 1%
LAP30
833 µM
1700 µM
3300 µM
6700 µM
10000 µM
Gel 24h
Gel 48h
Control 24h
Control 48h

B

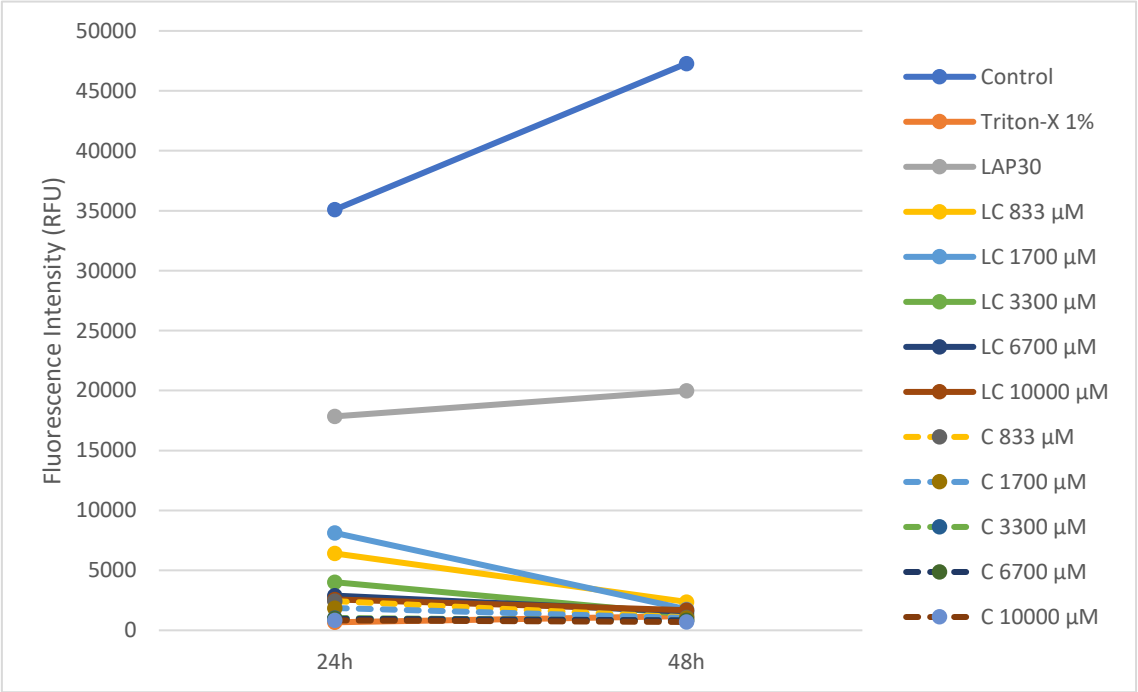
50000
45000
40000
35000
30000
25000
20000
15000
10000
5000
0
Fluorescence Intensity (RFU)
24h
48h
Control
Triton-X 1%
LAP30
LC 833 µM
LC 1700 µM
LC 3300 µM
LC 6700 µM
LC 10000 µM
C 833 µM
C 1700 µM
C 3300 µM
C 6700 µM
C 10000 µM

C

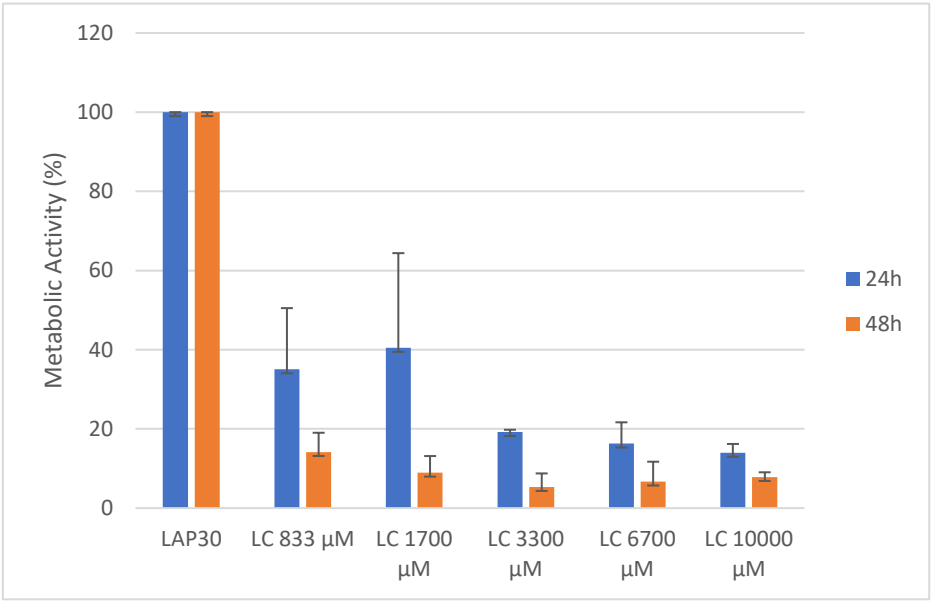

Figure 20 – Cytotoxicity of Laponite-Cisplatin gels at high cisplatin concentrations using A2780 cells (representative experiment from 3 assays). (A) Cell viability as a percentage of CONTROL 1 (cells adherent to the cell culture dish and cultured only in the presence of cell culture medium); (B) Cell viability as fluorescence intensity; and (C) Cell viability as a percentage of CONTROL 2 (cells adherent to the surface of the pristine Laponite hydrogel) for experiments involving gels. LAP30: Laponite gel at 30 $mgmL^{-1}$; LC – Laponite-Cisplatin gel with Laponite at 30 $mgmL^{-1}$ and the displayed cisplatin concentrations: 833, 1700, 3300, 6700 and 10000 µM. C - Cisplatin controls with the same concentrations used in the gels.

A

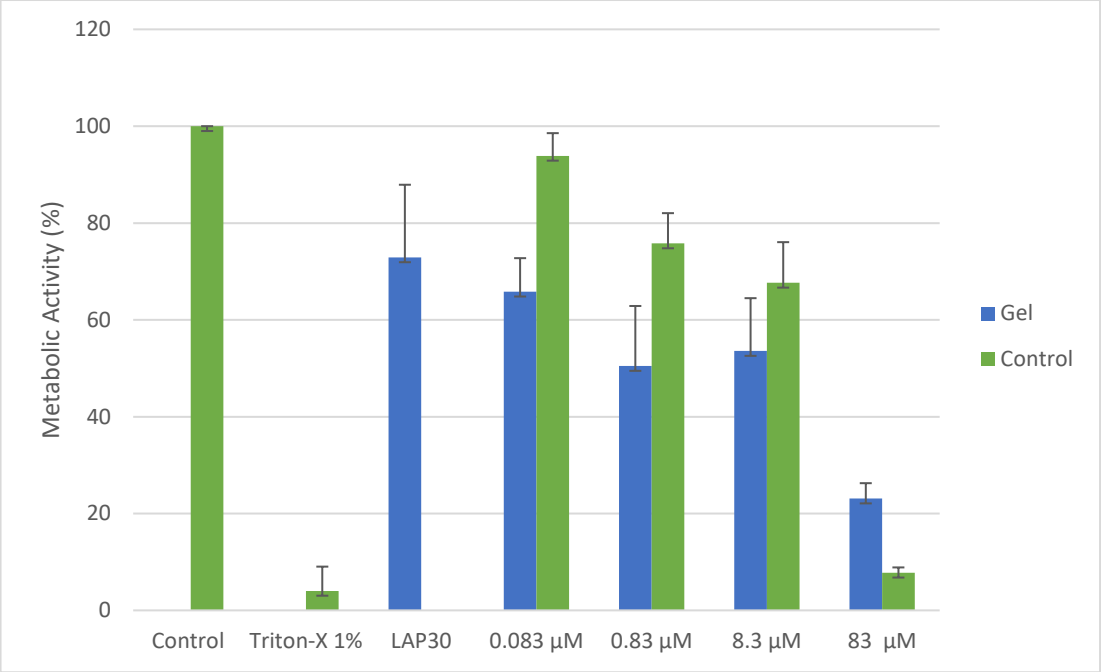

B

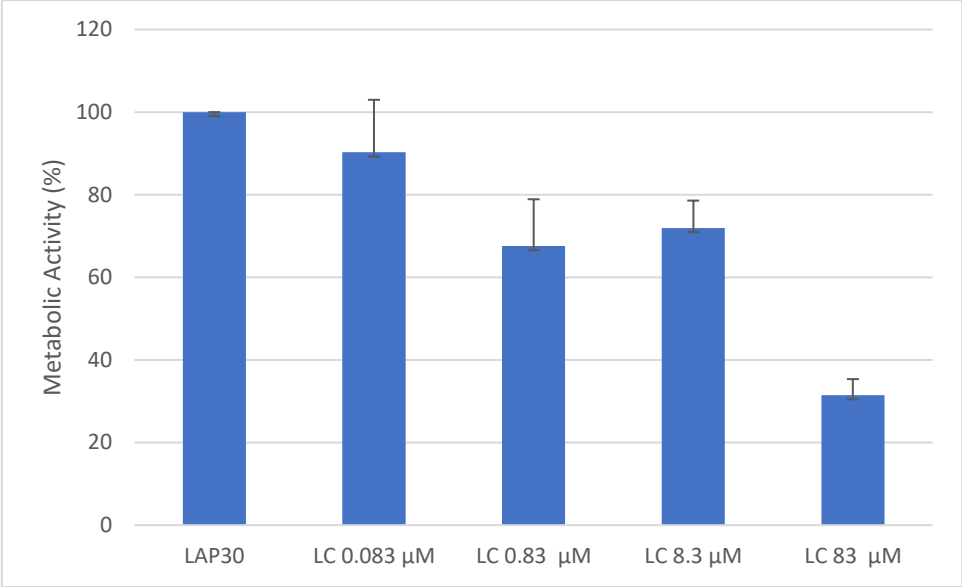

Figure 21 – Cytotoxicity of Laponite-Cisplatin gels at low cisplatin concentrations using A2780 cells after 24 hours (representative experiment from 3 assays). (A) Cell viability as a percentage of CONTROL 1 (cells adherent to the cell culture dish and cultured only in the presence of cell culture medium); and (B) Cell viability as a percentage of CONTROL 2 (cells adherent to the surface of the pristine Laponite hydrogel) for experiments involving gels. LAP30: Laponite gel at 30 $mgmL^{-1}$; LC – Laponite-Cisplatin gel with Laponite at 30 $mgmL^{-1}$ and the displayed cisplatin concentrations: 0.083, 0.83, 8.3 and 83 µM. Cisplatin controls were used with the same concentrations used in the gels.

A

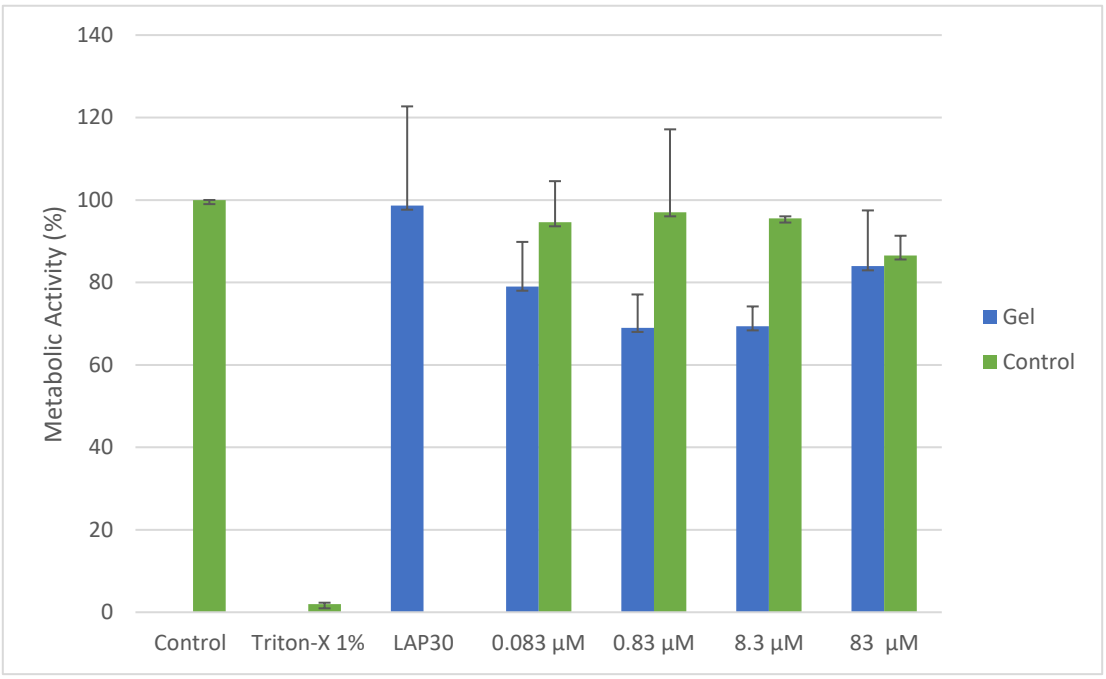

B

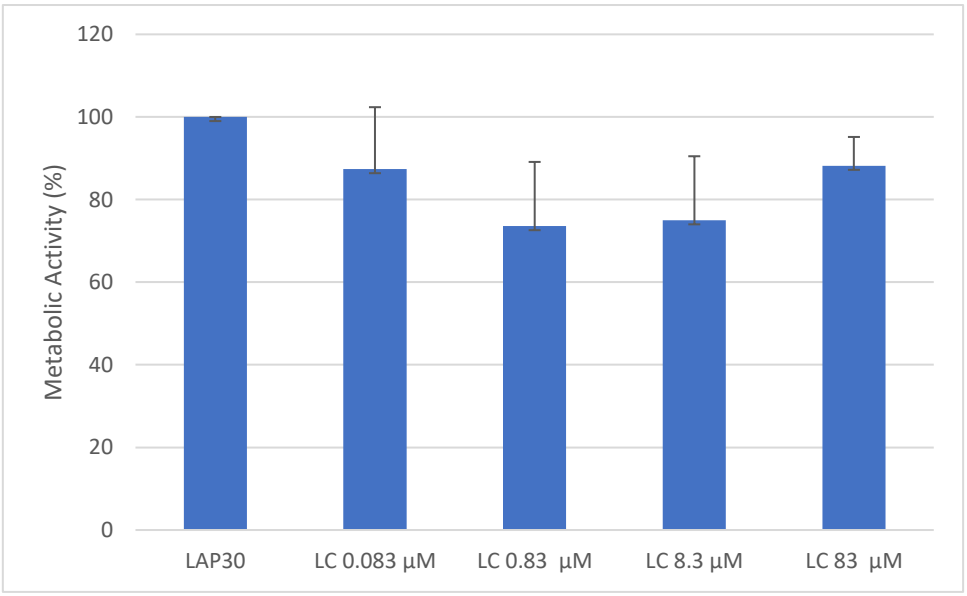

Figure 22 – Cytotoxicity of Laponite-Cisplatin gels at low cisplatin concentrations using A2780cis cells after 24 hours (representative experiment from 3 assays). (A) Cell viability as a percentage of CONTROL 1 (cells adherent to the cell culture dish and cultured only in the presence of cell culture medium); and (B) Cell viability as a percentage of CONTROL 2 (cells adherent to the surface of the pristine Laponite hydrogel) for experiments involving gels. LAP30: Laponite gel at 30 $mgmL^{-1}$; LC – Laponite-Cisplatin gel with Laponite at 30 $mgmL^{-1}$ and the displayed cisplatin concentrations: 0.083, 0.83, 8.3 and 83 µM. Cisplatin controls were used with the same concentrations used in the gels.

4.4.3. Cells cultured without direct contact with Laponite-Cisplatin hydrogels

As previously described, assays were also performed where the gels were placed inside inserts which were then placed on the cell culture wells. In this case, the cells grew on the plastic surface of the cell culture dishes and did not have direct contact with the gels. The results of representative experiments are summarized in Figures 23, 24, and 25.

A

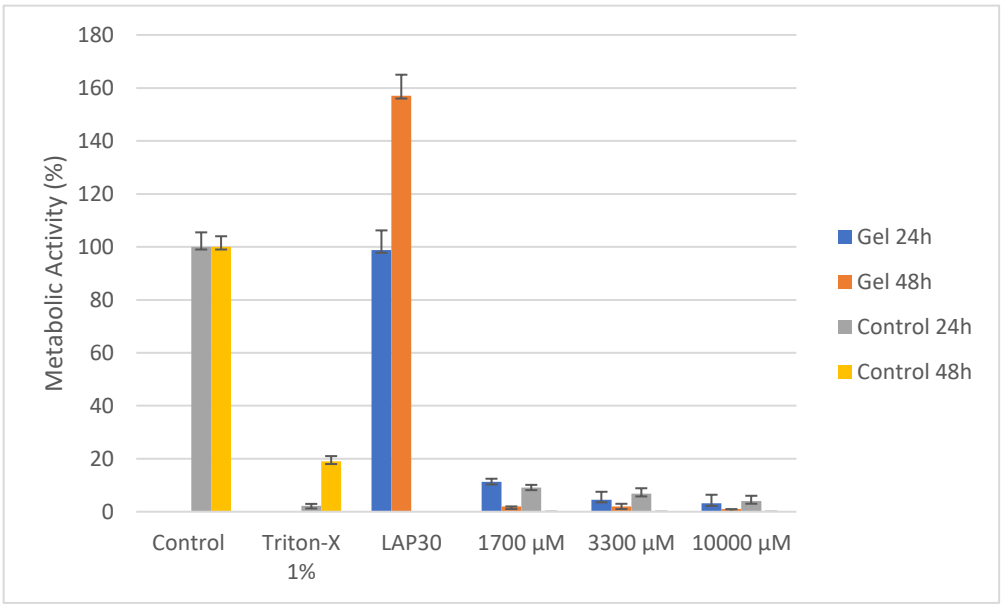

B

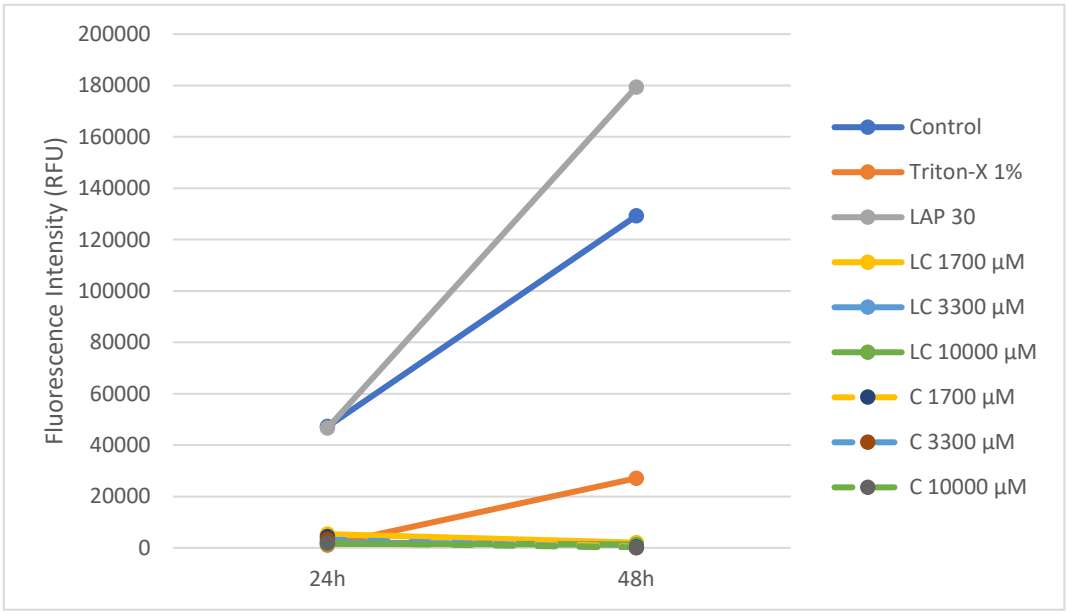

C

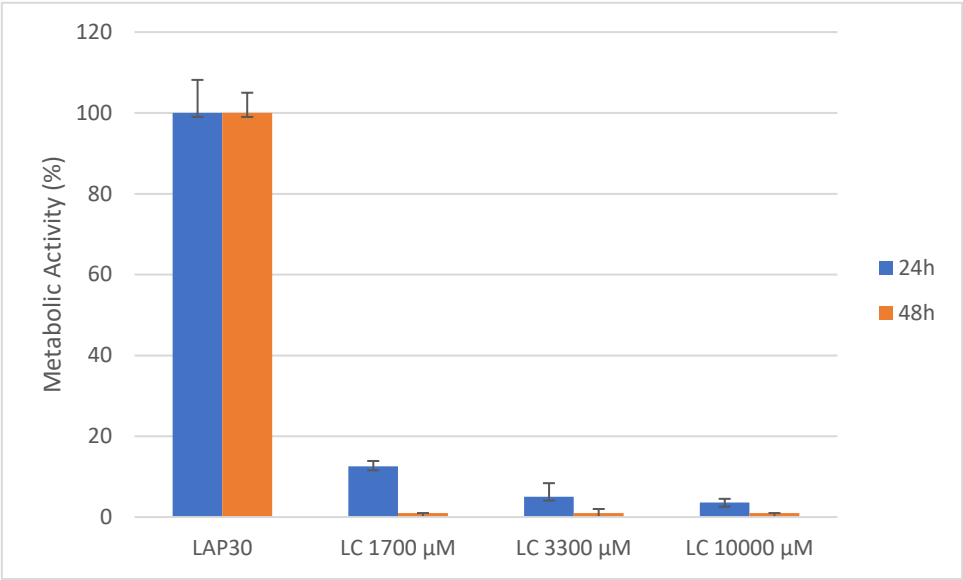

Figure 23 – Cytotoxicity of Laponite-Cisplatin gels (placed in inserts) at high cisplatin concentrations using A2780 cells (representative experiment from 3 assays). (A) Cell viability as a percentage of CONTROL 1 (cells adherent to the cell culture dish and cultured only in the presence of cell culture medium); (B) Cell viability as fluorescence intensity; and (C) Cell viability as a percentage of CONTROL 2 (experiments with gel in the insert but without cisplatin in the gel) for experiments involving gels. LAP30: Laponite gel at 30 $mgmL^{-1}$; LC – Laponite-Cisplatin gel with Laponite at 30 $mgmL^{-1}$ and the displayed cisplatin concentrations: 1700, 3300 and 10000 µM. C - Cisplatin controls with the same concentrations used in the gels.

Figure 23 shows the results obtained with the A2780 cell line when using gels containing cisplatin at high concentrations (in the range 1700-10000 µM). Graph A shows cell viability as a percentage of the control (CONTROL 1: cells adherent to the cell culture dish and cultured only in the presence of cell culture medium, without gel in the insert) and graph B shows cell viability as fluorescence intensity. Graph C is the same as graph A, but cell viability is presented as a percentage of the "real" control (CONTROL 2: experiments with gel in the insert but without cisplatin in the gel). In general, one can observe that cells grew from 24 to 48h in CONTROL 1, as well as in CONTROL 2. As such, it can be concluded that the presence of the gel did not have an impact on cell viability (by the contrary, cells grew a little bit more in CONTROL 2 as evidenced by the fluorescence intensity values after 48h). In the presence of cisplatin, the metabolic activity of cells was very low after 24h and continued to decrease until 48h, a fact attributed to cisplatin's high concentrations. Yet, it still could be observed that cytotoxicity was dependent on

cisplatin concentration, increasing even more for higher drug concentrations. When comparing the experiments where cisplatin was released by the Laponite gels in the inserts to those where cells were directly exposed to free cisplatin solutions (at equivalent amounts of cisplatin in the system), one can conclude that the cytotoxic effects, although always very strong, were even higher in the last case. Again, like the previous set of experiments when cells were in direct contact with the gels, this is consonant with a controlled release of cisplatin from the gels.

As before, experiments have been made at lower cisplatin concentrations too. These results are shown in Figure 24. Graph A and B show cell viability as a percentage of CONTROL 1 for A2780 cells and A2780cis cells, respectively. These assays led to lower cytotoxicity values as the drug concentration was much lower. The IC_{50} values for cisplatin were not determined in these cases as the number of experimental points was reduced. As in previous experiments, cytotoxicity was dependent on cisplatin concentration.

Comparing both approaches used in this study (direct and non-direct contact of cells with the hydrogel), after 24 hours in culture, it was observed that both A2780 and A2780cis cells were sensitive to the range of cisplatin concentrations used, although the level of cytotoxicity was not significantly different. In both situations, the Laponite hydrogel was effective as a cisplatin delivery system and demonstrated cytocompatibility on its own. Although it was expected a lower level of cytotoxicity when the hydrogels were present in the inserts, our results were not conclusive in that sense.

A

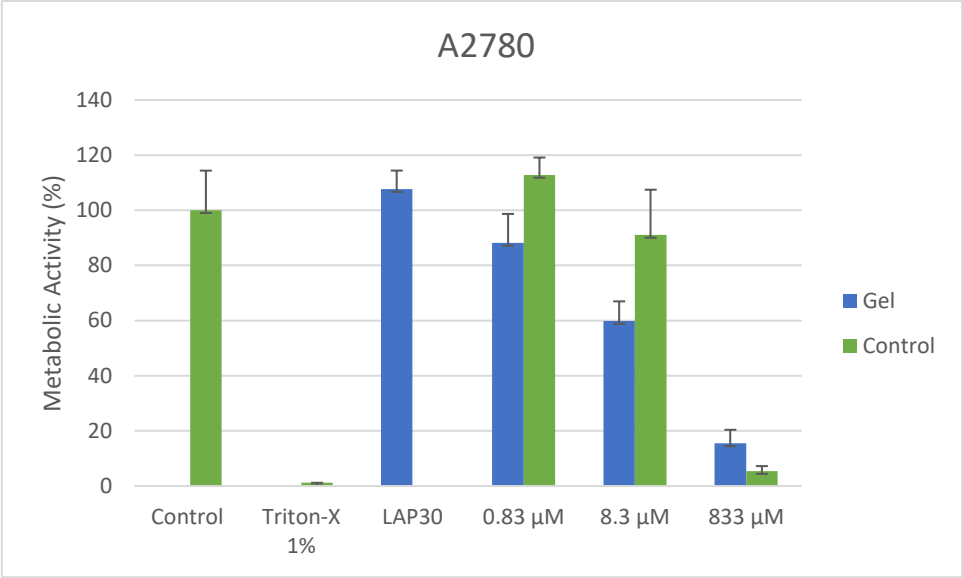

B

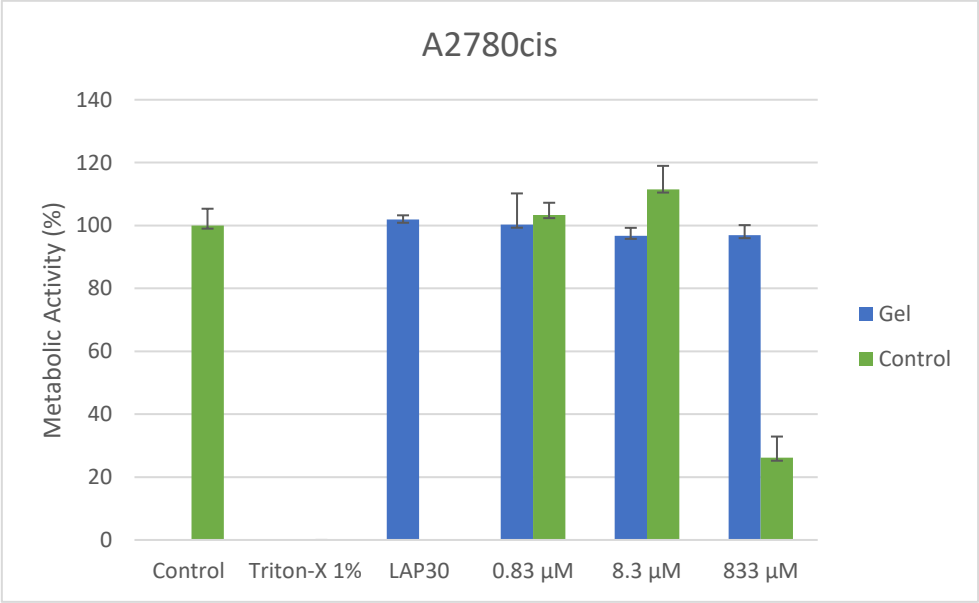

Figure 24 – Cytotoxicity of Laponite-Cisplatin gels (placed in inserts) after 24 hours at low cisplatin concentrations using (A) A2780 cells and (B) A2780cis cells (representative experiment from 3 assays for each cell line). Cell viability as a percentage of CONTROL 1 (cells adherent to the cell culture dish and cultured only in the presence of cell culture medium); LAP30: Laponite gel at 30 $mgmL^{-1}$; LC – Laponite-Cisplatin gel with Laponite at 30 $mgmL^{-1}$ and the displayed cisplatin concentrations: 0.83, 8.3, and 833 µM. Cisplatin controls were used with the same concentrations used in the gels.

In order to assess whether the metabolic activity measured in the assays reflected an actual decrease in the number of cultured cells, i.e., to confirm that there were no variables present that could affect the method used to evaluate cell viability itself (for example, Laponite gels could potentially impact the resazurin reduction assay), two additional simple experiments were conducted. In these experiments, the total protein content (determined using the BCA assay) was used as an indicative parameter of the cytotoxicity of cisplatin released by Laponite gels in non-direct contact with the cells after 48 hours. These experiments were carried out with A2780 and A2780cis cells after the resazurin reduction assay. Figures 25 and 26 present the results obtained in these assays for two cisplatin concentrations, 0.83 μM and 8.3 μM. As shown, for both cell types, a slight decrease in total protein in culture was also observed with an increase in cisplatin concentration (both in its free form and incorporated into Laponite gels). In comparison with the correspondent resazurin assay, it is possible to observe that in both assays both cisplatin concentrations studied had a cytotoxic effect, with this being more evident in the A2780 cells than A2780cis cells due to acquired drug resistance the latter have. Therefore, this suggest that the results of metabolic activity obtained in the studies conducted throughout this thesis should effectively reflect cisplatin-induced cytotoxicity.

A

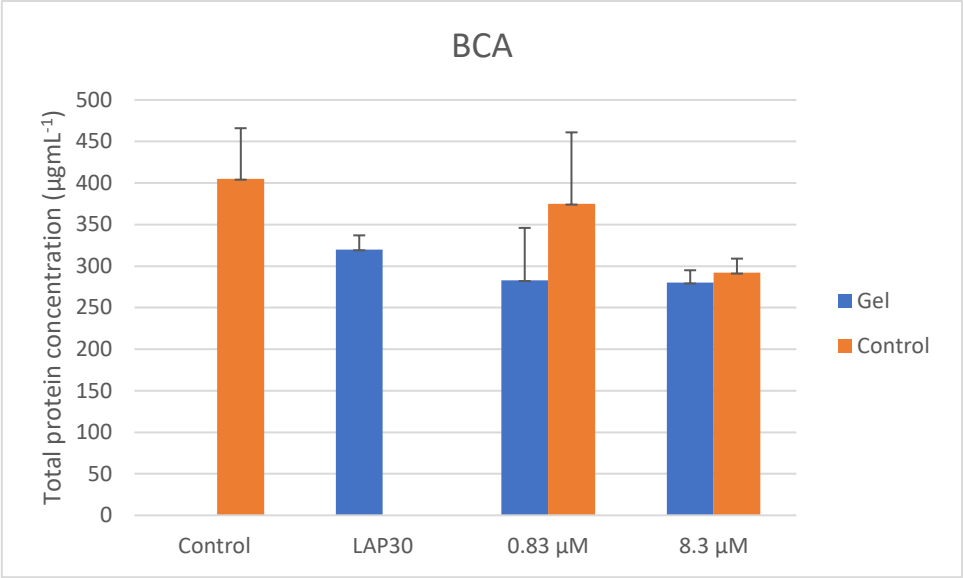

B

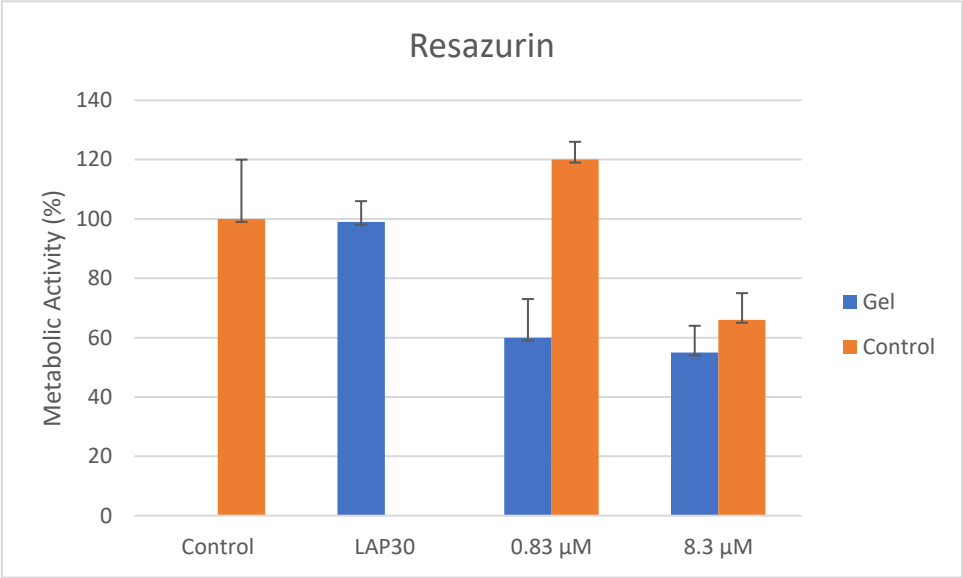

Figure 25 – (A) Total protein content (µgmL^{-1}) for A2780 cells exposed to increasing concentrations of free cisplatin and cisplatin incorporated in Laponite gels (gels were inside inserts) during 48h. (B) Corresponding resazurin reduction assay performed in the same cells prior to the BCA assay for comparison.

A

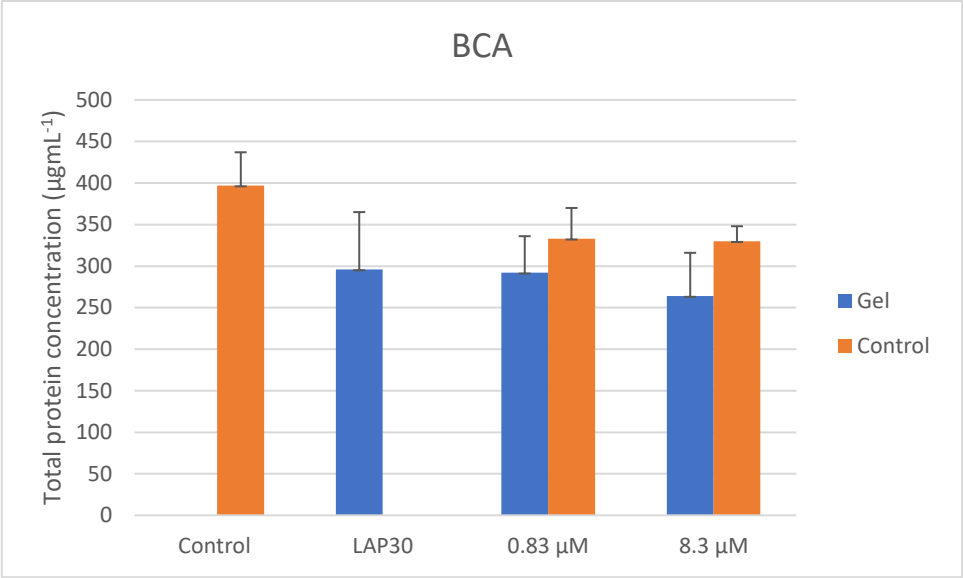

B

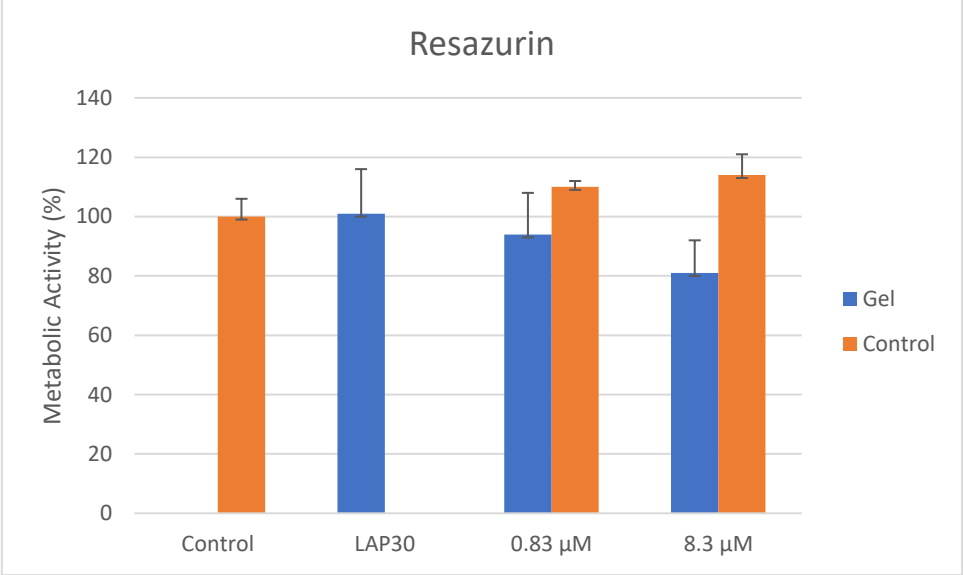

Figure 26 – (A) Total protein content (µgmL^{-1}) for A2780cis cells exposed to increasing concentrations of free cisplatin and cisplatin incorporated in Laponite gels (gels were inside inserts) during 48h. (B) Corresponding resazurin reduction assay performed in the same cells prior to the BCA assay for comparison.

5. Conclusions and future work

As one of the deadliest diseases of our time, cancer is a complex and harrowing condition to treat, with new methods being developed every day to combat it. Drug delivery systems play a big role in this research because of the role they play in the success of the treatment by the anti-neoplasic compounds. Hydrogels have emerged as systems able to not only actively deliver the drug to the tumor but to also maintain the microenvironment necessary for that drug to exert its effect. So, exploring gels' properties in drug delivery seems imperative when looking for new cancer therapies. Laponite and its ability to form gels under certain conditions, along with its properties regarding interactions with molecules and pH-sensitive nature, is a good material to study in this context.

In this work, Laponite gels were successfully formed and the gel-forming conditions, such as pH, temperature, and concentration, were studied and optimized. When cisplatin was added to form Laponite-Cisplatin gels, the gels were successfully formed under the same conditions. Indeed, it was found that self-standing Laponite gels could be prepared at 37 °C, in distilled water (previously adjusted to a pH of 7.0), by vigorously mixing using a vortex for 10s. Although the gelation rate was higher for higher Laponite concentrations, for technical reasons, a concentration of 30 $mgmL^{-1}$ was selected for further studies.

Interestingly, the Laponite-Cisplatin gels displayed a lower percentage of water content in comparison with pristine Laponite gels. After characterization of lyophilized gels by SEM/EDS to observe their morphology and composition, it was observed that the higher the cisplatin concentration in the gels, the more cohesive the structures seemed to be, with the stacks of Laponite sheets displaying higher organization. Thus, it could be concluded that cisplatin plays an important role in Laponite disks cohesion inside the gel. In terms of composition, the atomic concentrations found by EDS analysis matched the ratios present in Laponite empirical formula and confirmed the presence of cisplatin in Laponite-Cisplatin gels.

Regarding the *in vitro* drug release studies, it was found that the gels displayed sustained release behavior of cisplatin. However, the system was not sensitive to the environmental pH which can be explained by the characteristics of cisplatin that is not charged at pHs near neutrality.

Finally, the cytotoxicity assays performed *in vitro* (in A2780 and A2780cis cells) showed that pristine Laponite gels do not affect cell viability and, indeed, even seem to stimulate cells'

metabolic activity in a small extent (this may be related to the compounds/ions that Laponite can release into the medium, such as magnesium ions). Moreover, it was shown that in the higher range of cisplatin concentrations tested in the A2780 cells there were very elevated levels of cytotoxicity and that the gels displayed a more controlled release after 24h in comparison with the free drug. In the lower range of cisplatin concentrations tested, when IC_{50} values were compared, it was possible to conclude that the gels didn't potentiate cisplatin's toxicity in comparison with its free form in either of the cell lines tested. In the assays where the cells were not in direct contact with the gels, it was possible to conclude the same regarding the highest range of cisplatin concentrations in A2780 cells, in that cytotoxicity is dependent on drug concentration and that the gels display a controlled release after both 24h and 48h in comparison with the controls of free drug. Regarding the lower range of concentrations, it was once again observed that cytotoxicity was dependent on cisplatin's concentration and that the gels exerted a less cytotoxic effect in the A2780cis cells in comparison with A2780 after 24h, due to their resistance to the drug. Finally, in relation to the BCA assay performed as a complementary assay for the resazurin assays where the cells and gels had no direct contact, it is possible to conclude that lower metabolic activity evaluated in the resazurin assays indeed corresponded to a higher cell death, corroborating the results presented in this dissertation regarding cytotoxicity. In summary, Laponite hydrogels proved to be effective delivery systems for cancer treatment in both A2780 and A2780cis cells. They displayed cytocompatibility, the ability to release cisplatin, and the drug induced a cytotoxic effect on the cells.

In conclusion, in this work, exploratory studies on the development of Laponite gels as new delivery systems for cisplatin in cancer cells were performed. The drug release behavior of Laponite-Cisplatin gels and their cytotoxic effects on cells were studied using two different approaches: with and without direct cell-gel contact. For future work, the gel-forming studies need to be repeated to ensure reproducibility and the gels should be further characterized for their mechanical properties, utilizing techniques like Atomic Force Microscopy (AFM) or Rheometry. The incorporation of polymers inside the gels in order to try to modulate their drug release properties could also be an interesting study to do. Furthermore, the cisplatin's release profile of these gels may be evaluated at different conditions and the gels' cytotoxic effects may be tested in more cell lines (for example, melanoma cells as the system could be potentially applied in the skin).

6. References

1. WHO. Global health estimates: Leading causes of death [Internet]. [cited 2023 Dec 28]. Available from: https://www.who.int/data/gho/data/themes/mortality-and-global-health-estimates/ghe-leading-causes-of-death

2. Senapati S, Mahanta AK, Kumar S, Maiti P. Controlled drug delivery vehicles for cancer treatment and their performance. *Signal Transduct. Target. Ther.* **2018**; 3:7. https://doi.org/10.1038/s41392-017-0004-3

3. Sun Z, Song C, Wang C, Hu Y, Wu J. Hydrogel-Based Controlled Drug Delivery for Cancer Treatment: A Review. *Mol. Pharm.* **2020**; 17:373–91. https://doi.org/10.1021/acs.molpharmaceut.9b01020

4. Bahram M, Mohseni N, Moghtader M, Bahram M, Mohseni N, Moghtader M. An Introduction to Hydrogels and Some Recent Applications. In: Majee, SB, editor. *Emerging Concepts in Analysis and Applications of Hydrogels.* **2016**. p. 9-38. http://dx.doi.org/10.5772/64301

5. Jayakumar A, Jose VK, Lee JM. Hydrogels for Medical and Environmental Applications. *Small Methods.* **2020**; 4:1900735. https://doi.org/10.1002/smtd.201900735

6. Mantha S, Pillai S, Khayambashi P, Upadhyay A, Zhang Y, Tao O, et al. Smart Hydrogels in Tissue Engineering and Regenerative Medicine. *Materials.* **2019**; 12:3323. https://doi.org/10.3390/ma12203323

7. Chyzy A, Tomczykowa M, Plonska-Brzezinska ME. Hydrogels as Potential Nano-, Micro- and Macro-Scale Systems for Controlled Drug Delivery. *Materials*. **2020**; 13:188. https://doi.org/10.3390/ma13010188

8. Norahan MH, Pedroza-González SC, Sánchez-Salazar MG, Álvarez MM, Trujillo de Santiago G. Structural and biological engineering of 3D hydrogels for wound healing. *Bioact. Mater.* **2023**; 24:197-235. https://doi.org/10.1016/j.bioactmat.2022.11.019

9. Shen Z, Zhang C, Wang T, Xu J. Advances in Functional Hydrogel Wound Dressings: A Review. *Polymers.* **2023**; 15:2000. https://doi.org/10.3390/polym15092000

10. Nasra S, Patel M, Shukla H, Bhatt M, Kumar A. Functional hydrogel-based wound dressings: A review on biocompatibility and therapeutic efficacy. *Life Sci.* **2023**; 334:122232. https://doi.org/10.1016/j.lfs.2023.122232

11. Zhang H, Wu S, Chen W, Hu Y, Geng Z, Su J. Bone/cartilage targeted hydrogel: Strategies and applications. *Bioact. Mater.* **2023**; 23:156–69. https://doi.org/10.1016/j.bioactmat.2022.10.028

12. Zhu S, Li Y, He Z, Ji L, Zhang W, Tong Y, et al. Advanced injectable hydrogels for cartilage tissue engineering. *Front. Bioeng. Biotechnol*. **2022**; 10:954501. https://doi.org/10.3389/fbioe.2022.954501

13. Mutlu Z, Shams Es-haghi S, Cakmak M. Recent Trends in Advanced Contact Lenses. *Adv. Healthc. Mater.* **2019**; 8:1801390. https://doi.org/10.1002/adhm.201801390

14. Herrmann A, Haag R, Schedler U. Hydrogels and Their Role in Biosensing Applications. *Adv. Healthc. Mater.* **2021**; 10:2100062. https://doi.org/10.1002/adhm.202100062

15. Chen W, Zhang C, Peng S, Lin Y, Ye Z. Hydrogels in Dental Medicine. *Adv. Therap.* **2023**; 2300128. https://doi.org/10.1002/adtp.202300128

16. Mitura S, Sionkowska A, Jaiswal A. Biopolymers for hydrogels in cosmetics: review. *J. Mater. Sci.-Mater. Med.* **2020**; 31:50. https://doi.org/10.1007/s10856-020-06390-w

17. Kapusta O, Jarosz A, Stadnik K, Giannakoudakis DA, Barczyński B, Barczak M. Antimicrobial Natural Hydrogels in Biomedicine: Properties, Applications, and Challenges-A Concise Review. *Int. J. Mol. Sci.* **2023**; 24:2191. https://doi.org/10.3390/ijms24032191

18. Li J, Mooney DJ. Designing hydrogels for controlled drug delivery. *Nat. Rev. Mater.* **2016**; 1:16071. https://doi.org/10.1038/natrevmats.2016.71

19. Meng D, Yang S, Yang Y, Zhang L, Cui L. Synergistic chemotherapy and phototherapy based on red blood cell biomimetic nanomaterials. *J Control Release*. **2022**; 352:146–62. https://doi.org/10.1016/j.jconrel.2022.10.019

20. Lee JH, Tachibana T, Yamana K, Kawasaki R, Yabuki A. Simple Formation of Cancer Drug-Containing Self-Assembled Hydrogels with Temperature and pH-Responsive Release. *Langmuir*. **2021**; 37:11269–75. https://doi.org/10.1021/acs.langmuir.1c01700

21. Lu Z, Zheng X, Ding C, Zou Z, Liang Y, Zhou Y, et al. Deciphering the Biological Effects of Radiotherapy in Cancer Cells. *Biomolecules.* **2022**; 12:1167. https://doi.org/10.3390/biom12091167

22. Fu Z, Li H, Xue P, Yu H, Yang S, Tao C, et al. Implantable Bioresponsive Hydrogel Prevents Local Recurrence of Breast Cancer by Enhancing Radiosensitivity. *Front Bioeng Biotechnol*. **2022**; 10:881544. https://doi.org/10.3389/fbioe.2022.881544

23. Chen M, Wang Z, Suo W, Bao Z, Quan H. Injectable Hydrogel for Synergetic Low Dose Radiotherapy, Chemodynamic Therapy and Photothermal Therapy. *Front Bioeng Biotechnol*. **2021**; 9:757428. https://doi.org/10.3389/fbioe.2021.757428

24. Wang N, Gao Q, Tang J, Jiang YQ, Yang LS, Shi XX, et al. Anti-tumor effect of local injectable hydrogel-loaded endostatin alone and in combination with radiotherapy for lung cancer. *Drug Deliv.* **2021**; 28:183–94. https://doi.org/10.1080/10717544.2020.1869864

25. Zhang J, Yang L, Huang F, Zhao C, Liu J, Zhang Y, et al. Multifunctional Hybrid Hydrogel Enhanced Antitumor Therapy through Multiple Destroying DNA Functions by a Triple-Combination Synergistic Therapy. *Adv Healthc Mater*. **2021**; 10:2101190. https://doi.org/10.1002/adhm.202101190

26. Liu C, Yang M, Zhang D, Chen M, Zhu D. Clinical cancer immunotherapy: Current progress and prospects. *Front Immunol*. **2022**; 13:961805. https://doi.org/10.3389/fimmu.2022.961805

27. Liu Y, Geng Y, Yue B, Lo PC, Huang J, Jin H. Injectable Hydrogel as a Unique Platform for Antitumor Therapy Targeting Immunosuppressive Tumor Microenvironment. *Front Immunol*. **2022**; 12:832942. https://doi.org/10.3389/fimmu.2021.832942

28. Jin H, Wan C, Zou Z, Zhao G, Zhang L, Geng Y, et al. Tumor Ablation and Therapeutic Immunity Induction by an Injectable Peptide Hydrogel. *ACS Nano*. **2018**; 12:3295–310. https://doi.org/10.1021/acsnano.7b08148

29. van der Zee J, Vujaskovic Z, Kondo M, Sugahara T. The Kadota Fund International Forum 2004--clinical group consensus. *Int J Hyperthermia*. **2008**; 24:111–22. https://doi.org/10.1080/02656730801895058

30. Hannon G, Tansi FL, Hilger I, Prina-Mello A. The Effects of Localized Heat on the Hallmarks of Cancer. *Adv Ther (Weinh)*. **2021**; 4:2000267. https://doi.org/10.1002/adtp.202000267

31. Long X, Zhang X, Chen Q, Liu M, Xiang Y, Yang Y, et al. Nucleus-Targeting Phototherapy Nanodrugs for High-Effective Anti-Cancer Treatment. *Front Pharmacol*. **2022**; 13:905375. https://doi.org/10.3389/fphar.2022.905375

32. Zhang K, Xue K, Loh XJ. Thermo-Responsive Hydrogels: From Recent Progress to Biomedical Applications. *Gels*. **2021**; 7:77. https://doi.org/10.3390/gels7030077

33. Yang Z, Liu J, Lu Y. Doxorubicin and CD-CUR inclusion complex co-loaded in thermosensitive hydrogel PLGA-PEG-PLGA localized administration for osteosarcoma. *Int J Oncol*. **2020**; 57:433-44. https://doi.org/10.3892/ijo.2020.5067

34. Li X, Xu X, Xu M, Geng Z, Ji P, Liu Y. Hydrogel systems for targeted cancer therapy. *Front Bioeng Biotechnol*. **2023**; 11:1140436. https://doi.org/10.3389/fbioe.2023.1140436

35. de Lima CSA, Balogh TS, Varca JPRO, Varca GHC, Lugão AB, Camacho-Cruz LA, et al. An Updated Review of Macro, Micro, and Nanostructured Hydrogels for Biomedical and Pharmaceutical Applications. *Pharmaceutics*. **2020;** 12:970. https://doi.org/10.3390/pharmaceutics12100970

36. Majumder P, Singh A, Wang Z, Dutta K, Pahwa R, Liang C, et al. Surface-fill Hydrogel Attenuates the Oncogenic Signature of Complex Anatomical Surface Cancer in a Single Application. *Nat Nanotechno*. **2021**; 16:1251-9. https://doi.org/10.1038/s41565-021-00961-w

37. Minhas MU, Ahmad M, Anwar J, Khan S. Synthesis and Characterization of Biodegradable Hydrogels for Oral Delivery of 5-Fluorouracil Targeted to Colon: Screening with Preliminary In Vivo Studies. *Adv. Polym. Technol*. **2018**; 37:221–9. https://doi.org/10.1002/adv.21659

38. Soni KS, Desale SS, Bronich TK. Nanogels: an overview of properties, biomedical applications and obstacles to clinical translation. *J Control Release*. **2016**; 240:109-26. https://doi.org/10.1016/j.jconrel.2015.11.009

39. Zhang D, Tian S, Liu Y, Zheng M, Yang X, Zou Y, et al. Near infrared-activatable biomimetic nanogels enabling deep tumor drug penetration inhibit orthotopic glioblastoma. *Nat. Commun.* **2022** 13:6835. https://doi.org/10.1038/s41467-022-34462-8

40. Kumari N, Mohan C. Basics of Clay Minerals and Their Characteristic Properties. In: Nascimento G, editor. *Clay and Clay Minerals*. **2021**. p. 1-29. http://dx.doi.org/10.5772/intechopen.97672

41. Andrade FA, Al-Qureshi HA, Hotza D. Measuring the plasticity of clays: A review. *Appl. Clay Sci.* **2011**; 51:1–7. https://doi.org/10.1016/j.clay.2010.10.028

42. Awasthi A, Jadhao P, Kumari K. Clay nano-adsorbent: structures, applications and mechanism for water treatment. *SN Appl. Sci.* **2019**; 1:1076. https://doi.org/10.1007/s42452-019-0858-9

43. Park JH, Shin HJ, Kim MH, Kim JS, Kang N, Lee JY, et al. Application of montmorillonite in bentonite as a pharmaceutical excipient in drug delivery systems. *J. Pharm. Investig.* **2016**; 46:363–75. https://doi.org/10.1007/s40005-016-0258-8

44. Biddeci G, Spinelli G, Colomba P, Di Blasi F. Nanomaterials: A Review about Halloysite Nanotubes, Properties, and Application in the Biological Field. *Int. J. Mol. Sci.* **2022**; 23:11518. https://doi.org/10.3390/ijms231911518

45. Sandri G, Bonferoni MC, Rossi S, Ferrari F, Aguzzi C, Viseras C, et al. Clay minerals for tissue regeneration, repair, and engineering. In: Ågren, MS, editor. *Wound Healing Biomaterials, Vol.2: Functional Biomaterials.* **2016**; p. 385–402. https://doi.org/10.1016/B978-1-78242-456-7.00019-2

46. Tomás H, Alves CS, Rodrigues J. Laponite®: A key nanoplatform for biomedical applications? *Nanomedicine.* **2018**; 14:2407–20. https://doi.org/10.1016/j.nano.2017.04.016

47. Huang XB, Sun JS, Huang Y, Yan BC, Dong XD, Liu F, et al. Laponite: a promising nanomaterial to formulate high-performance water-based drilling fluids. *Pet. Sci.* **2021**; 18:579–90. https://doi.org/10.1007/s12182-020-00516-z

48. BYK Additives & Instruments. Laponite: performance additives. Technical Information B-RI 21; **2014.**

49. Tawari SL, Koch DL, Cohen C. Electrical Double-Layer Effects on the Brownian Diffusivity and Aggregation Rate of Laponite Clay Particles. *J. Colloid Interface Sci.* **2001**; 240:54–66. https://doi.org/10.1006/jcis.2001.7646

50. Mongondry P, Tassin JF, Nicolai T. Revised state diagram of Laponite dispersions. *J. Colloid Interface Sci.* **2005**; 283:397–405. https://doi.org/10.1016/j.jcis.2004.09.043

51. Ruzicka B, Zaccarelli E. A fresh look at the Laponite phase diagram. *Soft Matter*. **2011**; 7:1268–86. https://doi.org/10.1039/C0SM00590H

52. Jatav S, Joshi YM. Chemical stability of Laponite in aqueous media. *Appl. Clay Sci.* **2014**; 97–98:72–7. https://doi.org/10.1016/j.clay.2014.06.004

53. Nandi U, Trivedi V, Douroumis D, Mendham AP, Coleman NJ. Layered Silicate-Alginate Composite Particles for the pH-Mediated Release of Theophylline. *Pharmaceuticals.* **2020**; 13:182. https://doi.org/10.3390/ph13080182

54. Valencia GA, Djabourov M, Carn F, Sobral PJA. Novel Insights on Swelling and Dehydration of Laponite. *Colloid Interface Sci. Commun*. **2018**; 23:1–5. https://doi.org/10.1016/j.colcom.2018.01.001

55. Kiaee G, Dimitrakakis N, Sharifzadeh S, Kim HJ, Avery RK, Moghaddam KM, et al. Laponite-based Nanomaterials For Drug Delivery. *Adv. Healthc. Mater.* **2022**; 11:2102054. https://doi.org/10.1002/adhm.202102054

56. Das SS, Neelam, Hussain K, Singh S, Hussain A, Faruk A, et al. Laponite-based Nanomaterials for Biomedical Applications: A Review. *Curr. Pharm. Design* **2019**; 25:424–43. https://doi.org/10.2174/1381612825666190402165845

57. Furth ME, Atala A. Tissue Engineering: Future Perspectives. In: Lanza R, Langer R, Vacanti J, editors. *Principles of Tissue Engineering*. 4th Ed. **2014**; p. 83–123. https://doi.org/10.1016/B978-0-12-398358-9.00006-9

58. Reffitt DM, Ogston N, Jugdaohsingh R, Cheung HFJ, Evans BAJ, Thompson RPH, et al. Orthosilicic acid stimulates collagen type 1 synthesis and osteoblastic differentiation in human osteoblast-like cells in vitro. *Bone.* **2003**; 32:127–35. https://doi.org/10.1016/s8756-3282(02)00950-x

59. Boskey AL, Wright TM, Blank RD. Collagen and bone strength. *J. Bone Miner. Res.* **1999**; 14:330–5. https://doi.org/10.1359/jbmr.1999.14.3.330

60. Henriksen K, Karsdal MA. Type I Collagen. In: Karsdal MA, editor. *Biochemistry of Collagens, Laminins and Elastin: Structure, Function and Biomarkers.* **2016**; p. 1–11. https://doi.org/10.1016/B978-0-12-809847-9.00001-5

61. Swaminathan R. Magnesium Metabolism and its Disorders. *Clin. Biochem. Rev.* **2003**; 24:47-66.

62. Pohl HR, Wheeler JS, Murray HE. Sodium and potassium in health and disease. In: Sigel A, Sigel H, Sigel R, editors. *Interrelations between Essential Metal Ions and Human Diseases. Metal Ions in Life Sciences*. **2013**; Vol.13, p. 29–47. https://doi.org/10.1007/978-94-007-7500-8_2

63. Williams R, Ryves WJ, Dalton EC, Eickholt B, Shaltiel G, Agam G, et al. A molecular cell biology of lithium. *Biochem. Soc. Trans.* **2004**; 32:799–802. https://doi.org/10.1042/BST0320799

64. Gonzaga V de AM, Poli AL, Gabriel JS, Tezuka DY, Valdes TA, Leitão A, et al. Chitosan-laponite nanocomposite scaffolds for wound dressing application. *J. Biomed. Mater. Res. B Appl. Biomater.* **2020**; 108:1388–97. https://doi.org/10.1002/jbm.b.34487

65. Felbeck T, Hoffmann K, Lezhnina MM, Kynast UH, Resch-Genger U. Fluorescent nanoclays: Covalent functionalization with amine reactive dyes from different

fluorophore classes and surface group quantification. *J. Phys. Chem. C*. **2015**; 119:12978–87. https://doi.org/10.1021/acs.jpcc.5b01482

66. Tzitzios V, Basina G, Bakandritsos A, Hadjipanayis CG, Mao H, Niarchos D, et al. Immobilization of magnetic iron oxide nanoparticles on laponite discs – an easy way to biocompatible ferrofluids and ferrogels*. J. Mater. Chem.* **2010**; 20:5418-28. https://doi.org/10.1039/c0jm00061b

67. Ding L, Hu Y, Luo Y, Zhu J, Wu Y, Yu Z, et al. LAPONITE®-stabilized iron oxide nanoparticles for in vivo MR imaging of tumors. *Biomater. Sci.* **2016**; 4:474–82. https://doi.org/10.1039/C5BM00508F

68. Ding L, Wang R, Hu Y, Xu F, Zhang N, Cao X, et al. Folic acid-modified Laponite®-stabilized Fe3O4 nanoparticles for targeted T2-weighted MR imaging of tumor. *Appl. Clay Sci.* **2020**; 186:105447. https://doi.org/10.1016/j.clay.2020.105447

69. Liu R, Xu F, Wang L, Liu M, Cao X, Shi X, et al. Polydopamine-Coated Laponite Nanoplatforms for Photoacoustic Imaging-Guided Chemo-Phototherapy of Breast Cancer. *Nanomaterials.* **2021**; 11:394. https://doi.org/10.3390/nano11020394

70. Dawson JI, Oreffo ROC. Clay: new opportunities for tissue regeneration and biomaterial design. *Adv. Mater.* **2013**; 25:4069–86. https://doi.org/10.1002/adma.201301034

71. Roozbahani M, Kharaziha M, Emadi R. pH sensitive dexamethasone encapsulated laponite nanoplatelets: Release mechanism and cytotoxicity. *Int. J. Pharm.* **2017**; 518:312–9. https://doi.org/10.1016/j.ijpharm.2017.01.001

72. Stealey ST, Gaharwar AK, Zustiak SP. Laponite-Based Nanocomposite Hydrogels for Drug Delivery Applications. *Pharmaceuticals.* **2023**; 16:821. https://doi.org/10.3390/ph16060821

73. Aray Y, Marquez M, Rodriguez J, Coll S, Simon-Manso Y, Gonzalez C, et al. Electrostatics for Exploring the Nature of Water Adsorption on the Laponite Sheets' Surface. *J. Phys. Chem. B*. **2003**; 107:8946–52. https://doi.org/10.1021/jp0302257

74. Ghadiri M, Hau H, Chrzanowski W, Agus H, Rohanizadeh R. Laponite clay as a carrier for in situ delivery of tetracycline. *RSC Adv.* **2013**; 3:20193–201. https://doi.org/10.1039/C3RA43217C

75. Yang H, Hua S, Wang W, Wang A. Composite Hydrogel Beads Based on Chitosan and Laponite: Preparation, Swelling, and Drug Release Behaviour. *Iran. Polym. J.* **2011**; 20:479-90.

76. Wang S, Zheng F, Huang Y, Fang Y, Shen M, Zhu M, et al. Encapsulation of amoxicillin within laponite-doped poly(lactic-co-glycolic acid) nanofibers: preparation, characterization, and antibacterial activity. *ACS Appl. Mater. Interfaces*. **2012**; 4:6393–401. https://doi.org/10.1021/am302130b

77. Martínez Martínez VM, López Arbeloa F, Bañ Uelos Prieto J, Arbeloa López T, López Arbeloa I. Characterization of Supported Solid Thin Films of Laponite Clay.

Intercalation of Rhodamine 6G Laser Dye. *Langmuir* **2004**; 20:5709–17. https://doi.org/10.1021/la049675w

78. Yang JH, Lee JH, Ryu HJ, Elzatahry AA, Alothman ZA, Choy JH. Drug–clay nanohybrids as sustained delivery systems. *Appl. Clay Sci.* **2016**; 130:20–32. https://doi.org/10.1016/j.clay.2016.01.021

79. Schmaljohann D. Thermo- and pH-responsive polymers in drug delivery. *Adv. Drug Deliv. Rev.* **2006**; 58:1655–70. https://doi.org/10.1016/j.addr.2006.09.020

80. Paula FLO, da Silva GJ, Aquino R, Depeyrot J, Fossum JO, Knudsen KD, et al. Gravitational and magnetic separation in self-assembled clay-ferrofluid nanocomposites. *Braz. J. Phys.* **2009**; 39:163–70. https://doi.org/10.1590/S0103-97332009000200007

81. Kiaee G, Mostafalu P, Samandari M, Sonkusale S. A pH-Mediated Electronic Wound Dressing for Controlled Drug Delivery. *Adv. Healthc. Mater.* **2018**; 7:1800396. https://doi.org/10.1002/adhm.201800396

82. Xiao S, Castro R, Maciel D, Gonçalves M, Shi X, Rodrigues J, et al. Fine tuning of the pH-sensitivity of laponite-doxorubicin nanohybrids by polyelectrolyte multilayer coating. *Mater. Sci. Eng. C- Mater. Biol. Appl.* **2016**; 60:348–56. https://doi.org/10.1016/j.msec.2015.11.051

83. Jung H, Kim HM, Choy Y Bin, Hwang SJ, Choy JH. Itraconazole–Laponite: Kinetics and mechanism of drug release. *Appl. Clay Sci.* **2008**; 40:99–107. https://doi.org/10.1016/j.clay.2007.09.002

84. Li P, Kim NH, Hui D, Rhee KY, Lee JH. Improved mechanical and swelling behavior of the composite hydrogels prepared by ionic monomer and acid-activated Laponite. *Appl. Clay Sci.* **2009**; 46:414–7. https://doi.org/10.1016/j.clay.2009.10.007

85. Brazel CS, Peppas NA. Modeling of drug release from swellable polymers. *Eur. J. Pharm. Biopharm.* **2000**; 49:47–58. https://doi.org/10.1016/S0939-6411(99)00058-2

86. Wang S, Wu Y, Guo R, Huang Y, Wen S, Shen M, et al. Laponite nanodisks as an efficient platform for Doxorubicin delivery to cancer cells. *Langmuir*. **2013**; 29:5030–6. https://doi.org/10.1021/la4001363

87. Thompson DW, Butterworth JT. The Nature of Laponite and Its Aqueous Dispersions. *J. Colloid Interface Sci.* **1992**; 151:236-43. https://doi.org/10.1016/0021-9797(92)90254-J

88. Mohanty RP, Joshi YM. Chemical stability phase diagram of aqueous Laponite dispersions. *Appl. Clay Sci.* **2016**; 119:243–8. https://doi.org/10.1016/j.clay.2015.10.021

89. Gaharwar AK, Mihaila SM, Swami A, Patel A, Sant S, Reis RL, et al. Bioactive Silicate Nanoplatelets for Osteogenic Differentiation of Human Mesenchymal Stem Cells. *Adv. Mater.* **2013**; 25:3329–36. https://doi.org/10.1002/adma.201300584

90. Ghadiri M, Chrzanowski W, Lee WH, Rohanizadeh R. Layered silicate clay functionalized with amino acids: wound healing application. *RSC Adv.* **2014**; 4:35332–43. https://doi.org/10.1039/C4RA05216A

91. Gaharwar AK, Kishore V, Rivera C, Bullock W, Wu CJ, Akkus O, et al. Physically crosslinked nanocomposites from silicate-crosslinked PEO: mechanical properties and osteogenic differentiation of human mesenchymal stem cells. *Macromol. Biosci.* **2012**; 12:779–93. https://doi.org/10.1002/mabi.201100508

92. Câmara GBM, Barbosa R de M, García-Villén F, Viseras C, Almeida Júnior RF de, Machado PRL, et al. Nanocomposite gels of poloxamine and Laponite for β-Lapachone release in anticancer therapy. *Eur J Pharm Sci*. **2021**; 163:105861. https://doi.org/10.1016/j.ejps.2021.105861

93. Jafari H, Namazi H. pH-sensitive biosystem based on laponite RD/chitosan/polyvinyl alcohol hydrogels for controlled delivery of curcumin to breast cancer cells. *Colloids Surf B Biointerfaces*. **2023**; 231:113585. https://doi.org/10.1016/j.colsurfb.2023.113585

94. Gonçalves M, Figueira P, Maciel D, Rodrigues J, Shi X, Tomás H, et al. Antitumor Efficacy of Doxorubicin-Loaded Laponite/Alginate Hybrid Hydrogels. *Macromol Biosci*. **2014**; 14:110–20. https://doi.org/10.1002/mabi.201300241

95. Gonçalves M, Figueira P, Maciel D, Rodrigues J, Qu X, Liu C, et al. pH-sensitive Laponite(®)/doxorubicin/alginate nanohybrids with improved anticancer efficacy. *Acta Biomater*. **2014**; 10:300–7. https://doi.org/10.1016/j.actbio.2013.09.013

96. Becher TB, Mendonça MCP, De Farias MA, Portugal R V., De Jesus MB, Ornelas C. Soft Nanohydrogels Based on Laponite Nanodiscs: A Versatile Drug Delivery Platform for Theranostics and Drug Cocktails. *ACS Appl. Mater. Interfaces*. **2018**; 10:21891–900. https://doi.org/10.1021/acsami.8b06149

97. Heragh BK, Javanshir S, Mahdavinia GR, Jamal MRN. Hydroxyapatite grafted chitosan/laponite RD hydrogel: Evaluation of the encapsulation capacity, pH-responsivity, and controlled release behavior. *Int J Biol Macromol*. **2021**; 190:351–9. https://doi.org/10.1016/j.ijbiomac.2021.08.220

98. Luo J, Ma Z, Yang F, Wu T, Wen S, Zhang J, et al. Fabrication of Laponite-Reinforced Dextran-Based Hydrogels for NIR-Responsive Controlled Drug Release. *ACS Biomater Sci Eng*. **2022**; 8:1554–65. https://doi.org/10.1021/acsbiomaterials.1c01389

99. Anthony EJ, Bolitho EM, Bridgewater HE, Carter OWL, Donnelly JM, Imberti C, et al. Metallodrugs are unique: opportunities and challenges of discovery and development. *Chem. Sci.* **2020**; 11:12888–917. https://doi.org/10.1039/D0SC04082G

100. Rottenberg S, Disler C, Perego P. The rediscovery of platinum-based cancer therapy. *Nat. Rev. Cancer.* **2020**; 21:37–50. https://doi.org/10.1038/s41568-020-00308-y

101. Chen X, Wang J, Fu Z, Zhu B, Wang J, Guan S, et al. Curcumin activates DNA repair pathway in bone marrow to improve carboplatin-induced myelosuppression. *Sci Rep.* **2017**; 7:17724. https://doi.org/10.1038/s41598-017-16436-9

102. Mehmood RK. Review of Cisplatin and Oxaliplatin in Current Immunogenic and Monoclonal Antibody Treatments. *Oncol. Rev.* **2014**; 8:256. https://doi.org/10.4081/oncol.2014.256

103. Corinti D, Coletti C, Re N, Piccirillo S, Giampà M, Crestoni ME, et al. Hydrolysis of cis- and transplatin: structure and reactivity of the aqua complexes in a solvent free environment. *RSC Adv.* **2017**; 7:15877–84. https://doi.org/10.1039/C7RA01182B

104. Martinho N, Santos TCB, Florindo HF, Silva LC. Cisplatin-Membrane Interactions and Their Influence on Platinum Complexes Activity and Toxicity. *Front Physiol.* **2018**; 9:1898. https://doi.org/10.3389/fphys.2018.01898

105. Wang D, Lippard SJ. Cellular processing of platinum anticancer drugs. *Nat. Rev. Drug Discov.* **2005**; 4:307–20. https://doi.org/10.1038/nrd1691

106. Shen DW, Pouliot LM, Hall MD, Gottesman MM. Cisplatin Resistance: A Cellular Self-Defense Mechanism Resulting from Multiple Epigenetic and Genetic Changes. *Pharmacol. Rev.* **2012**; 64:706-21. https://doi.org/10.1124/pr.111.005637

107. Huang S, He P, Xu D, Li J, Peng X, Tang Y. Acidic stress induces apoptosis and inhibits angiogenesis in human bone marrow-derived endothelial progenitor cells. *Oncol. Lett.* **2017**; 14:5695–702. https://doi.org/10.3892/ol.2017.6947

108. Anilanmert B, Yalçin G, Ariöz F, Dölen E. The Spectrophotometric Determination of Cisplatin in urine, using o-phenylenediamine as derivatizing agent. *Anal. Lett.* **2001**; 34:113–23. https://doi.org/10.1081/AL-100002709

109. Smith PK, Krohn RI, Hermanson GT, Mallia AK, Gartner FH, Provenzano MD, et al. Measurement of protein using bicinchoninic acid. *Anal. Biochem.* **1985**; 150:76–85. https://doi.org/10.1016/0003-2697(85)90442-7

110. Wiechelman KJ, Braun RD, Fitzpatrick JD. Investigation of the bicinchoninic acid protein assay: identification of the groups responsible for color formation. *Anal. Biochem.* **1988**; 175:231–7. https://doi.org/10.1016/0003-2697(88)90383-1

111. Ding B, Zeng P, Huang Z, Dai L, Lan T, Xu H, et al. A 2D material–based transparent hydrogel with engineerable interference colours. *Nat Commun*. **2022**; 13:1212. https://doi.org/10.1038/s41467-021-26587-z

112. Tran VT, Mredha MTI, Jeon I. High-water-content hydrogels exhibiting superior stiffness, strength, and toughness. *Extreme Mech Lett.* **2020**; 37:100691. https://doi.org/10.1016/j.eml.2020.100691

113. Alamán-Díez P, Borau C, Guerrero PE, Amaveda H, Mora M, Fraile JM, et al. Collagen-Laponite Nanoclay Hydrogels for Tumor Spheroid Growth. *Biomacromolecules*. **2023**; 24:2879–91. https://doi.org/10.1021/acs.biomac.3c00257

114. Pirozzi NM, Kuipers J, Giepmans BNG. Sample preparation for energy dispersive X-ray imaging of biological tissues. *Methods Cell Biol*. **2021**; 162:89–114.

115. Zhang Q, Colazo J, Berg D, Mugo SM, Serpe MJ. Multiresponsive Nanogels for Targeted Anticancer Drug Delivery. *Mol Pharm*. **2017**; 14:2624–8. https://doi.org/10.1021/acs.molpharmaceut.7b00325

116. Wang J, Wang G, Sun Y, Wang Y, Yang Y, Yuan Y, et al. In Situ formation of pH-/thermo-sensitive nanohybrids via friendly-assembly of poly(N-vinylpyrrolidone) onto LAPONITE®. *RSC Adv.* **2016**; 6:31816–23. https://doi.org/10.1039/C5RA25628C

117. Salahshoori I, Ramezani Z, Cacciotti I, Yazdanbakhsh A, Hossain MK, Hassanzadeganroudsari M. Cisplatin uptake and release assessment from hydrogel synthesized in acidic and neutral medium: An experimental and molecular dynamics simulation study. *J. Mol. Liq.* **2021**; 344:117890. https://doi.org/10.1016/j.molliq.2021.117890

118. A2780. Culture Collections [Internet]. [cited 2024 Jan 13]. Available from: https://www.culturecollections.org.uk/nop/product/a2780

119. A2780cis. Culture Collections [Internet]. [cited 2024 Jan 13]. Available from: https://www.culturecollections.org.uk/nop/product/a2780cis

120. Zoń A, Bednarek I. Cisplatin in Ovarian Cancer Treatment—Known Limitations in Therapy Force New Solutions. *Int. J. Mol. Sci.* **2023**; 24:7585. https://doi.org/10.3390/ijms24087585

121. Lavogina D, Lust H, Tahk MJ, Laasfeld T, Vellama H, Nasirova N, et al. Revisiting the Resazurin-Based Sensing of Cellular Viability: Widening the Application Horizon. *Biosensors-Basel*. **2022**; 12:196. https://doi.org/10.3390/bios12040196

122. Rampersad SN. Multiple applications of Alamar Blue as an indicator of metabolic function and cellular health in cell viability bioassays. *Sensors*. **2012**; 12:12347–60. https://doi.org/10.3390/s120912347

123. Costa P, Gomes ATPC, Braz M, Pereira C, Almeida A. Application of the Resazurin Cell Viability Assay to Monitor Escherichia coli and Salmonella Typhimurium Inactivation Mediated by Phages. *Antibiotics-Basel* [Internet]. **2021**; 10:974. https://doi.org/10.3390/antibiotics10080974

124. Riss TL, Moravec RA, Niles AL, Duellman S, Benink HA, Worzella TJ, et al. Cell Viability Assays. In: Markossian S, Grossman A, Brimacombe K, et al., editors. *Assay Guidance Manual*. **2016**; p. 403-29. https://www.ncbi.nlm.nih.gov/books/NBK144065/

125. Toté K, Vanden Berghe D, Levecque S, Bénéré E, Maes L, Cos P. Evaluation of hydrogen peroxide-based disinfectants in a new resazurin microplate method for rapid efficacy testing of biocides. *J. Appl. Microbiol.* **2009**; 107:606–15. https://doi.org/10.1111/j.1365-2672.2009.04228.x

126. Kuete V, Karaosmanoğlu O, Sivas H. Anticancer Activities of African Medicinal Spices and Vegetables. In: Kuete V, editor. *Medicinal Spices and Vegetables from Africa: Therapeutic Potential Against Metabolic, Inflammatory, Infectious and Systemic Diseases*. **2017**; p. 271–97. https://doi.org/10.1016/B978-0-12-809286-6.00010-8

127. Gouveia M, Figueira J, Jardim MG, Castro R, Tomás H, Rissanen K, et al. Poly(alkylidenimine) Dendrimers Functionalized with the Organometallic Moiety $[Ru(\eta^5\text{-}C_5H_5)(PPh_3)_2]^+$ as Promising Drugs Against Cisplatin-Resistant Cancer Cells and Human Mesenchymal Stem Cells. *Molecules.* **2018**; 23:1471. https://doi.org/10.3390/molecules23061471

7. Annexes

Annex 1. Laponite XLG data sheet

BYK

LAPONITE-XLG

Data sheet
Issue 11/2023

LAPONITE-XLG

Rheology additive based on synthetic phyllosilicate for aqueous systems to provide thixotropic stabilization in personal care applications.

Product data

Composition
Synthetic (modified) phyllosilicate
(INCI: Lithium Magnesium Sodium Silicate (nano))

Vegan

Typical properties
The values indicated in this data sheet describe typical properties and do not constitute specification limits.

Bulk density:	1000 kg/m³
pH value (2 % in H_2O):	approx. 10
Moisture content:	max. 10 %
Sieve residue (60 mesh/250 µm):	max. 2 %
Surface area:	370 m²/g
Gel strength:	min. 22 g
Gel time:	max. 6 min
Dispersion rate:	max. 25
Clarity:	max. 22
Lead content:	max. 5 mg/kg
Arsenic content:	max. 1 mg/kg
Total viable count:	max. 750 cfu/g
Color:	white
Delivery form:	free-flowing powder

Storage and transportation
LAPONITE-XLG is hygroscopic and should be transported and stored dry in the unopened original container at temperatures between 0 °C and 30 °C.

Applications

Personal care

Special features and benefits
LAPONITE-XLG is suitable for use in formulations with a pH value of 6.5 and lower. In water or aqueous solutions of alcohols, it swells to clear and colorless colloidal dispersions, leading to the formation of a gel structure. At additive concentrations of more than 2 % in water, strongly thixotropic gels are formed. The unique thixotropic properties provided by LAPONITE-XLG improve the skin feel of personal care products and create a light, non-sticky texture. In addition, the additive enhances the stability of emulsions and prevents the settling of particles, pigments, and solid actives. It is also effective for stabilizing oil-in-water emulsions and is compatible with solutions of up to 40 % ethanol. When used in combination with co-thickeners, it can be added to formulations containing > 60 % ethanol.

A member of ALTANA

Recommended use

Creams and lotions	■
Sunscreen products	■
Depilatory creams	■
Toothpastes	■
Shower gels and shampoos	■
Liquid makeup	■
Eye makeup	■

■ especially recommended □ recommended

Recommended levels

0.1–5 % additive (as supplied) based on the total formulation, depending on the application. T

he above recommended levels can be used for orientation. The optimum dosage should be determined by application-related test series.

Incorporation and processing instructions

LAPONITE-XLG should be added steadily to deionized water at a temperature of 15 to 25 °C under high shear within 10 to 30 seconds. It should be stirred fast enough that a turbulent vortex current is formed, so that the powder is well dispersed and clumps are avoided. After complete addition, stirring is continued for 20 minutes. At complete dispersion, a clear, colorless, and low-viscosity pre-mix is obtained. Once this pre-mix is combined with other components of the formulation, viscosity develops instantaneously. This can be affected by temperature, electrolytes, or pH value.

Special note

LAPONITE-XLG is not compatible with cationic compounds. Therefore, for pH adjustment, citric acid, lactic acid, or sodium dihydrogen phosphate are recommended to lower the pH value and sodium hydroxide to increase the pH value. As the additive is a weak base and can thus lead to an increase in pH, it may be necessary to adjust the initial pH to a value below the target pH value.

Your local contact

BYK-Chemie GmbH
Abelstraße 45
46483 Wesel
Germany
Tel +49 281 670-0
Fax +49 281 65735

info@byk.com
www.byk.com

Annex 2. Bicinchoninic Acid Protein Assay Kit

SIGMA-ALDRICH®

sigma-aldrich.com

3050 Spruce Street, St. Louis, MO 63103 USA
Tel: (800) 521-8956 (314) 771-5765 Fax: (800) 325-5052 (314) 771-5757
email: techservice@sial.com sigma-aldrich.com

Product Information

Bicinchoninic Acid Protein Assay Kit

Catalog Numbers **BCA1 AND B9643**

TECHNICAL BULLETIN

Synonym: BCA

Product Description
Protein determination is one of the most common operations performed in biochemical research. The principle of the bicinchoninic acid (BCA) assay is similar to the Lowry procedure,[1] in that both rely on the formation of a Cu^{2+}-protein complex under alkaline conditions, followed by reduction of the Cu^{2+} to Cu^{1+}. The amount of reduction is proportional to the protein present. It has been shown that cysteine, cystine, tryptophan, tyrosine, and the peptide bond[2] are able to reduce Cu^{2+} to Cu^{1+}. BCA forms a purple-blue complex with Cu^{1+} in alkaline environments, thus providing a basis to monitor the reduction of alkaline Cu^{2+} by proteins.[3]

The BCA assay is more sensitive and applicable than either biuret or Lowry procedures. In addition, it has less variability than the Bradford assay. The BCA assay has many advantages over other protein determination techniques:

- It is easy to use.
- The color complex is stable.
- There is less susceptibility to detergents.
- It is applicable over a broad range of protein concentrations.

In addition to protein determination in solution, the BCA protein assay has other applications, including determination of protein covalently bound to agarose supports and protein adsorbed to multiwell plates.

There are two distinct ways to perform a protein assay. A protein assay can be set up to measure the concentration of the unknown protein sample (mg/ml), or it can be set up to determine the total amount of protein in the unknown protein sample (mg). The BCA assay has a linear concentration range between 200–1,000 µg of protein per milliliter. In the standard assay, only 0.1 ml protein sample is used, so the assay has a total linear protein range of 20–100 µg.

Reagents
Bicinchoninic Acid Solution, Catalog Number B9643
Reagent A is a 1,000 ml solution containing bicinchoninic acid, sodium carbonate, sodium tartrate, and sodium bicarbonate in 0.1 N NaOH (final pH 11.25).

Copper(II) Sulfate Pentahydrate 4% Solution, Catalog Number C2284
Reagent B is a 25 ml solution containing 4% (w/v) copper(II) sulfate pentahydrate.

Protein Standard (Bovine Serum Albumin - BSA) Solution, Catalog Number P0914
This product is supplied in 5 flame-sealed glass ampules, each containing 1.0 ml of a solution consisting of 1.0 mg/ml bovine serum albumin in 0.15 M NaCl with 0.05% sodium azide as a preservative.

Materials required depending on assay format used but not provided
- Spectrophotometer capable of accurately measuring absorbance in the 560 nm region.
- 96 well plates, Catalog Number M0156
- 96 well plate sealing film, Catalog Number Z369667
- Test tubes, 13 × 100 mm, Catalog Number CLS980013
- 1 ml Disposable Plastic Cuvettes, Catalog Number C5416

Precautions and Disclaimer
This product is for R&D use only, not for drug, household, or other uses. Please consult the Material Safety Data Sheet for information regarding hazards and safe handling practices.

Preparation Instructions
The BCA Working Reagent is prepared by mixing 50 parts of Reagent A with 1 part of Reagent B. Mix the BCA Working Reagent until it is light green in color.

Storage/Stability
Store Reagents A and B at room temperature. Reagent A, without Reagent B added, is stable for at least one year at room temperature in a closed container. The BCA Working Reagent (Reagent A mixed with Reagent B) is stable for one day.

Store the Protein Standard at 2–8 °C.

Procedure
In the standard assay, 20 parts of the BCA Working Reagent are then mixed with 1 part of a protein sample. For the 96 well plate assay, 8 parts of the BCA Working Reagent are mixed with 1 part of a protein sample. The sample is either a blank, a BSA protein standard, or an unknown sample. The blank consists of buffer with no protein. The BSA protein standard consists of a known concentration of bovine serum albumin, and the unknown sample is the solution to be assayed.

BCA assays are routinely performed at 37 °C. Color development begins immediately and can be accelerated by incubation at higher temperatures. Higher temperatures and/or longer incubation times can be used for increased sensitivity. Incubation at lower temperatures can slow down color development (see Procedures A and B). The absorbance at 562 nm is recorded and the protein concentration is determined by comparison to a standard curve.

A. Standard 2.1 ml Assay Protocol
(Linear concentration range is 200-1,000 µg/ml or 20-100 µg of total protein)
This is the standard assay that can be performed in a test tube. This procedure uses 0.1 ml of a protein sample and 2 ml of the prepared BCA Working Reagent. The instructions are a step-by-step procedure on how to perform the standard assay. If a nonstandard assay is used (96 well plate) adjust the volumes accordingly.
Note: It is necessary to create a standard curve during each assay, regardless of the format used.

1. Prepare the required amount of BCA Working Reagent needed for the assays (see Table 1). The final volume used in the assay depends upon the application and the equipment available. Table 1 can be used to determine the volume of BCA Working Reagent to prepare, depending on how many blanks, BSA protein standards, and unknown samples are to be assayed. Combine the volumes of Reagents A and B specified in the table. Mix until the BCA Working Reagent is a uniform, light green color.

Table 1.
Volume of BCA Working Reagent to prepare. This is dependent on how many blanks, BSA protein standards, and unknown samples are to be assayed.

Number of Assays		Amount of Each Reagent Used		
Number of 2.1 ml Standard Test tube assays	Number of wells in a 96 well plate assay	Reagent A (ml)	Reagent B (ml)	Total volume of BCA Working Reagent (ml)
4	40	8	0.16	8.16
8	80	16	0.32	16.32
9	96	19	0.38	19.38
12	127	25	0.5	25.5

2. Prepare standards of different concentrations. These BSA protein standards can range from 200–1,000 µg/ml (20–100 µg of total protein). This is accomplished by making serial dilutions starting from the 1 mg/ml standard, and then using 0.1 ml of each diluted standard in the assay. It is best to make the dilutions in the same buffer as the unknown sample (see Table 2). Deionized water may be used as a substitute for the buffer, but any interference due to the buffer will not be compensated for in the BSA protein standards.

Table 2
EXAMPLE of Standard Assay Set Up Table
For protein samples with unknown concentrations, it may be necessary to prepare a dilution scheme to ensure the concentration is within the linear range of 200–1,000 µg/ml. Two different unknown samples are represented in Table 2 by tubes 7 and 8. Tube 7 is an unknown sample with a 5-fold dilution, while tube 8 is a different unknown sample at a 10-fold dilution. Researchers must determine their own dilution schemes based on their estimation of the concentration of each unknown sample.

Tube No.	Sample (ml)	[BSA] Protein Standard (µg/ml)	BCA Working Reagent (ml)
1	0.1	0	2
2	0.1	200	2
3	0.1	400	2
4	0.1	600	2
5	0.1	800	2
6	0.1	1,000	2
7	0.1	(unknown 1)	2
8	0.1	(unknown 2)	2

3. Add 2 ml of the BCA Working Reagent to 0.1 ml of each BSA protein standard, blank, and unknown sample. Vortex gently for thorough mixing. The total liquid volume in the test tube is 2.1 ml.

4. The following incubation parameters may be used:
   60 °C for 15 minutes **Or**
   37 °C for 30 minutes **Or**
   25 °C (Room Temperature) from 2 hours to overnight

5. If required, allow the tubes to cool to room temperature.

6. Transfer the reaction solutions into a cuvette.

7. Measure the absorbance of the solution at 562 nm. Color development continues slowly after cooling to room temperature, but no significant error is seen if all the tubes are read within 10 minutes of each other. Create an assay table as needed and a standard curve based on either the BSA protein standard concentration or on the amount of protein present in the BSA protein standard (Examples are shown in the results).

8. Determine protein concentration by comparison of the absorbance of the unknown samples to the standard curve prepared using the BSA protein standards.

Results Based on the Standard Assay
Create a table with the absorbance results obtained during the assay. A separate standard curve should be generated for each assay performed. The amount of protein for tubes 1–6 was obtained from the known amount of BSA protein standard added.
Note: The data below should not be used as a replacement of a standard curve. The absorbance of the BSA protein standards (tubes 1–6) in each assay will differ from those presented here. The amount of protein recorded for tubes 7 and 8 was obtained from the standard curve.

Table 3.
EXAMPLE of Assay Data Table

Tube No.	A_{562}	Net A_{562}	Amount of protein (µg) in sample	[Protein] of protein sample (µg/ml)	Dilution Factor
1	0.045	0	0	0	-
2	0.207	0.162	20	200	-
3	0.364	0.319	40	400	-
4	0.510	0.465	60	600	-
5	0.661	0.616	80	800	-
6	0.823	0.778	100	1,000	-
7	0.587	0.542	70	700	5
8	0.743	0.698	90	900	10

After obtaining the results, create a standard curve to determine the protein concentration in the unknown sample. Plot the Net Absorbance at 562 nm versus the BSA protein standard concentrations (µg/ml, Tubes 1–6).

Graph 1.
Standard Curve produced from Assay Data

The standard curve indicates the unknown protein sample in test tube 7 (Net A_{562} = 0.542) contains 700 µg/ml of protein.

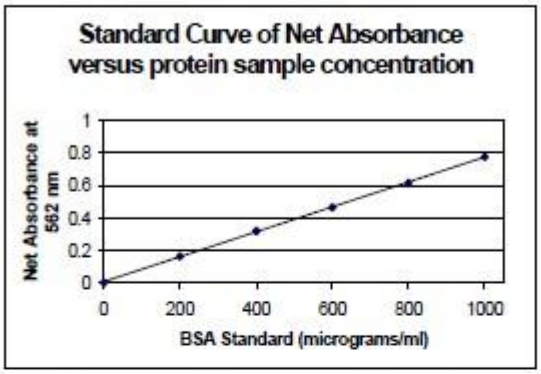

The actual concentration of protein present in the unknown sample is calculated as follows:

(µg/ml of unknown protein sample) times (Dilution Factor)

(700 µg/ml) × (5) = 3,500 µg/ml of protein

B. 96 Well Plate Assay
(Linear concentration range is 200-1,000 µg/ml or 5-25 µg of total protein)
The BCA assay can be adapted for use in 96 well plates. These plates can be used as long as five main points remain unchanged:

1. Read the absorbance at 562 nm. For a plate reader, which does not have the exact wavelength filter, a filter in the range of 540-590 nm can be substituted.

2. The ratio of BCA Working Reagent to protein sample will have to be modified from the Standard Assay.
   Examples:
   Standard Assay - (Test Tube): 0.10 ml protein sample to 2 ml BCA Working Reagent (1:20)

   96 well plate - 25 µl protein sample to 200 µl BCA Working Reagent (1:8). When using multiwell plates, make sure the unknown samples, blanks, or standards are present in the wells prior to adding the BCA Working Reagent to facilitate mixing.

3. Make sure the protein assay containers are sealed (cover the plates with film) and incubate the samples for:
   60 °C for 15 minutes **Or**
   37 °C for 30 minutes **Or**
   25 °C (Room Temperature) from 2 hours to overnight

4. Keep the protein sample concentration between 200–1,000 µg/ml (5–25 µg total protein).

5. A separate standard curve will have to be determined for each assay protocol. The pathlength in each assay is dependent on the assay container (cuvettes or multiwell plates) and/or the reaction volume. These and others changes like the BCA Working Reagent to protein sample ratio affect the Net Absorbance values.

C. TCA Concentration-BCA Assay Protocol
By using this procedure it is possible to remove some of the interfering substances that are described in the compatibility chart. It is also possible to increase the concentration of the unknown sample using this procedure.

1. Add the unknown samples and BSA protein standards to separate microcentrifuge tubes and adjust the final volumes to 1 ml with deionized water. Larger volumes can also be used by adjusting the following volumes accordingly.

2. Add 0.1 ml of a 0.15% (w/v) solution of sodium deoxycholate (Catalog Number D5670) prepared with deionized water.

3. Mix and let stand for 10 minutes at room temperature. It is also acceptable to let stand on ice for 10 minutes.

4. Add 0.1 ml of 6.1 N (~100% w/v) solution of trichloroacetic acid (TCA, Catalog Number T0699).

5. Cap and vortex each sample.

6. Incubate for 5 minutes at room temperature. It is also possible to let stand on ice for 5 minutes.

7. Centrifuge the samples for 15 minutes at room temperature in a microcentrifuge at full speed.

8. Carefully decant or pipette the supernatant of each sample. Do not disturb the pellet.

9. Solubilize each pellet by adding 0.04 ml of a 5% (w/v) solution of sodium dodecyl sulfate (SDS, Catalog Number L6026) prepared with a 0.1 N sodium hydroxide solution (Catalog Number 72076). Mix well until the pellet is completely dissolved.
10. Pipette 0.06 ml of deionized water into the tube to bring the sample volume to 0.10 ml, which can then be used in the standard 2.1 ml assay procedure. It is possible to add less water if a smaller volume assay is to be performed.
11. Vortex each sample and proceed onto the 2.1 ml standard assay protocol or a custom assay.

Compatibility Chart
The amount listed is the maximum amount of material allowed in the protein sample without causing a noticeable interference.

Incompatible Substances	Amount Compatible
Buffer Systems	
N-Acetylglucosamine (10 mM) in PBS, pH 7.2	10 mM
ACES, pH 7.8	25 mM
Bicine, pH 8.4	20 mM
Bis-Tris, pH 6.5	33 mM
CelLytic™ B Reagent	undiluted no interference
Calcium chloride in TBS, pH 7.2	10 mM
CHES, pH 9.0	100 mM
Cobalt chloride in TBS, pH 7.2	0.8 M
EPPS, pH 8.0	100 mM
Ferric chloride in TBS, pH 7.2	10 mM
HEPES	100 mM
MOPS, pH 7.2	100 mM
Nickel chloride in TBS	10 mM
PBS; Phosphate (0.1 M), NaCl (0.15 M), pH 7.2	undiluted no interference
PIPES, pH 6.8	100 mM
Sodium acetate, pH 4.8	200 mM
Sodium citrate, pH 4.8 or pH 6.4	200 mM
Tricine, pH 8.0	25 mM
Triethanolamine, pH 7.8	25 mM
Tris	250 mM
TBS; Tris (25 mM), NaCl (0.15 M), pH 7.6 (Catalog Number T5030)	undiluted no interference
Tris (25 mM), Glycine (1.92 M), SDS (0.1%), pH 8.3 (Catalog Number T4904)	undiluted no interference
Zinc chloride (10 mM) in TBS, pH 7.2	10 mM

Incompatible Substances (Continued)	Amount Compatible
Buffer Additives	
Ammonium sulfate	1.5 M
Aprotinin	10 mg/L
Cesium bicarbonate	100 mM
Glucose	10 mM
Glycerol	10%
Guanidine•HCl	4 M
Hydrochloric acid	100 mM
Imidazole	50 mM
Leupeptin	10 mg/L
PMSF	1 mM
Sodium azide	0.20%
Sodium bicarbonate	100 mM
Sodium chloride	1 M
Sodium hydroxide	100 mM
Sodium phosphate	25 mM
Sucrose	40%
TLCK	0.1 mg/L
TPCK	0.1 mg/L
Sodium orthovanadate in PBS, pH 7.2	1 mM
Thimerosal	0.01%
Urea	3 M
Chelating agents	
EDTA	10 mM
EGTA	not compatible
Sodium citrate	200 mM
Detergents	
Brij™ 35	5%
Brij 52	1%
CHAPS	5%
CHAPSO	5%
Deoxycholic acid	5%
Nonidet P-40 (IGEPAL® CA-630)	5%
Octyl β-glucoside	5%
Octyl β-thioglucopyranoside	5%
SDS	5%
Span® 20	1%
TRITON® X-100	5%
TRITON X-114	1%
TRITON X-305	1%
TRITON X-405	1%
TWEEN® 20	5%
TWEEN 60	5%
TWEEN 80	5%
Zwittergents®	1%

Incompatible Substances (Continued)	Amount Compatible
Reducing & Thiol Containing Agents	
Dithioerythritol (DTE)	1 mM
Dithiothreitol (DTT)	1 mM
2-Mercaptoethanol	1 mM
Tributyl Phosphine	0.01%
Solvents	
Acetone	10%
Acetonitrile	10%
DMF	10%
DMSO	10%
Ethanol	10%
Methanol	10%

Note: This is not a complete compatibility chart. There are many substances that can affect different proteins in different ways. One may assay the protein of interest in deionized water alone, then in the buffer with possible interfering substances. Comparison of the readings will indicate if an interference exists. Refer to References for additional information on interfering substances.[1-4]

Note: Reagents that chelate metal ions, change the pH of the assay, or reduce copper will interfere with the BCA assay. Examples are shown below:

1. Metal chelators such as EDTA (>10 mM) and EGTA (any level).
2. Thiol containing reagents such as cysteine (any level), DTT (>1 mM), dithioerythritol (>1 mM), and 2-mercaptoethanol (>0.01%).
3. High salt or buffers concentrations such as ammonium sulfate (>1.5 M), Tris (>0.25 M), and sodium phosphate (>0.1 M).

Troubleshooting Guide - Protein sample contains incompatible reagents or substances.

1. If the starting concentration of the protein is high, try diluting the sample so the substance no longer interferes.
2. Use the TCA Concentration-BCA procedure and discard the incompatible liquid after the pellet is spun down.
3. The interference caused by chelating reagents decreases when the relative amount of the copper(II) sulfate solution is increased in the prepared BCA Working Reagent. The standard preparation has 50 parts of bicinchoninic acid solution to 1 part copper(II) sulfate solution. The amount of copper(II) sulfate solution may be increased to 3 parts.

Technical Tips

1. Make sure the glassware being used has been cleaned well.
2. Consider a different protein assay procedure. If certain incompatible reagents cannot be removed from the assay, consider the use of the Bradford Reagent (Catalog Number B6916).
3. If the protein levels are too low, try using the QuantiPro BCA Kit (Catalog Number QPBCA).

References

1. Lowry, O.H. et al., J. Biol. Chem., **193**, 265-275 (1951).
2. Wiechelman, K. et al., Anal. Biochem., **175**, 231-237 (1988).
3. Smith, P.K. et al., Anal. Biochem., **150**, 76-85 (1985).
4. Brown, R.E. et al., Anal. Biochem., **180**, 136-139 (1989).

FF,JDS,MAM 02/11-1

Annex 3. Standard curves for *in vitro* drug release studies

Curve obtained for assay at pH=7.4

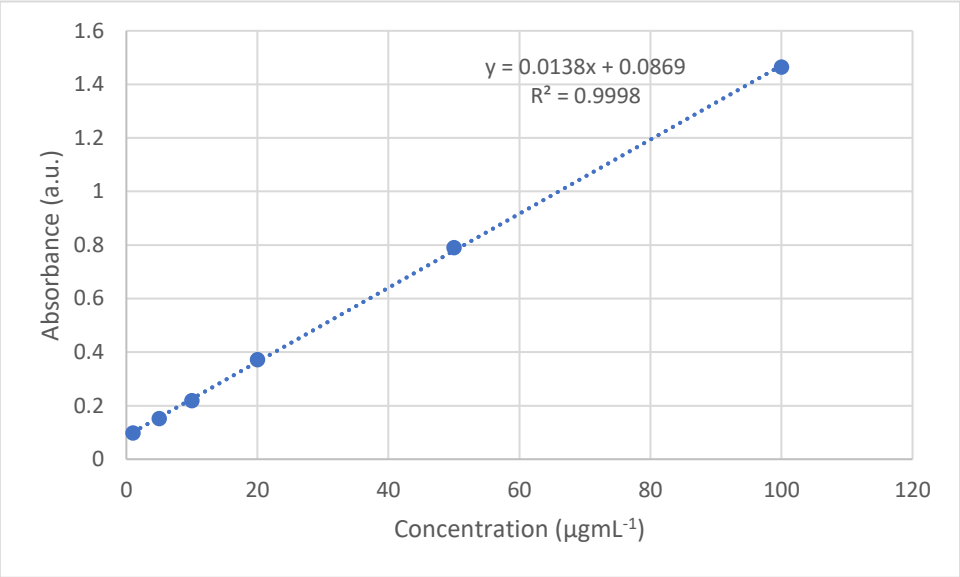

Curve obtained for assay at pH=6.5

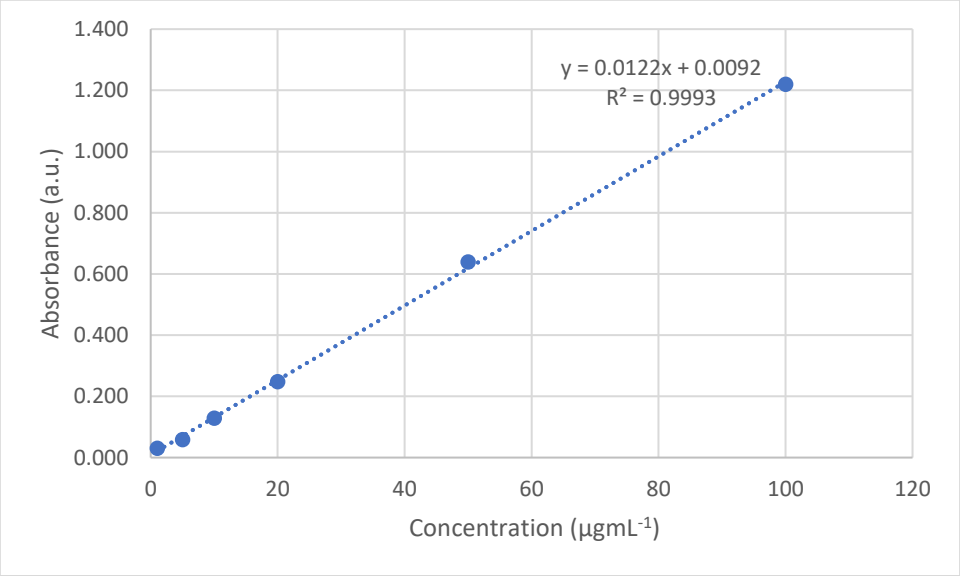


UNIVERSIDADE da MADEIRA


CQM
CENTRO DE QUÍMICA
DA MADEIRA


Molecular Materials
RESEARCH GROUP
MADEIRA ISLAND - PORTUGAL


fct
Fundação
para a Ciência
e a Tecnologia


arditi
agência regional para o
desenvolvimento da investigação
tecnologia e inovação